

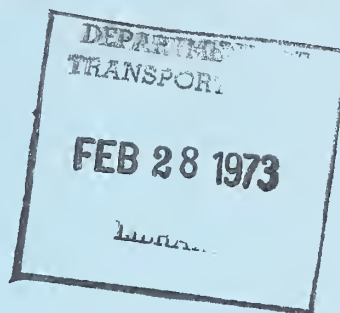
HE  
18.5

A37

no. DOT-  
TSC-UMTA  
71-6

T NO. DOT-TSC-UMTA-71-6.

# **URBAN VEHICLE COMMUNICATIONS & CONTROL**



R.E. BUCK, L.A. FRASCO,  
H.D. GOLDFEIN, S. KARP,  
L. KLEIN, E.T. LEONARD  
J. LIU, P. YOH  
TRANSPORTATION SYSTEMS CENTER  
55 BROADWAY  
CAMBRIDGE, MA. 02142



**AUGUST 1971  
ANNUAL REPORT  
VOLUME I**

Availability is Unlimited. Document may be Released  
To the National Technical Information Service,  
Springfield, Virginia 22151, for Sale to the Public.

Prepared for  
U.S. DEPARTMENT OF TRANSPORTATION  
URBAN MASS TRANSPORTATION ADMINISTRATION  
WASHINGTON, D. C. 20590

The contents of this report reflect the views of the Transportation Systems Center which is responsible for the facts and the accuracy of the data presented herein. The contents do not necessarily reflect the official views or policy of the Department of Transportation. This report does not constitute a standard, specification or regulation.

HE  
18.5  
A37  
10.  
DOT-  
TSC-  
UMTA-  
71-6

DEPARTMENT OF  
TRANSPORTATION

3. Recipient's Catalog No.

FEB 28 1973

1. Report No.

DOT-TSC-UMTA-71-6

2. Government Accession No.

4. Title and Subtitle

Ground Vehicle Communications &  
Control

5. Report Date

July 1971

6. Performing Organization Code

7. Author(s) R. E. Buck, L. A. Frasco, H. D.  
Goldfein, S. Karp, L. Klein, cont.

8. Performing Organization Report No.

9. Performing Organization Name and Address

Department of Transportation  
Transportation Systems Center  
55 Broadway  
Cambridge, MA 02142

10. Work Unit No.

R-2008

11. Contract or Grant No.

UM03-1

13. Type of Report and Period Covered

Annual Report

July 1970-June 1971

14. Sponsoring Agency Code

12. Sponsoring Agency Name and Address

Department of Transportation  
Urban Mass Transportation Admin.  
Washington, DC 20590

15. Supplementary Notes

authors cont. E. T. Leonard, J. Liu,  
and P. Yoh

16. Abstract A program for improving vehicular communications in the urban environment is described. The first major item was the development of a capability to measure and record both the multipath structure of any particular urban channel and the associated noise environment. This will be accomplished by outfitting a van to make noise measurements and also to be the receiving site for suitably designed probing signals which will be transmitted from fixed locations. The frequencies to be used are: 149.95, 416.6 and 902.2 MHz.

The second part of the program is directed toward analyzing the noise and multipath characteristics measured above. Effort has been directed toward constructing a channel simulator and a communication system simulator.

Contractor reports are included.

17. Key Words

land mobile communications,  
electromagnetic noise,  
channel characterization

18. Distribution Statement

Availability is Unlimited. Document may be Released  
To the National Technical Information Service,  
Springfield, Virginia 22151, for Sale to the Public.

19. Security Classif. (of this report)

Unclassified

20. Security Classif. (of this page)

Unclassified

21. No. of Pages

164

22. Price



# TABLE OF CONTENTS

## VOLUME I

	<u>Page</u>
SUMMARY . . . . .	1
Background . . . . .	1
Experimental Phase . . . . .	2
Analytical Phase . . . . .	3
Related Work . . . . .	3
TECHNICAL DISCUSSION. . . . .	5
Introduction . . . . .	5
General . . . . .	5
General Problem . . . . .	5
Noise Measurement Program . . . . .	6
Channel Characterization Experiment . . . . .	8
Outline of the Following Sections . . . . .	10
Equipment Specifications . . . . .	10
Receiver. . . . .	10
Transmitter . . . . .	15
Magnetic Tape Recorder I. . . . .	17
Magnetic Tape Recorder II . . . . .	19
Data Processor. . . . .	19
Designs of Experiments . . . . .	20
Noise Measurement . . . . .	20
Spectrum Occupancy. . . . .	25
Channel Measurement . . . . .	26
Milestones for FY'72 . . . . .	27
Installation and Checkout of the Mobile Van . . . . .	28
Channel Occupancy Measurements. . . . .	28
Calibration and Test Instruments. . . . .	28
Noise Measurements. . . . .	30
Channel Measurements. . . . .	30
Data Analysis and Modeling. . . . .	30
Simulator . . . . .	30

# TABLE OF CONTENTS

## VOLUME I (CONTINUED)

	<u>Page</u>
APPENDIX A . . . . .	31
Introduction. . . . .	31
Description of I/O Controller and Measurement Process . . . . .	31
Timing. . . . .	31
Measurement Accuracy. . . . .	32
Growth Potential. . . . .	36
Physical Description. . . . .	36
Programming . . . . .	36
Controller Operation. . . . .	38
REPRINTS OF IN-HOUSE PUBLICATIONS. . . . .	44
Urban EM Noise Measurement. . . . .	44
Measurement and Analysis of Urban Radio Channels for Communication System Design . . . . .	54
Survey of Multipath and Noise Measurements in Cities . . . . .	64
REPRINT OF SPECIAL CONTRACTOR REPORT . . . . .	99
Statistical-Physical Models of Urban Radio-Noise Environments by David Middleton . . . . .	99

TABLE OF CONTENTS

VOLUME II (CONTINUED)

VOLUME II

BIBLIOGRAPHY ON GROUND VEHICLE COMMUNICATIONS &  
CONTROL: A KWIC INDEX

W. I. THOMPSON, III

Report No. DOT-TSC-UMTA-71-3; issued July 1971		Page
1.0	Introduction . . . . .	1
1.1	General Description of the Bibliography . . . . .	1
1.2	Sources of Documents . . . . .	2
1.3	References to Chapter 1. . . . .	2
2.0	Bibliography List by Accession Number . . . . .	5
3.0	Author Index. . . . .	93
4.0	Negative Key Work List . . . . .	119
5.0	Key-Word-In-Context Index or Permuted Title Index. . . . .	123



# LIST OF ILLUSTRATIONS

<u>Figure</u>		<u>Page</u>
1.	Diagram of the Major Tasks and Problem Areas and the Logical Flow of the Data in the Measurement Program. . . . .	7
2.	Basic Receiver Block Diagram . . . . .	9
3.	Definition of Basic Signal Processing Operations in Prober Systems . . . . .	11
4.	Channel Playback Schematic Diagram . . . . .	12
5.	Block Diagram of the Receiver. . . . .	16
6.	Block Diagram of the Receiver. . . . .	18
7.	Measurement Action Sequence and Timing Data. . . . .	33
8.	Data Transfer Operations for Timing Estimation . . . . .	34
9.	Data Word Formats. . . . .	35
10.	Functional Block Diagram of I/O Controller and Measurement Hardware. . . . .	39
11.	Measurement Control Logic Block Diagram. . . . .	40
12.	Floating Point Counter Block Diagram . . . . .	41
13.	Address Counter. . . . .	42

## TABLE

1.	Time Schedule for Various Tasks. . . . .	29
----	--	----



# SUMMARY

## BACKGROUND

The purpose of the FY-71 effort was to initiate a program for improving vehicular communications in the urban environment and to provide UMTA with technical support in this and related areas. A general program outline is given in the PPA UM03-1 dated July 24, 1970.

Requirements imposed on land-mobile communication services have become more stringent in recent years. First, the number of users continues to increase, while available spectrum for this service remains severely restricted both for technical reasons and for reasons of public policy; second, the emerging interest in data communications and in automatic vehicle monitoring (AVM) systems implies demands for increased communication capacity utilizing wideband signalling methods.

Timely provision of this increased capacity requires that we understand in detail the urban communication environment. The measurement of these channel properties, therefore, is not academic; in fact, it is integral to both design and evaluation of communication systems capable of carrying out the difficult task of reliable urban communication at reasonable cost.

The analytic techniques and special purpose equipment being developed for UMTA by TSC have immediate, practical application to an important, continuing UMTA demonstration program, namely, the AVM tests presently planned for Philadelphia. Two main areas of application are envisaged: (1) spectrum occupancy and interference, and (2) design assistance for waveforms and modems.

### 1. Spectrum occupancy and interference

The AVM program can be assisted in several task areas using the TSC equipment.

- a. Quantitative measurements of RFI and EMI generated by the test systems can be made and their effect on the EM environment in their bands of operation can be calculated. These measurements can help set filtering and shielding requirements for transmitters and receivers.
- b. These data will provide essential information to be presented to the FCC when requesting approval for the use of certain bands or modulation formats.
- c. The TSC equipment will be available to carry out other spectrum occupancy measurements in response to FCC

requests for further data.

## 2. Design assistance

The channel characterization and noise measurement equipment can be used as a design tool in the formulation of range tone location systems and in the design and test of digital modems.

The TSC program consists of two parts described in the sections Experimental Phase and Analytical Phase.

### EXPERIMENTAL PHASE

First, a mobile experimental station is being developed with the capability to measure and record both the multipath structure of any particular urban channel and the associated noise environment. This will be accomplished by outfitting a van to make noise measurements and also to be the mobile receiving site for suitable designed probing signals which will be transmitted from fixed locations.

A thorough review of the literature has supported our view that the present measurements and standards for urban noise are inadequate. Consequently, we are preparing to make broad-band noise measurements over a wide dynamic range in order to preserve the basic noise structure. This data will be recorded on magnetic tape and will be available both for analysis and simulation. The results of the noise and multipath measurements will then be used in formulating a clearer description of these processes. This capability will also be available to make comprehensive measurements on the electromagnetic noise produced by electric vehicles. The effects of suppression techniques can also be measured and compared.

The probing signals will be specifically designed to decompose the multipath structure into its fundamental components. This is a standard technique in the study of fading dispersive channels which is being carried over directly to the urban channel. If done properly, each of these fundamental components can be recorded on tape and used as an input to a "playback" channel simulator. Therefore, the emphasis of the first part of this program is to assemble a channel simulator, designed to test hardware for the particular environment in which a demonstration is to take place. We estimate that it will be possible to record an environment and be prepared to evaluate equipment in a period of about four months. Hopefully, this will provide a quick reaction to programs and changes in programs as they develop.

## ANALYTICAL PHASE

The second part of this program is directed toward analyzing the noise and multipath characteristics and developing more reliable configurations for command and control. In particular, since UMTA will most likely be interested in the flow of digital data between terminals it will be necessary to study specifications and requirements for digital data flow over the existing voice links. At present, land mobile bands are allocated for voice transmission and only recently have proposals been made for digital data flow in the same channel. Allocations of channels for digital data transmission are available on an experimental basis. The intended use of these channels is exclusively for Automatic Vehicle Monitoring (AVM) systems, not for general digital transmission of voice and other message traffic. In addition, most of the available hardware is not suited for this use and is spectrally inefficient.

Thus, effort is to be directed toward the eventual construction of a communication system simulator into which the channel simulator could be inserted. This would allow detailed design and specification of command and control systems for the urban environment.

This approach to the command portion of the problem has the following merits.

As the frequency assignments change, it is relatively easy to retake the measurements without altering the basic system. Since the assemblage is modular in nature other channels of interest can be inserted without losing the capability of the communication simulator. Furthermore, the system can be directly employed in analyzing and designing various forms of AVM systems which use the land mobile bands. The great flexibility of a communication simulator will allow the designer to tailor his system to a close replica of the channel and to quickly evaluate competing techniques.

In addition, we will be in a position to suggest modifications of existing equipment that will yield the minimum impact on the cost of demonstration programs.

## RELATED WORK

During the course of the program, we have given support to the demonstration programs office in the assessment of competing AVM systems. This has been directed primarily at proposal evaluation and technical recommendations. The level of future TSC participation in the AVM program will be determined by the demonstration programs office and will be responsive to their

needs.

We are also undertaking preliminary investigation into the general area of traffic flow and traffic control in the urban area. This work is being directed toward assessing the status of present traffic control systems and determining what the state of the technology is in this area. Coordination is also being made with other groups within TSC who are working in this and related areas.

# TECHNICAL DISCUSSION

## INTRODUCTION

### GENERAL

A program was initiated at TSC to study the interference on the communication channel in the urban and suburban environments and to establish the capability for comparative evaluation of competing components, subsystems and systems. In this first year, major effort was concentrated on:

1. Defining the characteristics of interference
2. Establishing interference measuring facility
3. Constructing a channel simulator facility.

In the following sections, we will discuss the general problem, the noise program, and the channel characterization program.

### GENERAL PROBLEM

Reviewing the past experimental and theoretical work, we believe there are essentially three major types of interference in the urban and suburban environment; namely, additive noise -- Gaussian and impulsive, Co-channel interference, and fading dispersive interference -- reflection and scattering off the structures, terrain, etc. The experimental program was designed for the following purposes:

1. To study experimental techniques for the measurement of wideband man-made noise in the VHF-UHF region and to establish a capability for the routine performance of such measurements.
2. To identify the major sources of radiation that will interfere with the performance of any land transportation communication system being planned in the frequency band mentioned above.
3. To determine the information needed for the design and evaluation of any communication or command and control system of mass transit or land, air, water or highway communication. In combination with channel probing measurements this information will provide a complete characterization of the urban and suburban channel.
4. To determine the radiation characteristics of existing and proposed transportation systems such as electric cars, trolley cars, electric trains, etc.

Figure 1 shows the major tasks and problem areas and the logical flow of the data in the measurement program.

## NOISE MEASUREMENT PROGRAM

A communication system planner would like to know the detailed characteristics of the background noise in order to evaluate its effects on system performance. This information includes the time and space variation of the noise as well as, for prediction purposes, its correlation with factors such as population density, vehicular traffic, power consumption and topographical characteristics.

As has been mentioned, the requirements are more stringent for digital communication systems, which require a more thorough specification of the statistical characteristics of the noise than do analog systems. By and large this information is not currently available and this lack of design data hampers designers of wideband systems, i.e., for our purposes defined as systems whose bandwidth exceeds 10 kHz. Therefore, the purpose of the experiment under consideration is to measure broadband, wide dynamic range, impulsive-type noise in selected regions of the VHF and UHF bands. The bandwidth of the measuring system has been tentatively selected to be 1 MHz. The predominant noise is expected to be generated by man-made sources such as automobile engines, industrial equipment, etc.

One of the first tasks is, of course, the determination of the statistical quantities describing the noise which can be derived by suitable processing of the experimental data. Although a certain amount of data processing can be done in real time the decision has been made to record the IF waveform for later processing and for use in the simulation equipment. This means that most of the processing procedures can be decided upon at a later date. However, some initial consideration of what has to be measured is in order. A simple model of wideband man-made interference is the sum of an impulsive component and a Gaussian process. Both components can be expected to be nonstationary. It seems reasonable to measure at least the following quantities.

1. Average power over each measurement interval
2. Amplitude probability distribution function (pdf) of the peaks
3. Duration pdf of the impulses at given amplitude levels
4. Pulse spacing pdf
5. Crossing rate pdf

In addition to the above quantities some simpler parameters such as average and rms values after detection can be measured in real time. It is worth pointing out that instrumentation

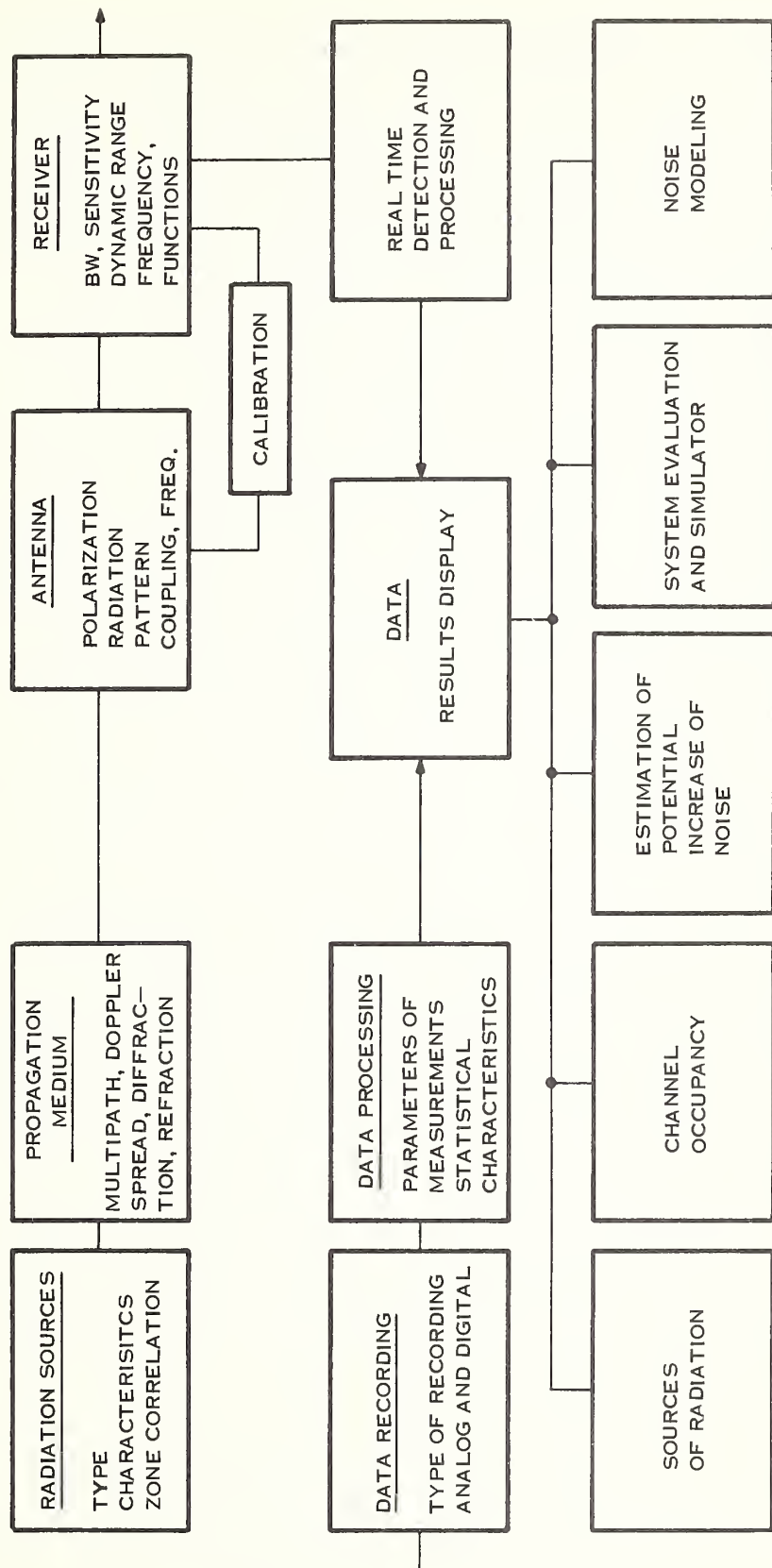


Figure 1. Diagram of the Major Tasks and Problem Areas and the Logical Flow of the Data in the Measurement Program

similar to that being studied for the noise measurements can be used in the future for the investigation of channel occupancy. By this we mean the evaluation of the probability that a given frequency region be occupied at a certain level by other transmitters. Because of the limited spectral region available for land mobile communication it is also important to determine the minimum allowed spatial separation of stations transmitting in the same frequency region in order to avoid appreciable cochannel interference. This type of measurement can also be performed by the system under consideration.

A simple block diagram of the noise measuring system is shown in Figure 2.

## CHANNEL CHARACTERIZATION EXPERIMENT

We now consider the experimental work planned for study of the second component of interference caused by the fading dispersive characteristics of the urban channel. This component arises from vehicle motion through a continually changing multipath environment. It is of equal importance to measure these deleterious effects and to analytically model them. Measurement is important because it provides a realistic, repeatable replica of the communication channel which can be used in optimizing or refining a system design, or in evaluating contending candidate systems at different times on an equal basis. Analytic work in this area is important in defining the form of a channel simulator even when the problem is too complex for a detailed mathematical analysis, and in providing the basic design for suitable transmitter waveforms for use in the fading environment.

Based on extensive research carried out over the last decade in the area of characterization of fading dispersive channels, it is now practical to build a channel simulator capable of presenting to a candidate communication system the simulated, stored replica of the distortion characteristics of any desired channel displaying multipath delay, Doppler spread and additive noise. This channel playback approach effectively brings the field conditions into the laboratory and makes possible the comparative evaluation of competing techniques under identical conditions. This stored channel simulation can represent an estimate of the channel characteristics based upon mathematical modeling or can in fact be a faithful reproduction of the channel under operating conditions. The availability of both approaches is desirable for a comprehensive simulator facility.

The proposed technique involves two procedures with corresponding equipment. The first procedure involves field tests employing specially designed transmitter probing signals which cover the frequency bands of interest in the planned program areas. The probing signals are processed in the moving vehicle

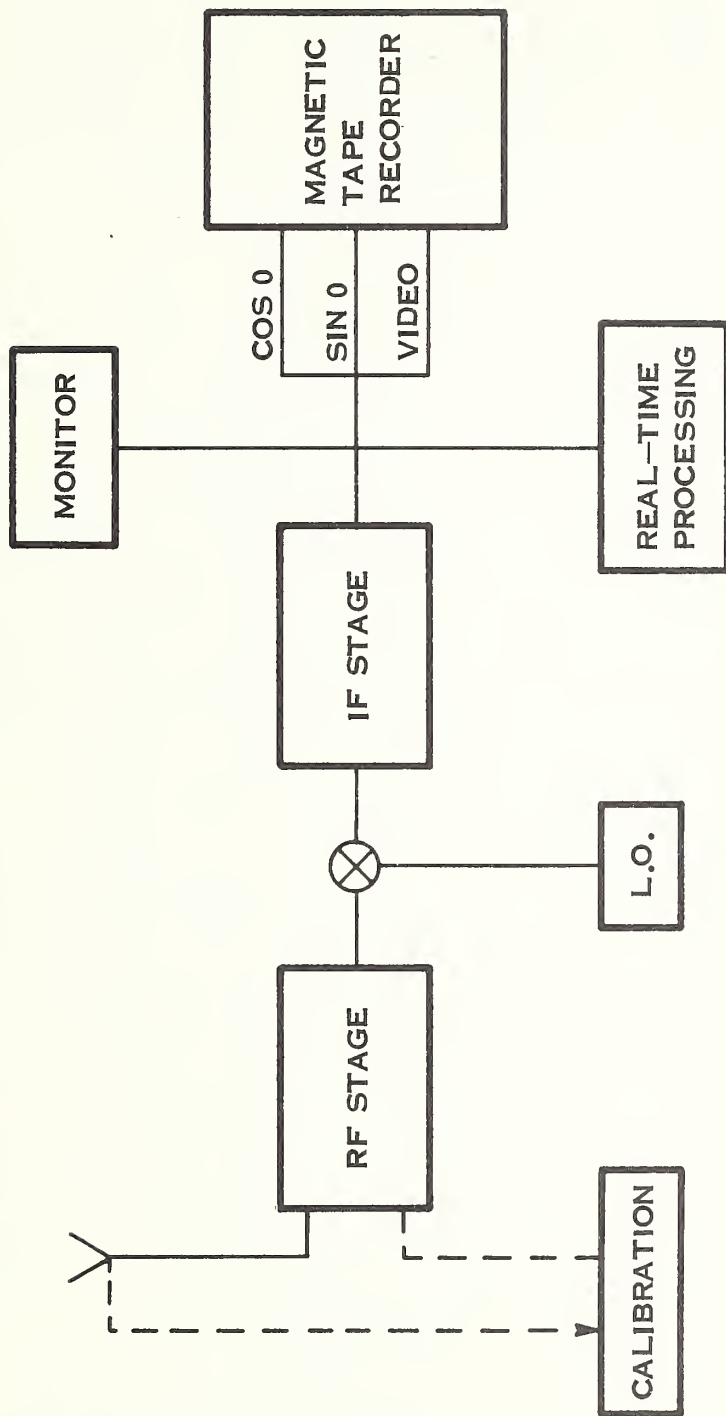


Figure 2. Basic Receiver Block Diagram

to extract the time-variant system function of the propagation environment or medium and record it on a multi-channel tape recorder. In addition, the additive noise would be recorded. A tape library could be built up which would adequately cover all environments for which systems are being developed. The replay procedure is carried out using these tape records. The time-varying channel, with the additive noise, would be played back repeatedly to enable tests of various systems to be made under the same field conditions. Basic block diagrams of the signal processing operations carried out in the channel prober and playback systems are shown in Figures 3 and 4.

Figure 3 defines the basic signal processing operations of the probing system. A periodic probing signal with complex envelope  $z(t)$  is filtered at the transmitter by IF and RF filters prior to transmission. All the filtering operations in the transmitter are lumped together as one filter, called the transmitter filter, which has impulse response  $h_T(t)$ . The propagation medium is represented by the complex time-variant impulse response  $h(t, \tau)$  and the additive noise by the complex process  $n(t)$ . All the linear operations in the receiver prior to the correlation operations are lumped together into one receiver filter with impulse response  $h_R(t)$ . The output of the filter is fed to a number of parallel correlators, only one of which is shown in the figure. Complex notation is used to describe the correlation operation as a multiplication of the receiver filter output by the complex conjugate of a shifted probing signal followed by a complex low pass filtering operation.

Channel playback is achieved with a tapped delay line as shown in Figure 4. The complex time-varying multipliers are just equal to the low pass filter outputs of the correlators which yield estimates of the impulse response for uniformly spaced values of delay separated by  $\tau$  seconds. Filtering operations necessary to avoid aliasing in the digital realization of the playback channel are shown in dashed lines.

## OUTLINE OF THE FOLLOWING SECTIONS

The specifications for all the major equipments are given in the next section. The planning of the experimental procedure, such as the number of measurements, frequency, and the length of each measurement will be discussed. Finally, a milestone for FY72 is given.

## EQUIPMENT SPECIFICATIONS

### RECEIVER

The function of the receiver is as follows: To make both wideband or narrowband measurements of man-made noise, spectrum

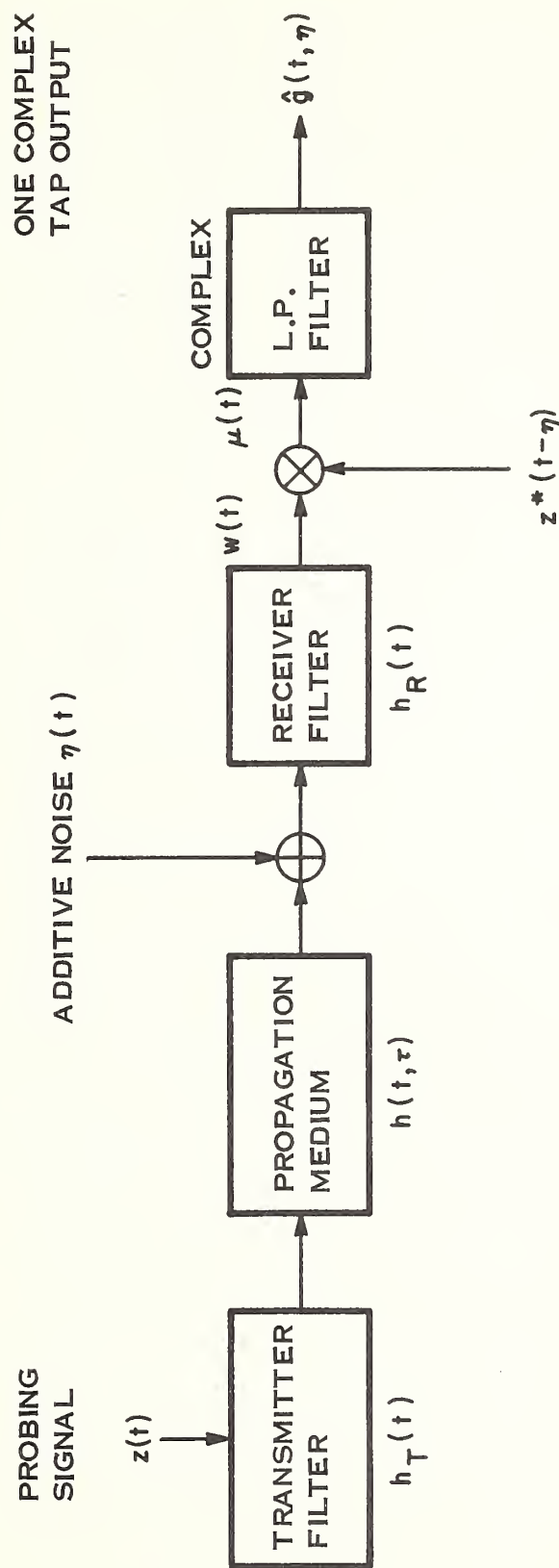


Figure 3. Definition of Basic Signal Processing Operations in Prober Systems

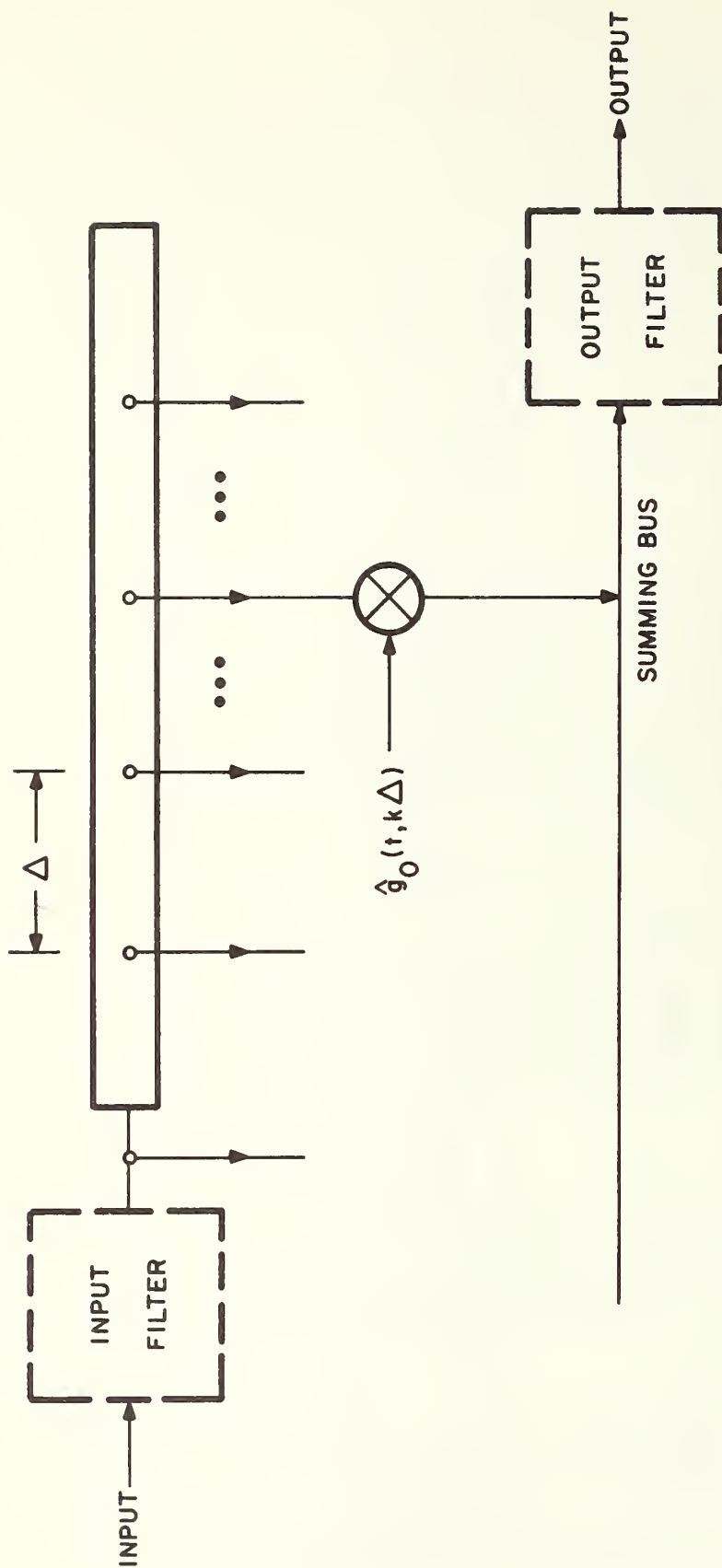


Figure 4. Channel Playback Schematic Diagram

occupancy and channel characterization of the time varying propagation media. These functions are carried out separately in time. The main receiver characteristics are the following:

1. Three selectable rf frequencies and their respective tunable frequency range:

<u>Frequency (MHz)</u>	<u>Range (MHz)</u>
149.95	135-165
416.6	400-480
902.2	850-950

2. Selectable i-f predetection BPF (3 dB):

2,1 and 0.2 MHz

3. Available outputs:

- a. I-F waveform
- b. Video amplitude for direct magnetic tape recording
- c. Two orthogonal components of the phase information, for direct magnetic tape recording
- d. RMS monitoring and recording for either magnetic tape or strip chart recording .

The receiver should have a wide dynamic range and sensitivity to detect any conceivable man-made noise (intentional and unintentional) in the urban and suburban environment.

#### Detailed Specifications:

##### Input Impedance:

50 ohms, VWSR < 1.5

##### RF Frequency:

1. 149.95 MHz  
Preselector rf passband (3 dB): 4.3 MHz  
Tunable range: 135-165 MHz  
Image rejection: 80 dB (min)  
Input power range: -104 to -19 dBm over  
1 MHz bandwidth
2. 416.6 MHz  
Preselector rf passband (3 dB): 5 MHz  
Tunable range: 400-480 MHz  
Image rejection: 80 dB (min)  
Input power range: -104 to -20 dBm over  
1 MHz bandwidth

3. 902.2 MHz  
 Preselector rf passband (3 dB): 18 MHz  
 Tunable range: 850-950 MHz  
 Image rejection: 80 dB (min)  
 Input power range: -108 to -23 dBm over  
 1 MHz bandwidth

<u>Noise Figure (max)</u>	<u>Frequency</u>
9 dB	149.95 MHz
9 dB	416.6 MHz
6 dB	902.2 MHz

Local Oscillators: In addition to three oscillators for the three center frequencies, an external reference oscillator port should be provided.

Stability:  $\pm 5$  kHz

I-F Frequency: 30 MHz

I-F Passband: Selectable and switchable according to the following predetection bandwidth:

1. 2 MHz  $\pm 10\%$
2. 1 MHz  $\pm 10\%$
3. 0.2 MHz  $\pm 10\%$

Rise Time:  $\frac{1}{2X \text{ bandwidth}}$

Overshoot: <10 percent

Outputs: All outputs, with the exception of i-f output, should have a maximum compressed dynamic range of 30 dB in order to match the dynamic range capability of an analog tape recorder.

1. I-F Output:  
 Accuracy:  $\pm 1$  dB  
 Maximum level: 10 dBm/MHz  
 Minimum level: -80 dBm/MHz  
 I-F Buffer amplifier should be provided with 50 ohms output impedance.
2. Baseband Output:  
 Accuracy:  $\pm 1$  dB  
 Maximum level: 5 V  
 Minimum level: 0.1 V  
 Compressed dynamic range: 30 dB  
 Output impedance: 75 ohms

3. Phase Information Output:  
Two orthogonal components of the phase information, or alternatively, the in-phase and quadrature components of the compressed i-f waveform.  
Phase accuracy:  $\pm 10^\circ$   
Level: 1 Vrms nominal  
Phase channel center frequency: 0.75 MHz  
Bandwidth (3 dB): 1 MHz

The output bandwidth should be compatible with the bandwidth of the tape recorder (400 Hz to 1.5 MHz).

4. RMS output:
5. Time constants: Variable in steps of 0.01, 0.1, 1 and 10 seconds.

Figure 5 shows the block diagram of the receiver.

## TRANSMITTER

The transmitter has the function of transmitting coded signals (binary PM) for measuring the multipath, frequency broadening, pulse broadening and other parameters while the receiving station is moving through urban and suburban environments. It should be capable of transmitting three selected frequencies, separately in time. The main transmitter characteristics are the following:

1. Three selectable rf frequencies:

149.95 MHz  
416.6 MHz  
902.2 MHz

2. Output power: 20 W (min)

### Detailed Specifications:

Frequency: 149.95 MHz  
416.6 MHz  
902.2 MHz

### Inputs:

1. Source Input  
Frequency: 79.95, 346.6 and 381.1 MHz  
Power level: 0 dBm  
Input impedance: 50 ohms, VSWR <1.5

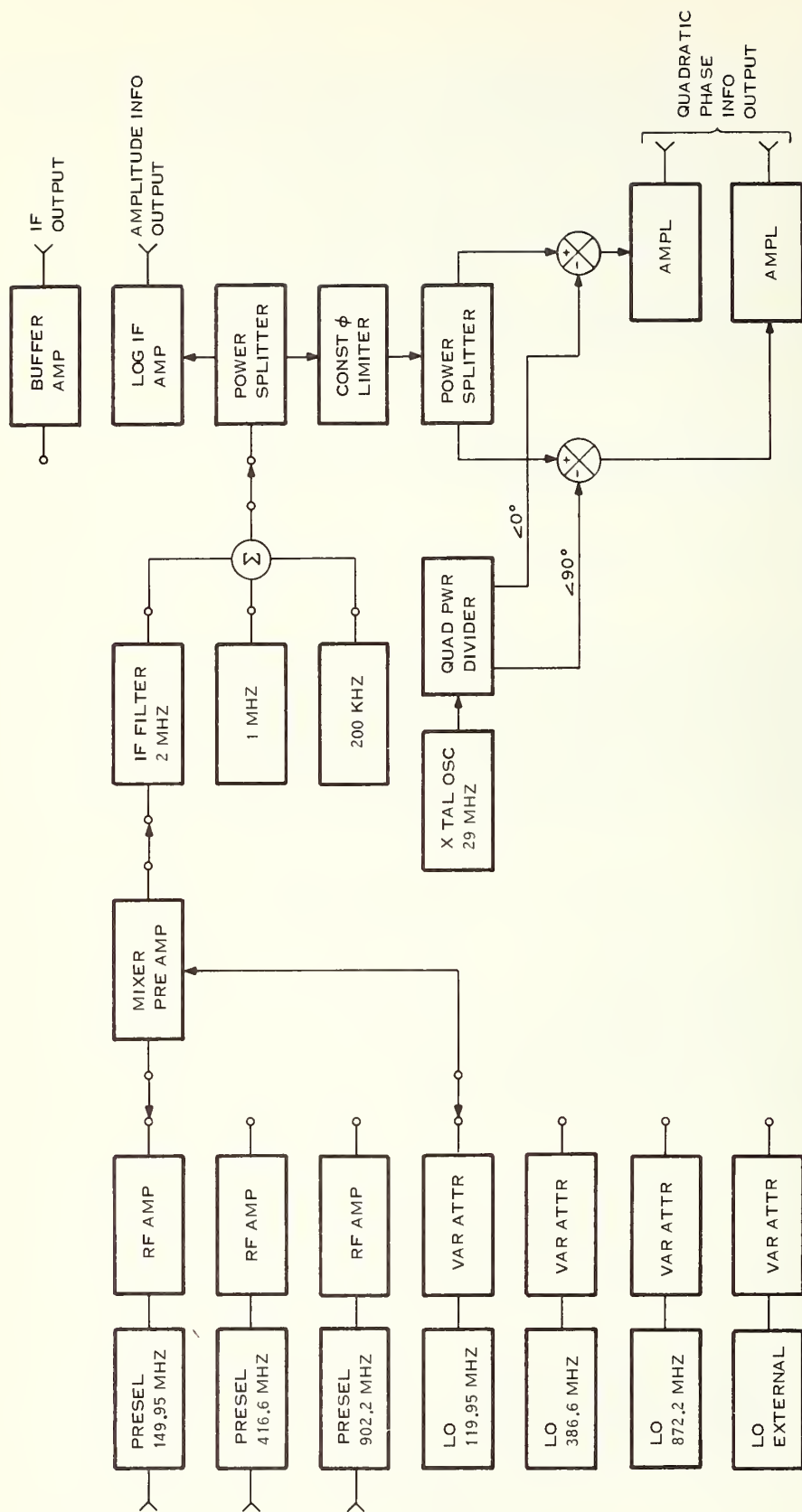


Figure 5. Block Diagram of the Receiver

## 2. L.O. Input

Frequency: 70 MHz  
Power level: -7 dBm  
Input impedance: 50 ohms  
VSWR <1.5

## Wideband Mixers

Operating frequency range: 140-460 MHz  
Output level: 16 dBm (min)

## Outputs:

### 1. 149.95 MHz

Bandwidth (3 dB): 5 MHz  
Power: 20 W (CW)

### 2. 416.6 MHz

Bandwidth (3 dB): 5 MHz  
Power: 20 W (CW)

### 3. 902.2 MHz

Bandwidth (3 dB): 10 MHz  
Power: 20 W (CW)

Linearity:  $\pm 1.5$  dB for all amplifiers

The block diagram is shown in Figure 6.

## MAGNETIC TAPE RECORDER I

This magnetic tape recorder has the purpose of recording all the information on man-made noise. The information to be recorded is the phase, the compressed baseband amplitude and the rms level for further processing. It should have the tape speeds: 120 ips (max) to 1-7/8 ips (min). The main specifications for the tape recorder are as follows:

Number of channels: 7

Flutter (peak-to-peak): 0.15% at 120 ips

Dynamic interchannel time-displacement error: 0.2  $\mu$ s at  
120 ips

Capstan speed accuracy:  $\pm 0.01$  percent

Instantaneous time base error: less than  $\pm 500$  ns at 120 ips

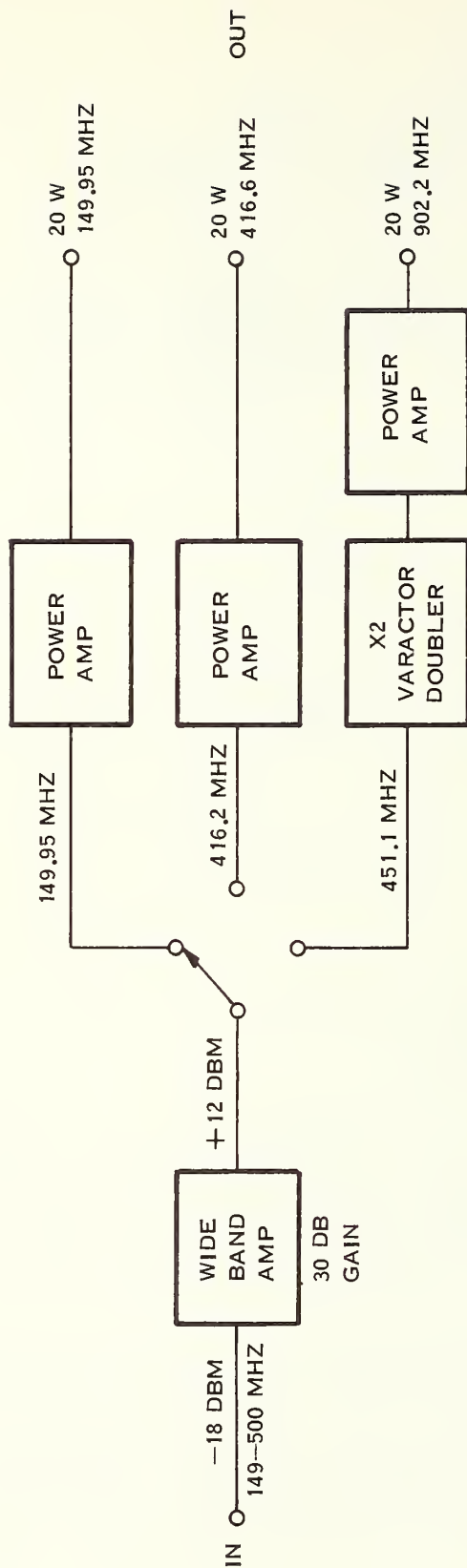


Figure 6. Block Diagram of the Receiver

#### Direct record/reproduce channel

Input sensitivity: 0.2 to 10 Vrms  
Input impedance: 75 ohms  
Output impedance: 75 ohms  
S/N ratio: 30 dB at 120 ips  
Bandwidth: 400 Hz to 1.6 MHz at 120 ips

#### Frequency modulation record/reproduce channel

Input sensitivity: 0.5 to 12.5 V peak  
Input impedance: 20,000 ohms  
Output impedance: 75 ohms  
S/N ratio: 50 dB at 120 ips  
Bandwidth: dc to 80 kHz at 120 ips

### MAGNETIC TAPE RECORDER II

The function of this magnetic tape recorder is to record the outputs of a 10 tap-delay line. Both in-phase and quadrature components of the tap outputs will be recorded. The tape recorder should have the tape speeds: 60 ips (max) to 1-7/8 ips (min).

The main specifications for the tape recorder are the following:

No. of channels: 14  
Capstan speed accuracy:  $\pm 0.05\%$  maximum  
Flutter (peak-to-peak): 0.7% at  $7\frac{1}{2}$  ips  
Bandwidth: DC to 1250 Hz at  $7\frac{1}{2}$  ips  
S/N ratio: 46 dB at  $7\frac{1}{2}$  ips  
Input level: 1 Vrms  
Input impedance: 75 ohms  
Output impedance: 1000 ohms  
Dynamic range: 35 dB

### DATA PROCESSOR

The function of the data processor is to analyze test data resulting from the man-made noise measurements, both real time while the van is in mobile operation, and in more detail following the taking of test data. The data processor consists of the following major components:

1. Interface between the magnetic tape recorder or receiver video output and a mini-digital computer.
2. A mini-digital computer which has the following main subsystems:
  - a. Central processor
  - b. Four 4K 16-bit read/write memories

- c. High speed paper tape reader (300 cps) and punch (50 cps)
- d. Analog to digital convertor

### 3. Graphic display system

Character plotting rate: 5000 characters/sec  
Point plotting rates: 100K pt/sec

Appendix A gives a detailed description of the data processing procedure.

In addition to the above major measuring instruments, a mobile van was furnished and modified. The van will be used as a mobile laboratory which will house the measuring equipment such as receiver, tape recorders, data processor, etc. The measurements will be made with two operators in the van. The locations and states (stationary and moving) of the van will be discussed in the following section.

## DESIGNS OF EXPERIMENTS

### NOISE MEASUREMENT

The characterization of the man-made noise present in the urban environment, and therefore the design of an appropriate experiment to derive such characterization, appears to be, at first, a rather hopeless task because of the multivarious variability of that noise with a number of variables such as time, space, hour of the day, traffic conditions, etc. In addition, the difficulty of the task is compounded by the fact that some of those variations, for example spatial variations, are seldom smooth owing to occasional sharp discontinuities in the distribution of noise sources and to the presence of standing wave noise patterns. Fortunately, however, a very large number of similar experiments have already been performed by other investigators and we can benefit from their findings and try to improve our knowledge of the urban noise in the iterative fashion that is typical of statistical experimentation.

The first important subdivision of the characterization problem comes from recognizing that there are basically three types of terminals in mobile communication:

1. stationary vehicles
2. moving vehicles
3. base stations.

We will thus break the design of our experiment into three categories corresponding to the three types of terminals.

For stationary vehicles we can start with a concept put forward in the FCC study, that of "activity zone". The FCC Report divides the total urban and suburban environment into areas characterized essentially by their level of man-made noise. General categories defined in the study were: clear areas, residences, businesses, industrial sites, transportation areas, institutional sites, automotive activities. For the purpose of locating most of these zones in a large city like the Greater Boston area, use can be made of an Urban Atlas recently published. This atlas contains detailed information on the characteristics of 20 large U.S. cities including Boston. Population density is, for example, given with a resolution grid of 250 m X 250 m and the different grids of each city are divided in five categories (50-200, 200-500, 500-1200, 1200-3600, 3600 and more people/grid). In the same document the following subdivisions are also identified for a large city: Airport, Institutional, Large Institutional, Park, Industrial, Commercial.

Examination of the FCC measurements and some additional thought suggests the following locations where measurements should be made with a stationary vehicle.

1. Clear areas
2. Residential - separation between homes 500 ft.
3. Residential - separation less than 30 ft. but detached
4. Residential - row houses
5. Apartment buildings - 2 stories
6. Apartment buildings - 6 stories and higher
7. Office buildings - 8 stories and more
8. Industrial plant
9. High power lines (220 kV)
10. Low power lines (33 kV)
11. Power plant
12. Hospitals
13. Main thoroughfare
14. Busy intersection
15. Large institution
16. Airport

It is expected that these "activity zones" will be sufficiently different in the amount and type of man-made noise present, to justify this subdivision. The experiment will, of course, confirm or modify this assumption. However, even if the noise characteristics were found to be very similar for two or more categories, the equivalence of different types of sites (say a power line and a congested traffic situation) will certainly constitute important information. It is also expected that for each site there will be at least one "control variable" to take into consideration: for example, the hour of the day in a residential area, the traffic at a busy intersection (smooth traffic versus a traffic jam), weather conditions for a power line, etc.

Economy of experimentation suggests the consideration of only two levels for this variable. It seems also advisable to replicate the same experiment at least twice for each type of site in order to gain some insight into the validity of the assumption of similarity. It must also be mentioned that, owing to the fact that automotive noise, whenever present, is an important source of noise, it will be probably impossible, or at least very difficult, to measure the noise characteristics of some of the sites mentioned without including automotive noise. This, however, must be considered a fact of life (office buildings are generally located in areas of high traffic) and it is therefore appropriate and relevant to measure the total noise present at those sites.

The total number of measurements required will in general be

$$N = C \times K \times M$$

where

C = number of activity areas identified

K = number of levels of the control variable

M = number of replicates for the same activity area

From the above considerations it seems that a minimum of 64 measurements is necessary for stationary vehicles. The number of sites is practically coincident with the number of measurements since, in general, changing the level of the control variable will prevent using a site for more than one measurement.

The time to be spent on each measurement depends on several factors. In general, it will be the sum of two terms: time necessary for preparatory and concluding procedures (calibration, validation of measurements, etc.) and the measurement time itself. The former will be dictated by practical considerations, the latter is related to the assumed stationarity of the environment and to the accuracy with which we estimate probability density functions and cumulative density functions. Here we must distinguish between on-line processing and off-line processing. It seems that as far as on-line processing is concerned, what one can determine is the cumulative distribution on a point-by-point basis, assuming stationarity of the underlying distribution. One gets, in essence, an estimate of  $p_\ell$ , i.e., the probability that a certain variable, say amplitude, exceeds the level  $\ell$ . The estimate is clearly given by  $x_\ell/n$  where  $x_\ell$  is the number of samples which exceed the level and  $n$  is the total number of samples. The random variable  $p_\ell$ , for each level, can be thought as the population parameter in a binomial distribution. The binomial distribution can be approximated by a Gaussian distribution when  $n$  becomes large. Since the mean of the population  $x_\ell/n$  is  $p_\ell$  and its variance is  $p_\ell q_\ell/n$  where  $q_\ell = 1 - p_\ell$  the

standard form of the variable  $x_\ell/n$  is

$$Z_\ell = \frac{(x_\ell/n) - p_\ell}{\sqrt{p_\ell q_\ell/n}}$$

A confidence interval for the estimate of  $p_\ell$  can easily be constructed. The  $1-\alpha$  confidence interval for  $Z_\ell$  is

$$-Z_{\alpha/2} < \frac{(x_\ell/n) - p_\ell}{\sqrt{p_\ell q_\ell/n}} < Z_{\alpha/2}$$

The  $1-\alpha$  confidence interval for  $p$  can be obtained by solving the previous inequality for  $p_\ell$ . Since, however, we do not know the standard deviation which is a function of  $p_\ell$  we must also estimate it from the data. The most logical estimate is

$$\text{Est } \sqrt{\frac{p_\ell q_\ell}{n}} = \sqrt{\frac{(x_\ell/n)[1 - (x_\ell/n)]}{n}}$$

and therefore the confidence interval for  $p_\ell$  is

$$\frac{x}{n} - Z_{\alpha/2} \sqrt{\frac{(x_\ell/n)[1 - (x_\ell/n)]}{n}} < p_\ell < \frac{x}{n} + Z_{\alpha/2} \sqrt{\frac{(x_\ell/n)[1 - (x_\ell/n)]}{n}}$$

The number  $n$ , from the sampling theorem, is given by the expression

$$n = 2WT$$

where  $W$  is the bandwidth of the receiver and  $T$  the duration of the measurement for that particular level. Thus, if one assumes stationarity, a clear tradeoff exists between the accuracy required (note that the accuracy is a function of  $p_\ell$ ) and the number of levels that one is willing to consider. If one does not want to assume stationarity, but an estimate is required of the validity of this assumption, the total time must be also subdivided in intervals corresponding to possible time constants

of stationarity. To get a feeling for the order of magnitude involved assume a total measurement time (per frequency) of 100 sec. Assume that we want to test stationarity in 10 intervals of 10 sec. each and that we quantify the pdf in 10 levels. The time available for each level is therefore 1 sec. Assume a bandwidth of 1 MHz. Then  $n = 2 \times 10^6$ . Assume also that we are testing a level of low probability, say  $x/n = 10^{-5}$ . The rms error in estimating  $p_\ell$  is

$$\frac{p_\ell q_\ell}{n} \approx \sqrt{\frac{10^{-5}}{10^6}} = 3.16 \cdot 10^{-6}$$

and the relative error becomes

$$3.16 \times \frac{10^{-6}}{10^{-5}} = 3.16 \times 10^{-1} .$$

Note that if the hypothesis of stationarity is sustained, one can obviously "pool" the estimates of variance and reduce it further.

Similar results hold for off-line processing where one determines a pdf simultaneously for a chosen number, say  $k$ , of quantization intervals. One has then, in essence, a multinomial distribution with  $k$  classes, where  $f_1, f_2, \dots, f_k$  are the experimental frequencies and  $p_1, p_2, \dots, p_k$  the true values of the probabilities. A simple application of a theorem due to Fischer shows that for large  $n$  (i.e.,  $n \gg 1, n \gg f_i$ )

$$\frac{\text{Var } (f_i n)}{(f_i n)^2} \sim \frac{1}{f_i} \quad \text{for each } i .$$

The characterization of the urban noise for a terminal on a moving vehicle should, in principle, require the duplication of the measurements taken at a stationary site. It seems, however, that the main difference between a moving vehicle and a stationary one arises when the moving vehicle is immersed in traffic. This point of view was implicitly taken in the FCC measurements where the only measurements from moving vehicles were made while riding in downtown traffic and on a busy suburban thoroughfare. These measurements should be duplicated, perhaps adding a few additional ones in other "activity zones" to compare the results with those obtained from a stationary vehicle.

Measurements of urban noise from base stations differ from the ones from stationary vehicles, essentially because of the height of the receiving antenna. Furthermore, most base stations are presently located either downtown or in busy suburban districts. It is suggested that the top of the TSC building be used for a set of such measurements. Two or three additional measurements with antennas located at various heights will probably suffice for the characterization of the base station noise. Remarks similar to the ones made for the accuracy achievable apply here also.

## **SPECTRUM OCCUPANCY**

The functions of the spectrum occupancy measurement are the following:

1. To determine the average rate of occupancy in the land mobile broadcasting bands 150-160 MHz and 450-470 MHz.
2. To develop techniques for determining the interference from a large distance, say a city 50 miles away.
3. To determine the center frequency and i-f bandwidth to be used for noise measurement, hence avoiding the confusion of two distinctive types of interference, i.e., narrowband - cw and wideband impulsive.

## Site Selection

For the implementation of the first two measurement functions, the initial choice of the roof of TSC management building seems to be an appropriate one. It is one of the highest buildings in a radius of two miles.

The area covered by transmission from the management building may include the Greater Boston Area, i.e. within Route 128. This seems to be a good start initially and any further expansion of the terminals will be decided by the results of initial measurements taken from the roof of TSC management building.

For the implementation of the last measurement function the sites selected are similar to the sites selected for noise measurements. The measurements will be taken from the mobile van. Because of the proximity of the antenna to the ground and to the urban environment, streets, buildings, expressway etc., it is not expected that the characteristics of the spectrum occupancy at the two frequency bands, 150-165 and 450-470 MHz, will be the same at these sites. Accordingly, the total number of the sites is the same as the number of activity areas defined in the noise measurements.

## Monitoring

In establishing the measurement procedure a HP spectrum analyzer (HP-855B/851B) and a recording system described in Appendix A will be used to monitor the spectrum at the site.

Three frequency bands will be monitored: 135-165, 400-480 and 850-950 MHz. The total spectrum is to be monitored at the site in 21 bands of 10 MHz each. Each band will be recorded only for a 5-minute run, with a complete cycle through all twenty-one bands requiring slightly less than two hours. This pattern will be repeated four times each day. In addition to daytime monitoring, nighttime monitoring may be needed if the results of initial daytime monitoring so indicate. The duration of nighttime monitoring will be decided upon after analysis of the initial data.

## **CHANNEL MEASUREMENT**

This section describes the planning of the urban channel measurements in the Greater Boston Area. The site selection of the transmitting terminals, the characteristic regions of urban and suburban environments, and the average time for individual measurements are discussed.

### Transmitting Terminals

Presently three different types of terminals are planned. These three terminals are: a) the top of a highrise building in urban area; b) the top of a low rise building in urban area; and c) a high tower in a suburban area. For the above three terminals we have selected the following:

1. The roof of the TSC management building because it is one of the highest buildings in the area.
2. The roof top of TSC Technology building, because it is a typical low rise building in the area.
3. The transmitting tower of New England Telephone Co. in Prospect Hill, Waltham, a suburb of Boston.

These terminals with the exception of 2, we believe, would represent typical terminals for all land mobile base stations. With the use of a low terminal (type 2), we hope to determine the effect of transmit antenna height in urban communications.

### Zoning Areas

In the urban and suburban environments one can characterize zones according to structures of the following types:

1. High rise buildings: In this area all the high rise buildings are congested together. An example of that is the downtown Boston area near Government Center.
2. High rise buildings scattered among low rise buildings: In this area a few high rise buildings are situated among the low rise buildings. Typical examples are the Back Bay area of Boston and the area near TSC in Cambridge.
3. Low rise buildings: In this area there is no high rise building over ten-stories. Brookline, the western part of Cambridge, and Somerville are a few typical areas in the Greater Boston area.
4. Individual houses located on a plain: This is a typical suburban area where all the houses are located on individual lots. Most of the suburbs of Boston fit in this category.
5. Houses located among the hills: This is another type of the suburbs. There are a number of places within the Greater Boston area which fit this description, for example, Belmont Hill.

### Measurement

Initially, five to ten runs in each zone for each terminal are planned at all three frequencies, 149.95, 416.6 and 902.2 MHz. Each run will take about 10 to 15 minutes. The basis for measuring time is the requirement that each measurement should cover a distance of three to five miles, on the assumption that the van is moving between 10 and 30 miles per hour.

### **MILESTONES FOR FY'72**

During FY'71 we were involved in getting to know the problems specific to urban communication systems, command and control of urban vehicles, and voice and digital communication in these channels. We found that there are three major interference sources which degrade a communication channel:

- a. Man-made noise
- b. Co-channel interference
- c. Multipath due to reflections off buildings and terrain.

With a view to characterizing the above three interference sources, a measurement program was initiated in FY'71. During FY'71 we have reviewed the past work on measurement and characterization of the electromagnetic interference, have planned and

designed a versatile measurement scheme for both man-made noise and multipath interference, and have initiated procurement of all the necessary equipment to establish a mobile laboratory. This laboratory includes a data processor and channel analyzer to be used for characterizing the interference, and for evaluating present and future communication systems.

For FY'72 the emphasis will be placed on actual measurements, analysis and simulation. The following table (Table 1) shows the time schedule of various tasks.

## **INSTALLATION AND CHECKOUT OF THE MOBILE VAN**

The mobile van was delivered at the end of FY'71. During the first two and a half months of FY'72, the following tasks are planned:

- a. Installation of antennas
- b. Layout of connecting cables between the equipment
- c. Arrangement equipment and console such that one operator can conduct the noise measurement.

Checkout of the mobile van includes the following:

- a. Performance of the van
- b. Performance of the cooling and heating systems
- c. Performance of the 5 kW power generator
- d. EM noise generated by the van and its accessories and find the proper way to suppress them if necessary.

## **CHANNEL OCCUPANCY MEASUREMENTS**

While the van is being checked out, the channel measurements can be conducted concurrently. The test instrument required is a spectrum analyzer which is presently available at the center. The channel occupancy measurements serve three functions as mentioned in the section Spectrum Occupancy. These measurements should be made before conducting the measurements on man-made noise. We plan to make these measurements from mid-July to the end of September. The total period is about two and a half months.

## **CALIBRATION AND TEST INSTRUMENTS**

The major experiment components are expected during the first few months of FY'72. Test and calibration of these components are required before field measurements are taken. Furthermore, TSC personnel may need to be trained to operate the instruments. A proper procedure of data taking will be planned.

Table 1. Time Schedule for Various Tasks

	J	A	S	O	N	D	J	F	M	A	M	J
INSTALLATION AND CHECKING OF THE VAN	△	△	△									
CHANNEL OCCUPANCY MEASUREMENT	△	△	△									
CALIBRATION AND TESTING INSTRUMENT AND DATA PROCESSOR	△	△	△	△	△							
NOISE MEASUREMENT				△	△				△			
CHANNEL MEASUREMENT				△	△				△			
DATA ANALYSIS		△	△									△
MODELING					△							△
SIMULATOR	△											△

## NOISE MEASUREMENTS

Initial noise measurements are expected to start sometime in October 1971. The time required to collect necessary and sufficient data for reasonable statistical modeling and simulating is estimated at approximately three to four months. Therefore, we expect the measurements will be completed by the end of March 1972. Note that the channel measurement will be conducted concurrently, though the channel measurements and noise measurements are not being made simultaneously. The estimated total time has taken into consideration winter weather conditions in the Boston area.

## CHANNEL MEASUREMENTS

The time schedule for channel characterization measurements is the same as that for the noise measurement.

## DATA ANALYSIS AND MODELING

Data analysis will begin as soon as the first measurements are made. The data analysis will interact with actual data collection as to the location, time, format of the data, etc. The initial data analysis will emphasize first order statistics such as pulse amplitude distribution, pulse duration distribution, pulse separation distribution and rms values. Further analysis will involve second order statistics such as correlation with traffic flow, zoning variations, time of the day, type of the station terminals and others. The period of the data analysis will carry to the end of FY'72.

The major effort of modeling will begin after the preliminary analysis has been completed. Because we have reviewed most of the modeling work which has been done in the past, it is our belief that any further work on modeling will be meaningless until a certain amount of data has been collected and analyzed using the new measuring equipment which is substantially different than any used before in studying the urban channel. The major differences include wideband techniques, large dynamic range, and different frequency ranges.

## SIMULATOR

The contractor, Signatron, Inc., has the chief responsibility for designing and building a channel analyzer for the fading dispersive channel with provision for including the additive noise. The delivery date of the simulator is approximately the end of 1971 (calendar year). During the interim, TSC personnel will keep close contact with Signatron, Inc. personnel to insure that contract requirements are met according to schedule. During

the ensuing six months, TSC personnel will be trained to test and operate the simulator. The tape recorded data for both channel and noise will be used for evaluation of existing equipment on an equal basis and for the design and evaluation of new signaling methods and new command and control equipment.

## **APPENDIX A**

### **INTRODUCTION**

This paper describes the noise measurement I/O Controller for the PDP-11.

Data in the sections Timing and Measurement Accuracy should be sufficient to determine the validity of the measurements and to plan algorithms for data evaluation and analysis. Programming provides information for writing programs which use the controller. The section Controller Operation describes the controller hardware and operation.

In the future this document will be expanded to include logic diagrams, maintain information, and sample programs.

This is a preliminary description and instruction manual for the noise measurement I/O controller. All specifications and parameters are preliminary and subject to change during device construction.

### **DESCRIPTION OF I/O CONTROLLER AND MEASUREMENT PROCESS**

The I/O controller is a direct memory access interface to the PDP-11. It is connected to the PDP-11 Unibus. The device has been designed to measure the significant parameters of an impulse noise random process and transfer them into the PDP-11 memory.

Three noise process parameters are measured for each noise impulse; elapsed time since last pulse, duration of pulse, and amplitude of pulse. These parameters are measured, and then transferred directly to the PDP-11 memory without any program interrupt. The program is interrupted only when a buffer is filled with three word records, one record from each noise impulse. Certain error conditions can also cause an interrupt; these will be described later.

### **TIMING**

The ability of the device to generate a representation of a noise process is strongly dependent on its timing characteristics. These are in turn dependent on the computer core memory organization and Unibus timing. Complete understanding of the

remainder of this section requires an understanding of the PDP-11 Unibus and possible memory organizations; for this information see the PDP-11 manuals. A flow chart of the I/O controller timing and control sequence is shown in Figure 7. It should be noted that timing is relatively complex and will typically be dependent on previous measured data. The A to D conversion time  $t_{AD}$  will be 11  $\mu$ s (approximately) in initial operation of the controller with the DEC AD01 analog to digital converter. This will be the limiting factor for controller operation. The A to D converter can be replaced by an 8 bit 1  $\mu$ s converter at a reasonable cost in which case memory write time (see Figure 8) will become the principal speed limitation. In the initial controller configuration a time of 16  $\mu$ s to process each impulse would be a good estimate. This time can be reduced to 4  $\mu$ s.

## MEASUREMENT ACCURACY

The peak amplitude measurement error comes from two sources: A to D converter error and peak value sampler errors. The peak value is sampled by waiting a preset time interval after the crossing of a threshold. This is based on the assumption that the noise pulse has a much broader bandwidth than the measurement system and that the rise time of the sampler input is proportional only to measurement system bandwidth. If measurement data fails to confirm this approximation a more complex peak detector can easily be installed. A to D converter accuracy is 10 bits which is far in excess of that required for this experiment. The sample-and-hold module supplied with the AH01 does not have sufficient bandwidth to allow the .01% accuracy of the A to D converter to be achieved. This error source will have to be examined during device calibration.

The time measurements are made by counting the pulses generated by a clock in the I/O controller. The counter cannot measure durations of less than 200 ns but this will not be a detectable limitation on system performance. The clock pulse rate can be up to 25 MHz but it will initially be set to 4 MHz (250 ns resolution). The counter will round off measured times to the next lowest integer time count. All time intervals of less than 200 ns will be indicated as 200 ns; counter error will be plus or minus one half count plus clock accuracy for times up to 4096 counts. For times above 4096 counts (initially 1024  $\mu$ s) accuracy is plus or minus .05% plus clock error.

The time measurements require a large dynamic range. To suppress overflow problems an unsigned floating point number representation was selected. This results in a word format as shown in Figure 9. The largest count before overflow is  $2^{15} * (2^{12} - 1) = 134\ 184\ 960$ . This will initially correspond to 33.5 seconds. The floating point representation will require no arithmetic

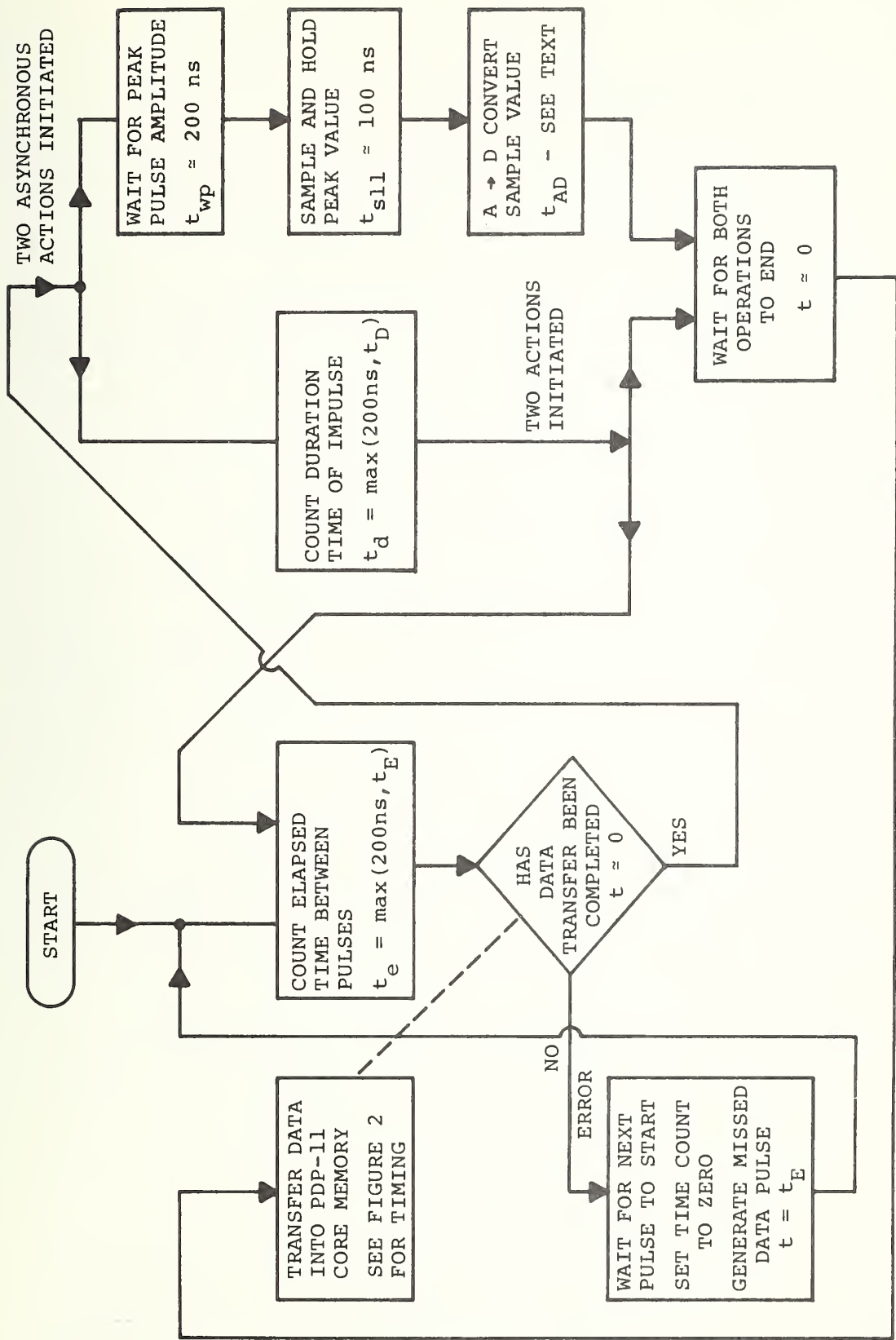


Figure 7. Measurement Action Sequence and Timing Data

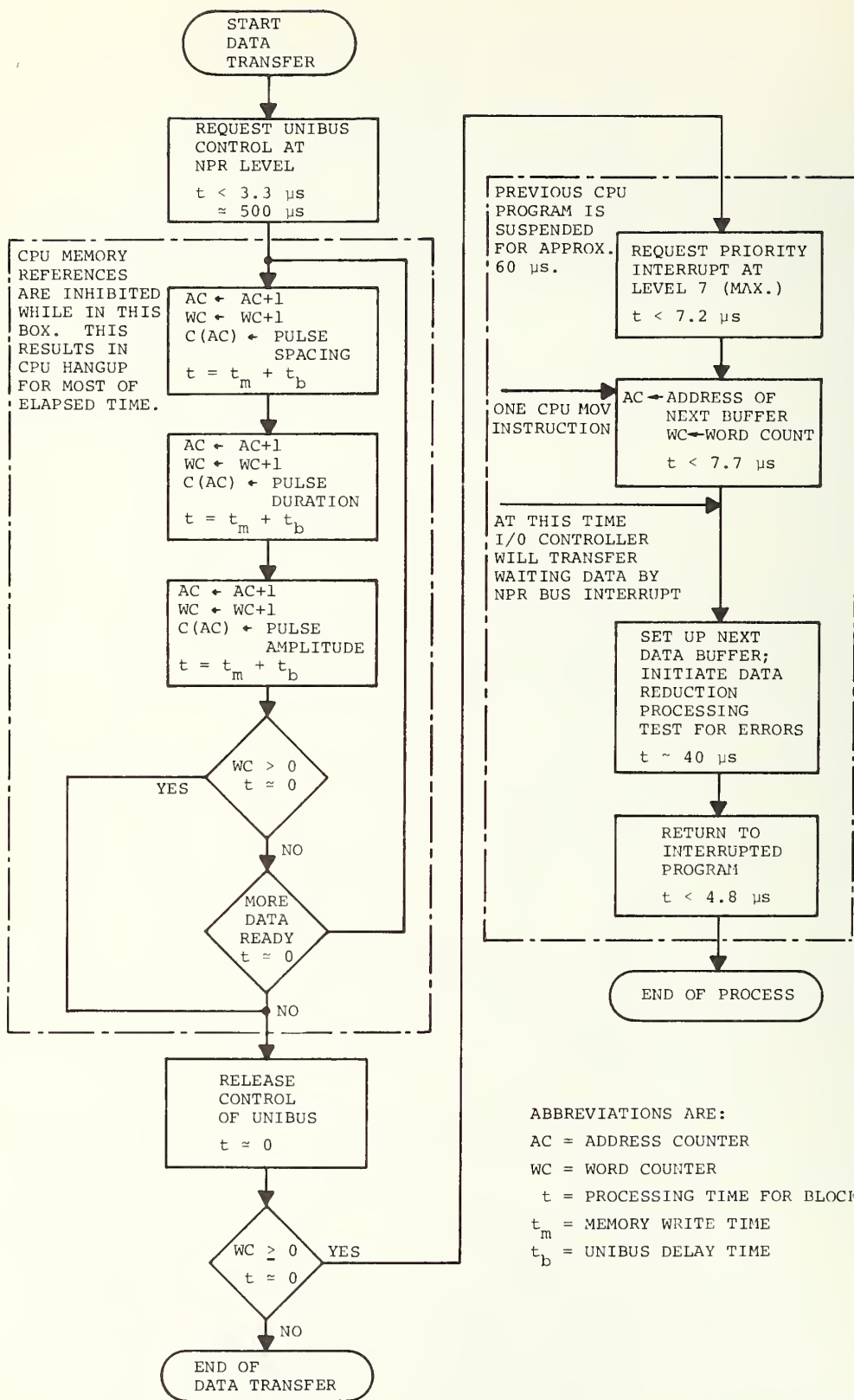


Figure 8. Data Transfer Operations for Timing Estimation

BIT	15	14	13	12	11	10	9	8	7	6	5	4	3	2	1	0
	DATA WORD FROM COUNTER															
	EXPONENT UNSIGNED				<div><div>FRACTION</div><div><div>0 IF &lt; 2048</div><div>1 IF ≥ 2048</div></div><div><div>FRACTION IS UNNORMALIZED IF &lt; 2048 NORMALIZED IF ≥ 2048</div></div></div>											
0 ≤ EXP ≤ 15					0 ≤ FRACTION ≤ 4095											

$$\text{NUMBER} = \text{FRACTION} * 2^{\text{EXPONENT}}$$

BIT	15	14	13	12	11	10	9	8	7	6	5	4	3	2	1	0
DATA WORD FROM A TO D CONVERTER																
0	MOST SIGNIFICANT DIGITS				LEAST SIGNIFICANT DIGITS				INSIGNI- FICANT DIGITS			0	1	1	1	1

Figure 9. Data Word Formats

operations for conversion to integer format when the count is less than 4096. This will be the situation most of the time.

## GROWTH POTENTIAL

Provision has been made to transfer an extra data word in the I/O controller if an additional parameter must be measured. This will require significant controller modifications. The time counters cannot easily be modified, but by changing the clock frequency a large range of resolutions and accuracies can be provided. The A to D converter can be easily changed or replaced by another measurement device. The pulse detector and peak detector circuits can be easily modified.

Two dc logic levels which can be set by the program are available for setting modes or gains.

A pulse is generated each time input noise impulses occur too closely spaced in time for the controller to measure one of them. These pulses can be counted by an external counter or the controller can be modified to interrupt the CPU when this condition occurs.

## PHYSICAL DESCRIPTION

The I/O controller is mounted on one DEC 5¼ inch high circuit card rack. Its power supply occupies 3½ inches of rack space. The controller should be mounted next to the AD-1-D Analog to Digital Converter in the computer rack. Total power consumption is less than 70 watts. No power is drawn from the computer.

## PROGRAMMING

The controller contains three registers which are addressable by the program. They are: Address Count (AC), Word Count (WC), and status (S). These registers are described below.

Word Count - Location 767774, write only

This register contains the buffer size in words. It need only be loaded when the controller is initialized or buffer size is changed.

Address Count - Location 767772, read/write

This register contains the address to which the next data word will be transferred. At the end of a buffer the address will be one beyond the last word of the buffer. If an error interrupt has occurred this value tells how many good words of data

have been transferred. Loading this register always causes the device status to be set to "run enabled," and resets Word Count to its initial value (the buffer size).

#### Status - Location 767770

The bits of the status register are:

Int Enb;

Bit 6,  
Read/Write,  
Initial state 0,  
Function: enables end of buffer and error interrupts

Run;

Bit 7,  
Read only,  
Set by loading AC,  
Reset on any error or end of buffer,  
Function: enables data transfer  
Initial state 0

Time Out;

Bit 15,  
Read only,  
Set by hardware or address range error,  
Reset by loading AC,  
Initial state 0.

In addition to these three bits other bits are described in the maintenance section. Status is set to its initial condition by the PDP-11 power-on sequence or by the RESET instruction (resets all devices).

In addition to these registers the Analog to Digital Converter status register must be set to 000030. The status register is location 776070. This location is reset to 000000 by power on or RESET. The word 000030 sets the converter gain to 2.5 v full scale.

#### Interrupt Vectors

At the end of a buffer the interrupt vector is location 000170. If any error occurs the interrupt vector will be 000174. If both error and end of buffer occur simultaneously the vector is 000174. If an error occurs the value of ac should be saved and then ac set to a new buffer. The old AC value can then be used immediately to recover all good data.

## CONTROLLER OPERATION

### Overview

The Unibus is described in the PDP-11 Handbook. A functional block diagram of the controller is shown in Figure 10. The measurement and data transfer parts of the controller are asynchronous and essentially independent of each other. The individual blocks in Figure 10 are described below.

### Measurement Control Logic

The measurement control logic consists of a precision Schmitt trigger circuit which acts as the pulse detector followed by timing and sequencing circuits to control the measurement. A block diagram of this circuit is shown in Figure 11.

### Measurement Devices

Performance of the floating point counter was described in the chapter Technical Discussion. The counter can count at a 25 MHz maximum rate but it takes approximately 200 ns for the count to propagate to the end of the count chain. When the count period ends, a one shot times out the 200 ns propagation delay. The counter contents are then transferred into one of two buffer registers (pulse duration or pulse spacing) and the counter is reset to the value that corresponds to the elapsed transfer time (200 ns approximately). The counter is always counting except when a data transfer occurs. A counter block diagram is shown in Figure 12.

The Analog to Digital converter is a standard DEC AD01-D; it is triggered through its external input (EXT IN A).

### Address Counter

The address counter and logic contains three registers; one for current address, one for current word count, and one for buffer size. When the controller is to be operated, the buffer size register (WC) must be loaded first. When the current address counter is loaded from the Unibus, the current word - counter is loaded from the buffer size register. Each single word data transfer results in the address count being incremented by two and the word count being decremented by two. End of buffer is signaled when the word count reaches zero.

This structure was selected to allow buffers to be swapped with one CPU instruction. Any buffer size or buffer location can be used; additional instructions are necessary only if errors occur or if buffer size must be changed. The Address Counter is described in Figure 13.

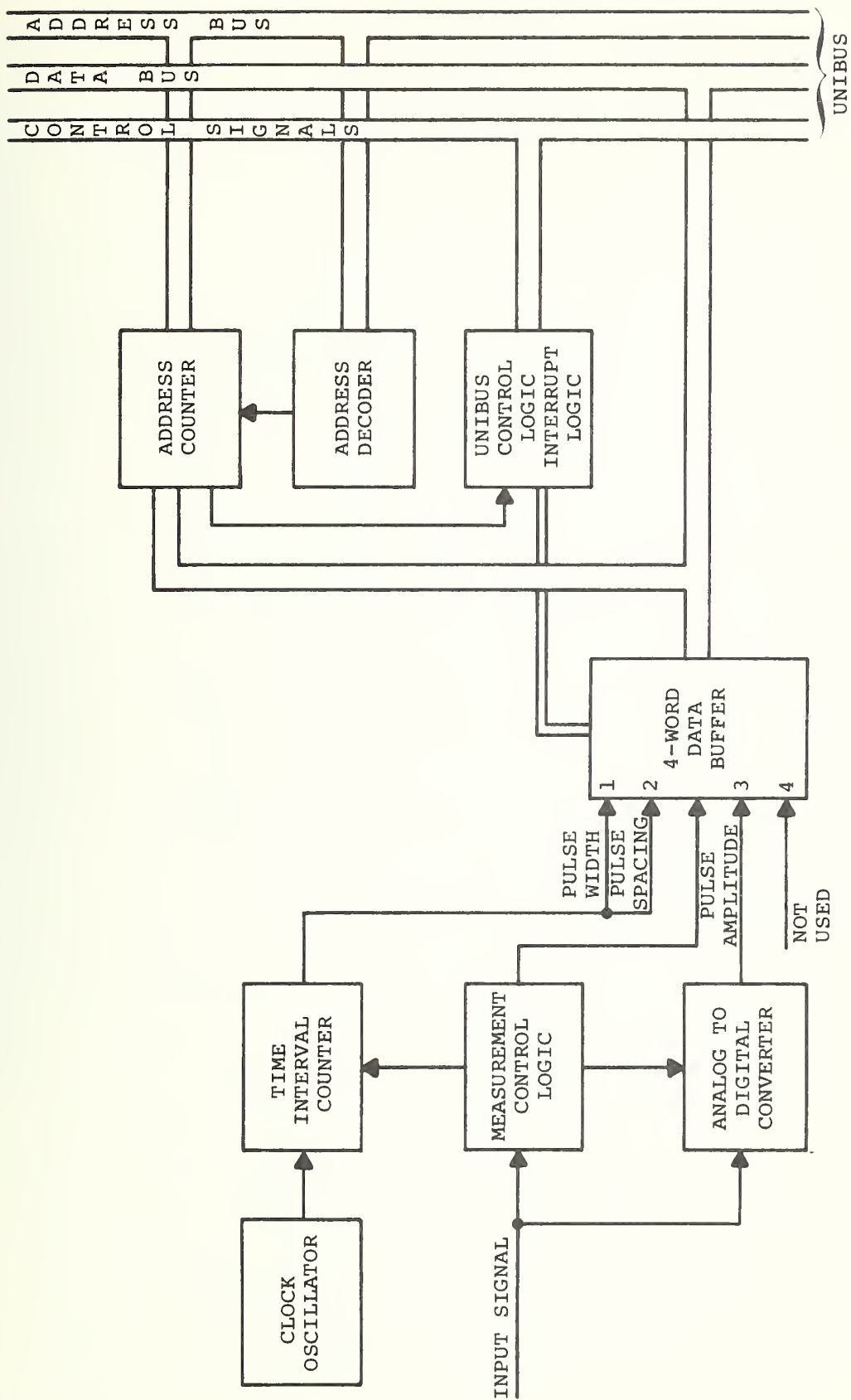


Figure 10. Functional Block Diagram of I/O Controller and Measurement Hardware

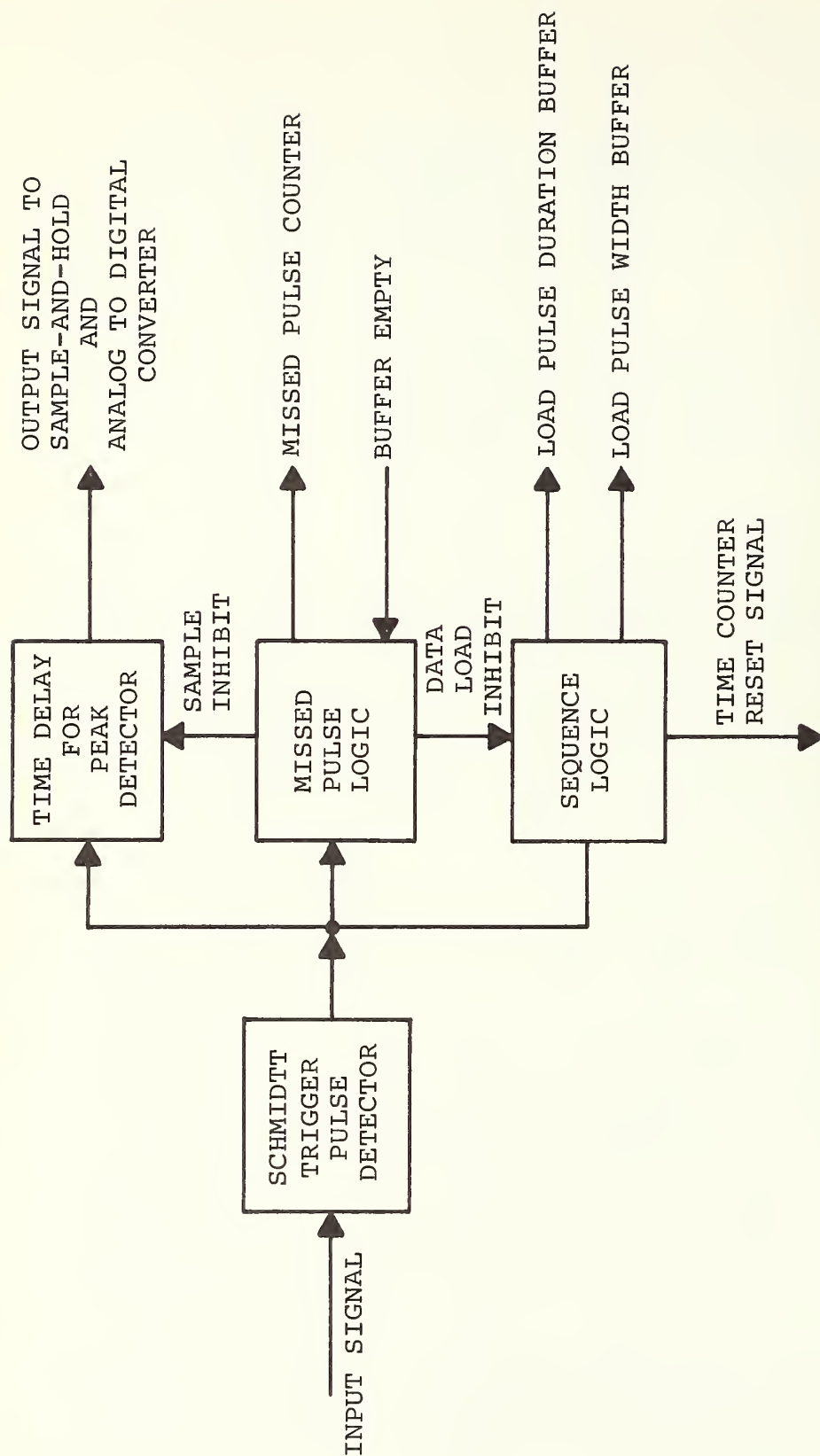


Figure 11. Measurement Control Logic Block Diagram



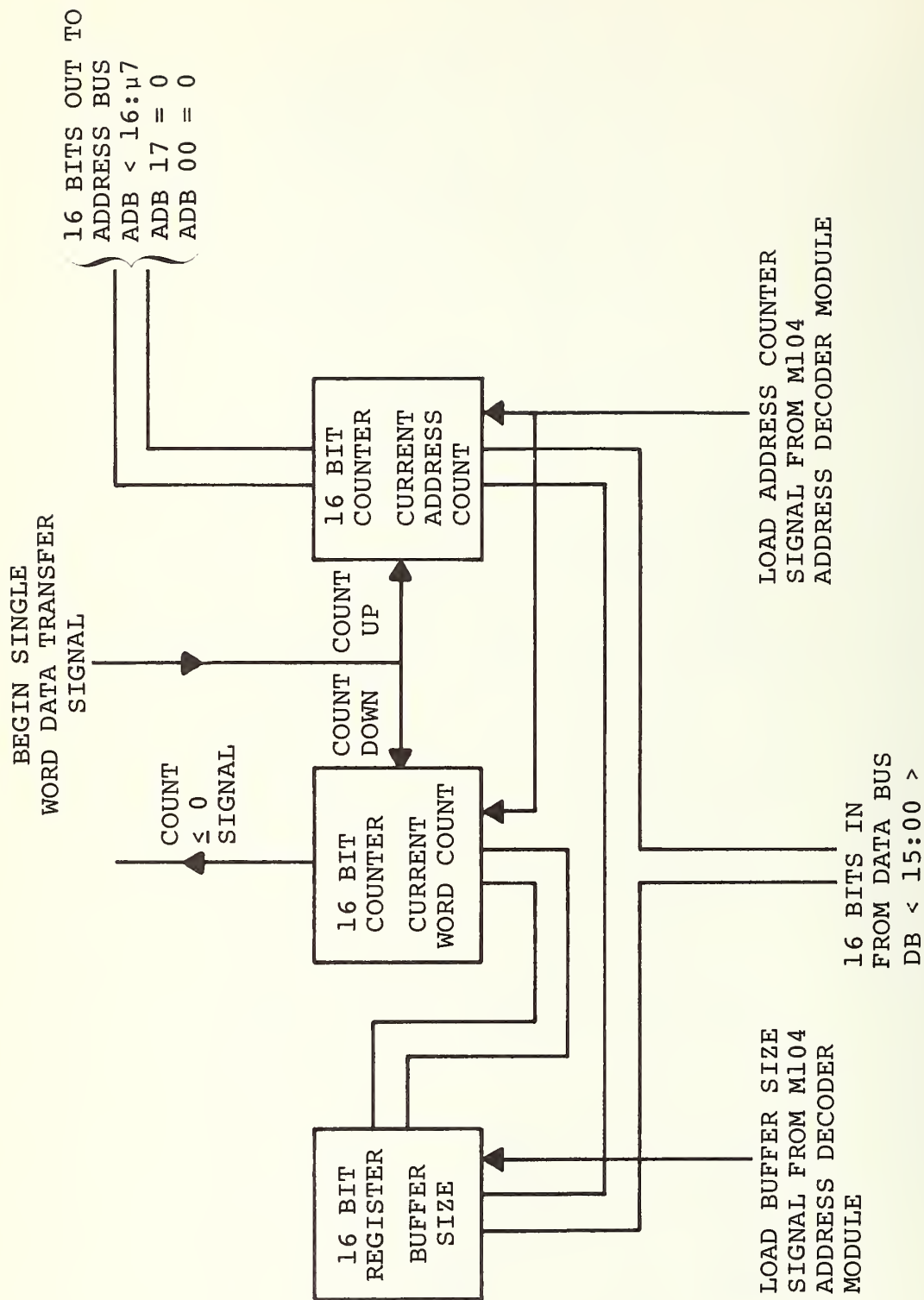


Figure 13. Address Counter

## Data Transfer Control Logic

The data transfer control logic is relatively standard. It is built around the DEC M782 Interrupt Control Module and the DEC M104 Address Decoder Module. The circuit is described in detail in the maintenance section.

# REPRINT OF IN-HOUSE PUBLICATIONS

URBAN EM NOISE MEASUREMENT, Jan 25, 1971, P. Yoh and R. Esposito

## INTRODUCTION

During the past several decades many measurements of man-made electromagnetic noise have been made at HF, VHF and UHF for different environments such as urban, suburban and rural areas. However, because of the instrumentation used and of the limited scope of most of the measurements, the results are often of limited use and sometimes misleading for the communication engineer. Basically, a communication system planner would like to know the detailed characteristics of the background noise in order to evaluate its effects on system performance. This information includes also the time and space variations of the noise as well as, for prediction purposes, the correlation with factors such as population density, vehicular traffic, power consumption and topographical characteristics. The requirements are more stringent for digital communication systems which, for example, demand a more thorough specification of the statistical characteristics of the noise. By and large this information is not currently available especially for wideband systems, i.e., for systems whose bandwidth exceeds 10 KHz. Therefore, the purpose of the experiment under consideration is to measure broadband, wide dynamic range, impulsive-type noise in selected regions of the VHF and UHF band. The bandwidth of the measuring system has been tentatively selected to be 1 MHz. The predominant noise is expected to be generated by man-made machines such as automobile engines, industrial equipment, etc.

The reasons for this experimental program are the following:

1. To study experimental techniques for the measurement of wideband man-made noise in the VHF-UHF region and establish a capability for the routine performance of such measurements.
2. To identify the major sources of radiation that will interfere with the performance of any transportation system being planned in the frequency region mentioned above.
3. To determine the information needed for the design and evaluation of any communication or command and control system of mass transit or land, air, water and highway communication. The combination with the measurements of the impulse response of the medium this information

will provide a complete characterization of the urban and suburban channel.

4. To determine the radiation characteristics of the existing and proposed transportation systems such as electric cars, trolley cars, guided way, electric trains, etc. Figure 1 indicates the major tasks and problem areas and the logical flow of data of the measurement program.

## NOISE MEASUREMENTS

One of the first tasks is, of course, the determination of the statistical quantities describing the noise which can be derived by suitable processing of the experimental data. Although a certain amount of data processing can be done in real time the decision has been made to record the IF waveform for later processing and for use in the simulation equipment. This means that most of the processing procedures can be decided upon at a later date. Some initial considerations on what has to be measured is, however, in order. A simple model of the wideband man-made interference is the sum of an impulsive component and of a Gaussian process. Both components can be expected to be nonstationary. It seems necessary to measure at least the following quantities:

1. Average power over each measurement interval
2. Percentage of power in the impulsive component and Gaussian component
3. Amplitude pdf of the peaks
4. Duration pdf of the impulses at given amplitude levels
5. Pulse spacing pdf
6. Crossing rate pdf.

In addition to the above quantities some simpler parameters such as average and rms values after detection can be measured in real time. It is worth pointing out that instrumentation similar to the one being studied for the noise measurements can be used in the future for the investigation of channel occupancy. By this we mean the evaluation of the probability that a given frequency region be occupied at a certain level, by other transmitters. Because of the limited spectral region available for land mobile communication it is also important to determine the minimum allowed spatial separation of stations transmitting in the same frequency region in order to avoid appreciable co-channel

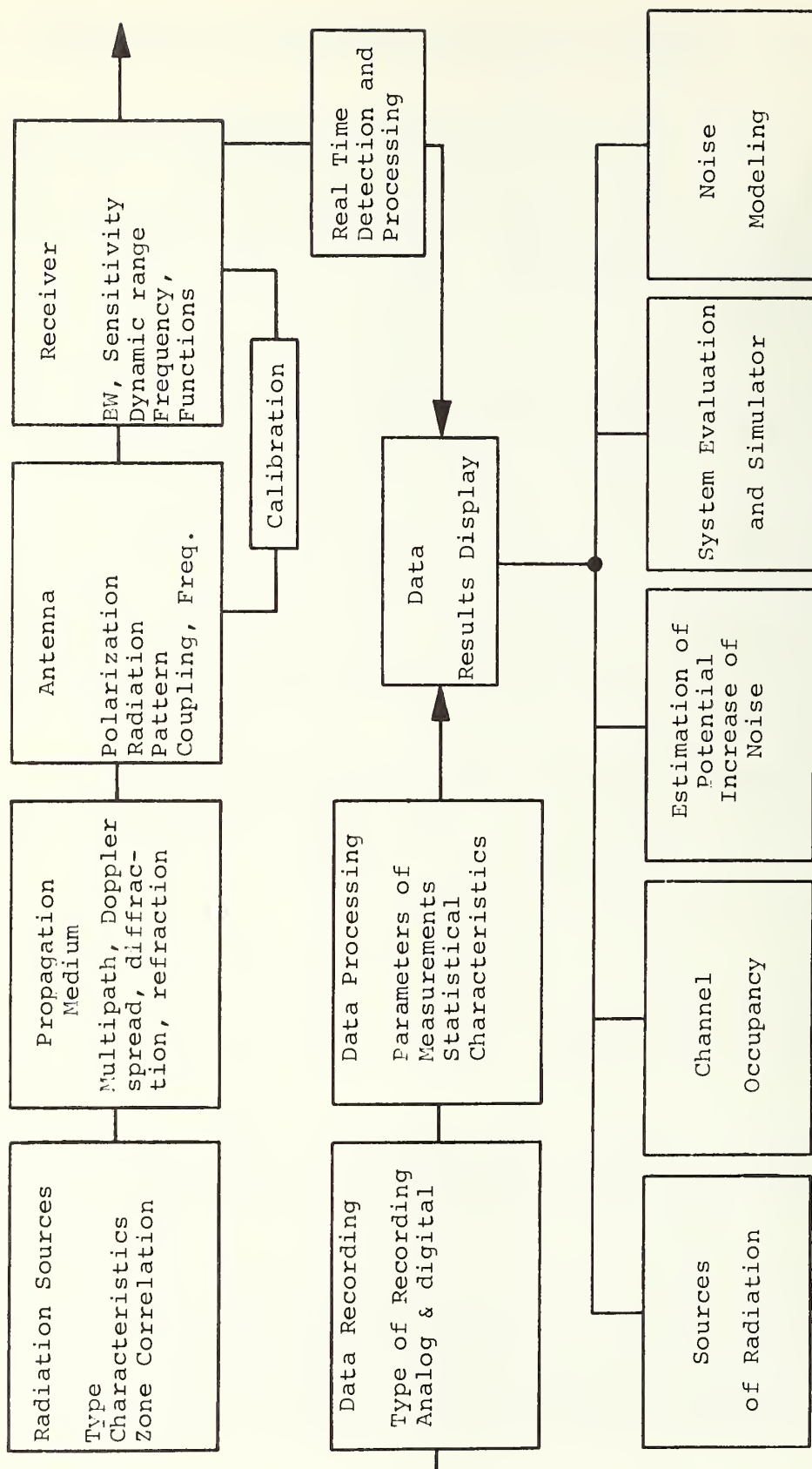


Figure 1.

interference. This type of measurements can also be performed by the system under consideration.

A simple block diagram of the noise measuring system is shown in Figure 2.

The following is a preliminary discussion of the specifications for the various blocks of the system and of the possible tradeoffs.

### Frequencies of Operation

The measurements will be taken in the neighborhood of 150, 450 and 900 MHz. Inquiries have been made to the FAA to determine whether a 1 MHz slot free from intelligible interference is available in the greater Boston area in the frequency regions mentioned.

### Antenna

In deciding on the type of antenna to be used a number of questions should be considered such as polarization, antenna pattern, gain, frequency response characteristics and mutual coupling if there are other antennas close by. All of the above factors depend on the type of measurements. It seems that for the spatial distribution expected from urban noise under different conditions the omnidirectional short dipole will be a good candidate. A directional antenna would, instead, be necessary if one wants to establish the location of the noise sources. Also antennas with different polarization are needed if polarization effects must be studied. Note that some of the measurements available indicate little difference between horizontal and vertical polarization. A number of closely spaced antennas would be needed if one wants to map the spatial distribution of the noise sources. Thus, the initial specifications for the antennas are:

Frequency:	150, 450 and 900 MHz within $\pm 10\%$
Polarization:	vertical over ground plane
Antenna Pattern:	Omnidirectional in azimuth and $\cos \theta$ in elevation, where $\theta$ is evaluation angle
Type:	Short dipole
Gain:	3 dB

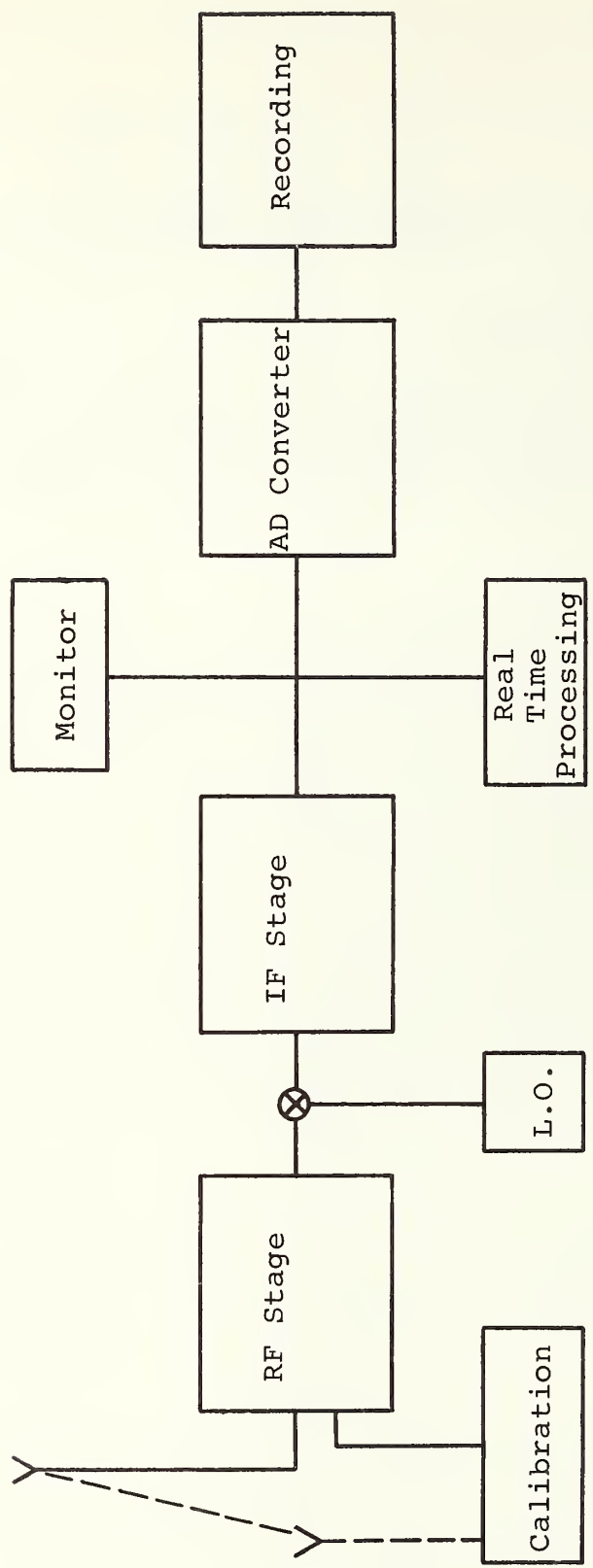


Figure 2.

Considerations for future extensions of the experiment are:

1. Simultaneous measurements of different polarizations
2. Simultaneous measurements of all three frequency bands
3. Array measurements at the same frequency, including the study of mutual coupling effects
4. Change of antenna pattern

#### RECEIVER - RF, Mixer, L.O. and IF State

The two essential quantities in the overall design of the receiver are sensitivity and dynamic range. These quantities are related since a high sensitivity requires a large dynamic range if the external noise has large variations. The system sensitivity is defined as the level at which external noise power equals the receiver noise power. The external noise has both natural and man-made origin. The natural noise is galactic, atmospheric and solar. However, in the frequency range of interest this noise is almost negligible with the exception of periods of high solar activity. The total contribution of these sources can be 3 dB above the receiver thermal noise level. Thus, if low level man-made noise is at 150 MHz and negligible above this frequency of interest, the sensitivity of the receiver should be as good as possible. Since the thermal noise level corresponding to thermal noise for a reference temperature of 288 K and 1 MHz bandwidth is 144 dBW (or -114 dBM) the receiver must be able to detect any signal above a level of about -140 dBW. For an input resistance of 50 ohms this implies a detectable noise level of 0.7  $\mu$ V. The minimum detectable noise field can be easily determined by using the capture area of the antenna.

$$A \approx \frac{1.6}{4\pi} \lambda^2$$

where  $\lambda$  is the wavelength.

The previous considerations suggest that the noise figure of the RF stage should be rather low, of the order of 3 or 4 dB if possible. It seems also desirable to make the bandwidth of the RF stage the same as the IF bandwidth in order to prevent overloading of the mixer. The RF stage should also have some gain (10 dB seems a good ballpark number) in order to prevent overall sensitivity degradation caused by mixer and local oscillator noise. The overall sensitivity of the receiver should be 1  $\mu$ V/m or better.

The next question is the determination of the dynamic range required. This is perhaps the most difficult parameter to determine since it involves an estimate of the unknown amplitude distribution of the man-made noise. Note that the dynamic range can always be expressed in percentiles of the amplitude distribution. For example, ITS measurements of amplitude probability density of man-made noise made in San Antonio, Texas at 50 MHz with a bandwidth of 10 KHz indicate a dynamic range of 86 dB between the  $10^{-6}$  and 0.99 probability levels. It is often stated that the dynamic range varies roughly as  $10 \log_{10}$  (bandwidth) and therefore, the dynamic range for 1 MHz should be 106 dB (with the further assumption that the dynamic range is independent of the frequency of operation). However, a closer look at the argument which yields the  $10 \log_{10}$  relation shows that it is not valid when the bandwidth is very large if the number of incoming impulses is not exceedingly large. In fact, one can argue that a wideband receiver can resolve the individual pulses and only very rarely will the impulses have enough overlap to cause a significant increase in the required dynamic range. Since each car radiates a few hundred impulses/sec and only very close by cars contribute to the upper part of the dynamic range the argument seems reasonable. Then, what is important for the determination of the dynamic range is the maximum peak value of impulses received from a car located very close to the receiving equipment. Some measurements made in England with a 2.5 MHz receiver indicate a maximum received field of 56 mV/m at 150 MHz when the radiating car is 30 feet away from the receiver. The maximum received field is about 5 dB higher at 450 MHz. This value, converted to a 1 MHz bandwidth, yields a value of about 80 dB of dynamic range based on an overall system noise figure of 7 dB at 150 MHz and a slightly lower value at 450 MHz. Since we are interested in events of as low a probability as  $10^{-6}$ , the effective dynamic range must be increased to take into account the possibility of overlapping of impulses coming from different cars. This increase can be estimated to be of the order of 10 dB. Therefore, the overall dynamic range seems to be of the order of 90 dB.

It is our intention to perform some simple measurements with instrumentation available in the laboratory to ascertain whether our estimate of the dynamic range required is correct.

### Recording and Data Processing

As mentioned before part of the processing will be done in real time and part by computer. This tradeoff is very important because, owing to the large dynamic range and bandwidth used in the experiment, some severe requirements are imposed on the recording and data processing system. To show this, assume a dynamic range of 90 dB and a 1 MHz bandwidth. In order to use

digital processing the data must be sampled at a rate of 2 MHz, while 10 bits are required for 10% accuracy (1 bit is the sign). Thus the measuring system generates data at a rate of 20 Mbit/sec. Assume now that each processing operation takes 30 computer cycles and that the computer cycle is 1  $\mu$ sec. Assume also that the tape is played back into the computer at a speed 4 times lower than the recording speed. For 100 sec of data the required processing time for each operation is thus

$$20 \cdot 10^6 \cdot 30 \cdot 10^{-6} \times 100 \times 4 = 2.4 \cdot 10^5 \text{ sec} = 66 \text{ hrs},$$

a large number indeed. One would still require over 16 hours if the tape were to be played back at the recording speed. Since most of the measurements we want to make, at least initially, probability density functions, the use of high speed threshold counters, operating over selected time intervals and energy levels must be considered for real time processing.

A simple example of the possible real time processor is shown below in Figure 3.

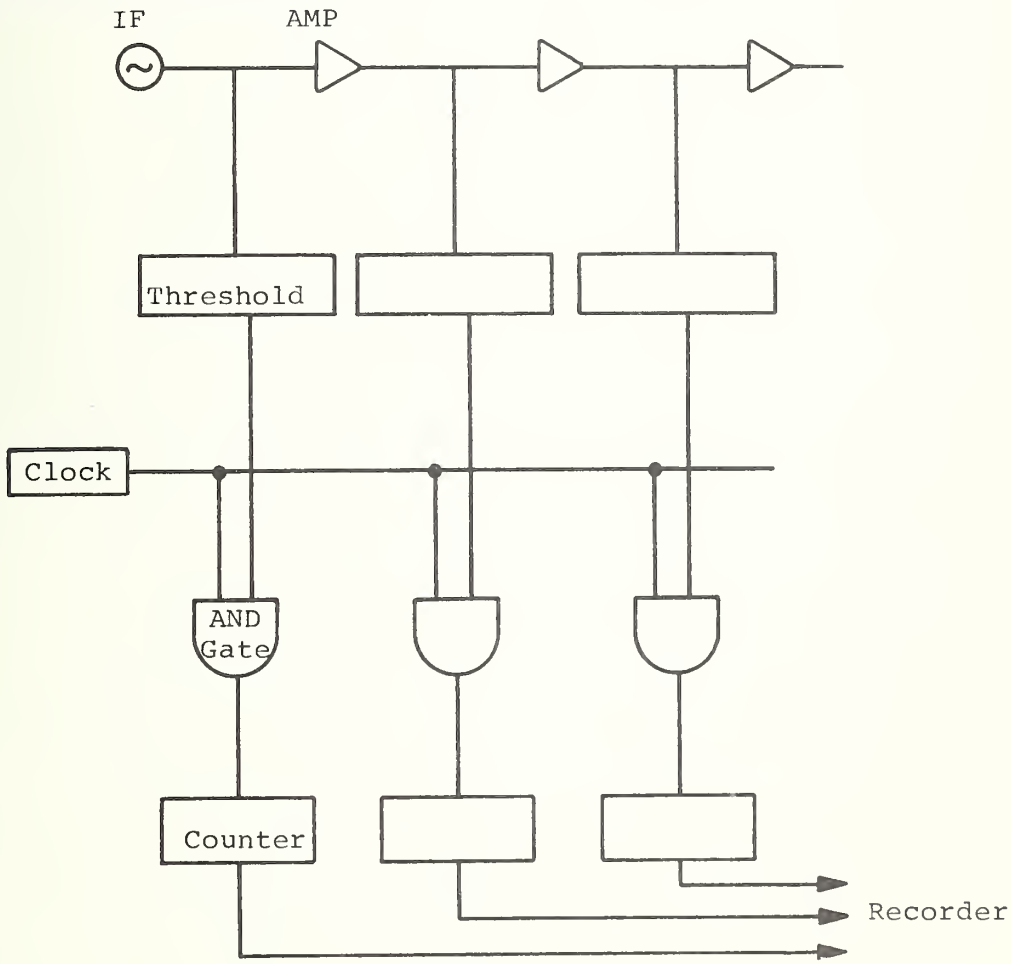


Figure 3.

## Calibration

This system shall have the necessary equipment to accurately and conveniently calibrate all channels for both noise and channel measurement, so hence the external noise or signal relative to the terminal of an equivalent lossless antenna system is measured in absolute units to accuracies of  $\pm 3$  dB. The receiver, detectors, and A-D converter output shall be calibrated to measure to accuracies of  $\pm 1$  dB.

The absolute calibration on the channel measurement is needed so that the simulation study can be conducted successfully.

## Operation

The equipment must be grouped together in a console so that it may be monitored by a single seated operator who can conveniently listen to the noise channel and make note on discrete signals when they occur. The operator must be able to observe the system outputs to ascertain the system is functioning properly. In case of malfunction or others the operator should try to adjust, eliminate or note.

## Procedure of Measurement

It is tentatively planned that, initially, a single frequency measurement will be made in the greater Boston area. Because of the large variety of the zones: commercial, industrial, residential, transportation terminals, high rise buildings, etc., it presents a great opportunity to measure the noise characteristics of a city. However, a single measurement can be made at any given time. Hence, it is strongly suggested to have a detailed plan on when and where the measurements shall be made. The following criteria may be useful for the planning:

1. Vehicle volume
2. Population density
3. Geometrical distribution of high rise building
4. Geographical and topological features of the city
5. Zoning characteristics

Measurement and Analysis of Urban Radio Channels for  
Communication System Design

By L. A. Frasco and H. D. Goldfein

The authors are at the U.S. Dept. of Transportation, Transportation Systems Center, Cambridge, Massachusetts

Abstract.- A program to measure VHF and UHF urban radio channels for playback and analysis in the laboratory is described. The measured data will be used to develop analytic models for channel behavior. A 50 KHz bandwidth tapped delay line real-time channel simulator is being built. Both the simulator and the models will be used for the design and evaluation of systems for communication and vehicular monitoring in the urban environment.

Presented at 1971 International Telemetry Conference, Washington, D.C. Proc. International Telemetering Conf. Vol. VII pp. 166-171, International Foundation for Telemetering, Woodland Hill, California, Reprinted by permission of the Instrument Society of America, publisher of the proceedings.

# Measurement and Analysis of Urban Radio Channels for Communication System Design

By L. A. Frasco and H. D. Goldfein

The authors are at the U.S. Dept. of Transportation, Transportation Systems Center, Cambridge, Massachusetts

## SUMMARY

This paper outlines a program to measure VHF and UHF urban radio channels for playback and analysis in the laboratory. These measurements are required for the design of high data rate communication equipment which makes efficient use of the radio spectrum. We include in this category data communication and surveillance equipment necessary to meet the demands of the variety of command and control functions envisioned for transportation systems by federal, state, and local governments. Included in the paper is a qualitative description of the channel followed by a discussion of the measurement techniques and hardware that will be used. The goal of the measurement program is to develop both analytic and experimental tools for the design and evaluation of advanced communication techniques specialized for signalling over the urban radio channel. These techniques will include modulation waveform design, coding, and the design of receiver structures including those which adapt to measured channel behavior. Future technology will permit complex hardware designs to be used in the implementation of these techniques while maintaining low system cost. The same techniques and approach used here for the urban channel can be applied to other radio channels that occur in transportation systems. In particular, they are applicable to data links for air-ground and high speed ground transportation system uses.

## Introduction

Requirements for communication in an urban environment have become much more stringent in recent years. Where traditionally voice channels have been sufficient to satisfy user needs, new requirements have emerged for data communication and surveillance to support proposals for command and control for transportation systems made by federal, state and local governments. For example, automatic vehicle monitoring and digital data links have been proposed for both public and private vehicles such as buses, taxis, private automobiles, and special services including police and fire (this latter category may also require some form of secure communication). Implicit in these system requirements are demands for increased communication capacity -- high data rates and efficient utilization of the rapidly disappearing available radio spectrum. In order to provide both the reliable and efficient communication needed, one must understand in detail

the urban communication environment. The measurement of the properties of this radio channel is, therefore, not academic. It is integral to the design *and* evaluation of communication equipment matched to the job in both performance and cost. The urban radio channel environment will be qualitatively described and a program will be outlined which will systematically measure and playback the channel for communication system design.

## PROGRAM DESCRIPTION

There are two basic technological problem areas in urban radio communication. The available spectral space is severely limited and will not grow appreciably in the future. At the same time both the number of users and the type and variety of services required are growing with time. The radio propagation medium in urban areas is characterized by severe multipath distortion and impulsive noise which makes the design of high performance non-voice communication systems difficult.

Short-term solutions for increasing radio traffic handling capacity are to open new frequency bands, use narrower bandwidth channels, and to promote good operating procedures for minimizing radio channel usage by individual users. These techniques will not provide the several orders of magnitude increase in traffic handling capacity that will be needed over longer time periods. The only efficient solution to this problem appears to be the use of semi or fully automatic digital data transmission with prespecified message formats and relatively complex polling or scheduling procedures for control of channel usage. The efficient transmission of digital data on urban radio channels is difficult because such channels exhibit complex multipath propagation, typically without any direct path between transmitter and receiver. This means that for reliable digital data transmission, signaling waveforms and modem structures must be carefully designed to match specific channel behavior. Some sort of coding will almost certainly be required. A detailed understanding of urban multipath propagation is also required for design or evaluation of surveillance systems which locate vehicles by measurement of radio propagation time. In addition to the multipath problem, radio noise in cities is especially complex and highly structured. Receivers designed for white gaussian noise will not perform efficiently. By taking advantage of the urban noise structure, performance will be improved.

There are a variety of techniques for designing communication systems which adapt to the time varying behavior of the urban radio channel. These range from adaptive equalizing channel measuring communication systems to systems which allocate channel usage time to individual users according to their measured performance.

In an adaptive equalizing system, the transfer function of the channel over the frequency range of interest must be measured and an inverse filter generated at either end of the link. Adaptive equalizing systems have the ability to allow high data rate transmission on badly dispersive channels. They are not a total cure for time dispersive channel problems in that they clearly can not increase the signal energy transferred over a fading channel. This in effect limits their usefulness to relatively broad bandwidth systems in which the signalling waveforms have sufficient range (or equivalently time) resolution to allow some of the multipath scattering structure of the channel to become measurable. Adaptive equalizing systems can only be designed if a broad bandwidth characterization of the multipath channel is available for the required analysis. The construction of such a system is made much easier by the ability to simulate the channel in the laboratory. There are a variety of adaptive equalizing concepts using different schemes for channel multipath measurement, and different schemes for apportioning hardware between transmitter and receiver. Several different techniques will be evaluated.

Other procedures for allowing a vehicular communication network to adapt to propagation conditions involve dynamic channel scheduling algorithms which attempt to take account of the spatially non-homogeneous nature of the urban radio channel. Also, error-detecting or correcting codes with two-way data links can allow a system to adapt to the error performance of individual network participants. There are a large variety of such systems which should be evaluated to determine their potential for providing reliable and economical communication. The performance of this type of system depends on the time variation of channel behavior. Such systems can be expected to provide good performance if reasonably large numbers of users are present. A broad bandwidth channel characterization is required for evaluation or design of any candidate system of this type.

Error-detecting or correcting codes can be considered for several purposes on the radio channels of interest here. A few of the most promising uses are: control of errors due to noise (a classical application), control of errors due to multiple users interfering with each other, providing redundant information for channel measurement while transmitting data, and facilitating the simple generation of waveforms with good properties for transmission over the multipath channel (e.g., spectral shaping). The channel characterization experiments will provide the required tools for evaluation of coding techniques for these purposes.

Security from both interception and jamming is also desired for a variety of civil communication systems (e.g., police).

It is much easier to provide secure coding for digital communications than it is for voice communications.

In order to design and evaluate digital communication systems a detailed understanding of the urban noise and propagation environment is required. At present a two-fold program for channel characterization and measurement is planned. An attempt will be made to generate analytic models for channel characterization which will be useful for system design. In addition, a real-time hardware simulator is being developed which will be used to play back the channel using the recorded measurement data permitting the design and evaluation of proposed modems in the laboratory (see Figure 1). The next phase in the program will be to evaluate a variety of modulation waveforms, coding techniques, and receiver structures including systems which adapt to measured channel behavior. The channel data to be measured will be selected to provide a realistic test of modem performance.

#### URBAN RADIO CHANNEL DESCRIPTION

The urban environment is composed of a variety of noise sources (e.g., ignition systems of motor vehicles, electrical machinery, high voltage power transformers, etc.). In addition, the physical character of urban areas with their dense construction present a variety of paths for transmitted radio signals -- often with the absence of a direct path from transmitter to receiver. These two situations and their interaction qualitatively describe the urban radio channel. The description of the channel can therefore be divided into two parts: 1) additive noise composed of high-level impulsive man-made noise and lower-level background noise; 2) multipath, a multiplicative noise due to the presence of multiple signalling paths and causing time-and-frequency dispersion of transmitted signals.

#### MULTIPATH CHANNEL MEASUREMENT

A characterization of the urban radio multipath channel is being developed which is experimentally exact for use in the design of systems with bandwidths up to 50 KHz and which, with appropriate care, will be useable out to 150 KHz. This should be adequate for the design and evaluation of systems developed for the present nominal bandwidth allocations and also allow sufficiently broad-band channel characterization to study some channel multiplexing strategies. The final choice of channel characterization bandwidth was based, of course, on the need to provide reasonable system design flexibility at a moderate cost. The equipment for measurement and hardware simulation of the urban multipath channel is being designed and built for DOT/TSC by Signatron, Inc..

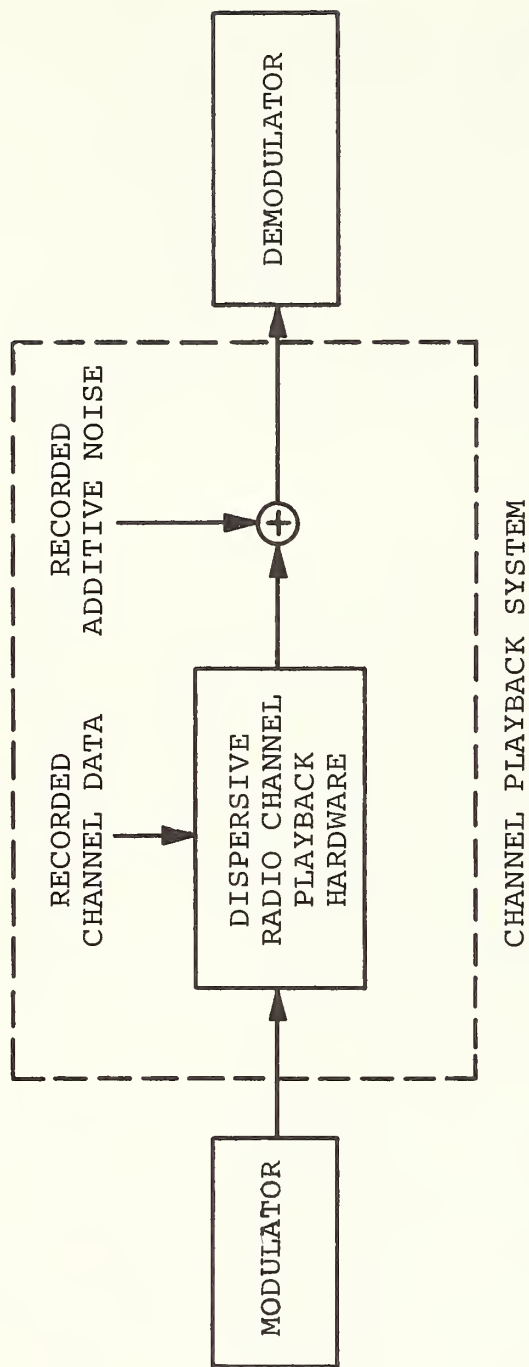


Figure 1. Communication System Simulator

The multipath measurement technique being used is a "pulse-probing" technique which determines the band-limited impulse response of the multipath channel. Previous measurements have indicated that the time duration of the channel impulse response determined by the multipath delay spread between the shortest and the longest propagation paths in the urban environment is on the order of 40  $\mu$ sec. A probing signal with an impulse-like time auto-correlation function is transmitted over the urban radio channel and the channel output is measured by correlation techniques, sampled, and recorded. A conceptual picture of this process is shown in Figure 2a.

To simulate the multipath channel, a filter with the recorded channel impulse response is generated by using a tapped delay line. The effects of the multipath channel on an arbitrary signalling waveform can be duplicated in the laboratory by applying this same signal to the input of this tapped delay line channel model and varying its tap gains according to the prerecorded channel data. This process is shown in Figure 2b. The mathematical theory of dispersive channel characterization has been extensively studied and is described in References 1, 2, and 3. Also, a survey of the variety of measurement techniques for these channels can be found in Reference 4.

The actual channel measurement transmitter hardware uses a 511 bit pseudo-random sequence of phase-modulated 5  $\mu$ sec long raised cosine pulses as its sharp auto-correlation function probing signal. The channel measurement receiver uses a bank of 10 pulse compression filters to continuously sample the estimated channel impulse response. These samples are then recorded for use as the 10 channel delay line model tap gains. Each tap gain is a low pass complex random process with its bandwidth proportional to the rate of change of the multipath environment, or, equivalently, to the doppler spread of the urban radio channel. Measurement data taken by others has indicated that doppler spreads of under a hundred cycles will be experienced in moving ground vehicles.

## NOISE MEASUREMENTS

Urban radio channels typically exhibit high-level impulsive man-made noise as well as low-level background noise. The noise environment will be recorded over a wide bandwidth (up to 1 MHz) and with extremely large dynamic range (85 dB). While only a relatively narrow band, lower dynamic range characterization of the additive noise (approximately 100 KHz) is needed for the channel simulator, the more detailed noise structure is necessary for analysis and modelling efforts. To support these latter efforts, a PDP-11 mini-computer along with a hardware interface which is presently being built will be used for real-time control

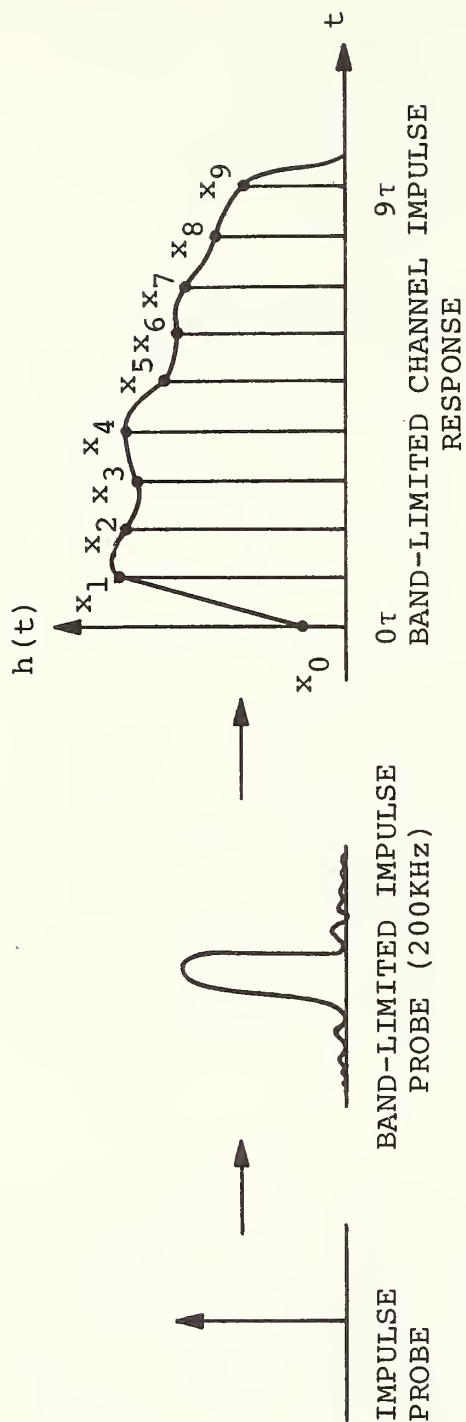


Figure 2a. Channel Measurement and Playback Technique (Simplified).

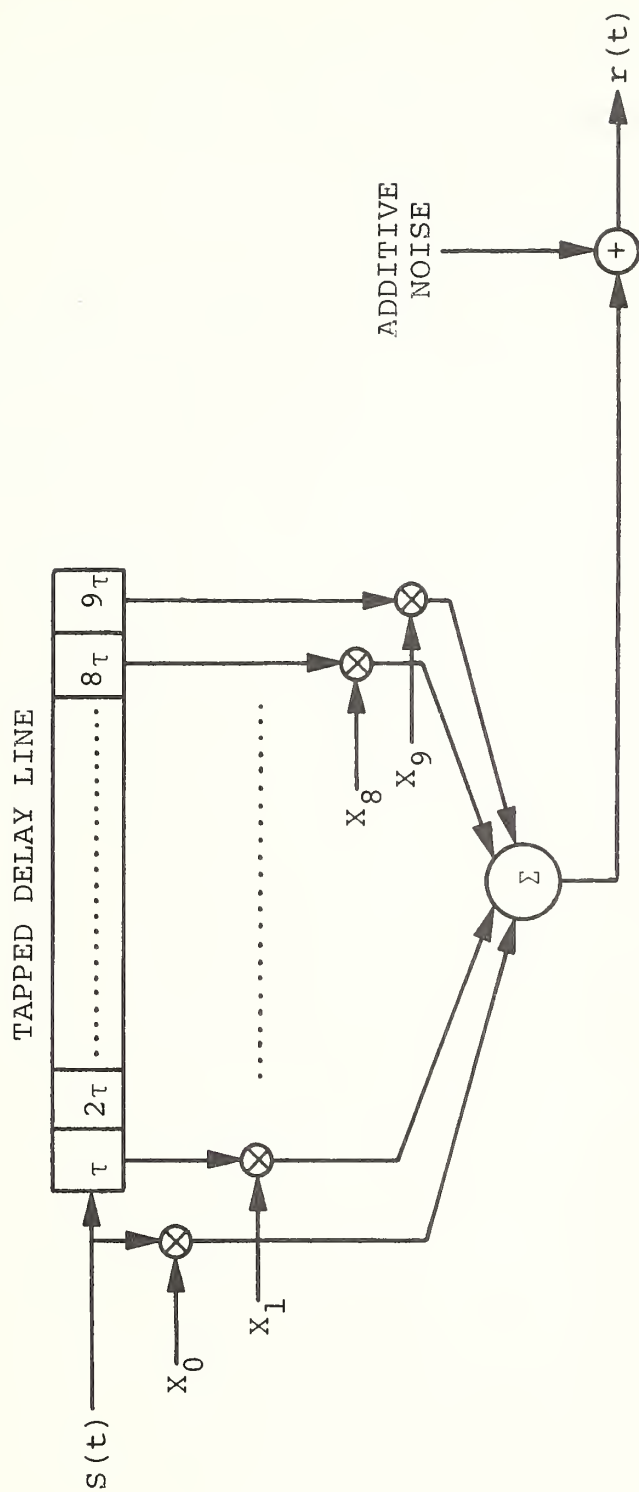


Figure 2b. Channel Measurement and Playback Technique (Simplified).

of the actual noise measurement. First-order statistics as well as tests of homogeneity will be computed for real-time evaluation of the validity, quality, and type of measurement data being taken; histograms will be computed as well as conventional moments such as rms noise power which alone are inadequate. Various bookkeeping functions will also be provided by the computer such as logging of the measurements and any other parts of the laborious measurement task which can be easily automated. An attempt will also be made in the near future to automate parts of the multipath measurement.

Further analysis of the measured noise will be performed back in the laboratory. These include a second-order analysis and further tests of homogeneity of the measured data. The details of this second level of analysis remain yet to be clearly defined. However, preliminary studies indicate that extensive use can be made of the homogeneity test to determine stationarity, classification and separation of noise phenomena, intervals of quasi-stationarity, and to aid in the estimation of second-order statistics of the noise process. Also, some preliminary work is being done to provide foundations for modelling both multipath and additive noise for the urban channel.

Several candidate techniques for taking advantage of the noise structure have been proposed. These include several multiplexing strategies, burst error-correcting codes, noise canceller, and two-way data link error information feedback. The noise measurements will provide the tools for the evaluation of these concepts.

## REFERENCES

1. T. Kailath, "Sampling Model for Linear Time-Variant Filters," M.I.T. Research Laboratory of Electronics, Cambridge, Mass., Rpt. No. 352; May 25, 1959.
2. P. Bello, "Characterization of Randomly Time-Variant Linear Channels," IEEE Communication Systems, Vol. CS-11, pp. 360-393; Dec. 1963.
3. R. G. Gallager, "Characterization and Measurement of Time-and-Frequency Spread Channels," M.I.T. Lincoln Laboratory, Lexington, Mass., Technical Rpt. 352; April 30, 1964.
4. P. Bello and R. Esposito, "Measurement Techniques for Time-Varying Dispersive Channels, "Alta Frequenza, N. 11 Vol. XXXIX, pp. 980-310E to 996-326E, 1970.

SURVEY OF MULTIPATH AND NOISE MEASUREMENTS IN CITIES

by

J. Liu  
P. Yoh  
L. Klein  
S. Karp

U.S. DEPARTMENT OF TRANSPORTATION  
TRANSPORTATION SYSTEMS CENTER  
CAMBRIDGE, MASSACHUSETTS 02142

INTERNATIONAL CONFERENCE ON COMMUNICATIONS

ICC 71

INSTITUTE OF ELECTRICAL AND ELECTRONIC ENGINEERS, INC.

MONTREAL, CANADA

June 14, 15, 16

## SURVEY OF MULTIPATH AND NOISE MEASUREMENTS IN CITIES

### ABSTRACT

This paper summarizes the available information on the statistical characteristics of the urban communication channel. This includes the results of measurements of the propagation properties of urban channels as well as the results of measurements of man-made and natural electromagnetic noise. Statistical models of the urban multipath channel based on these data are discussed. Some models of the various noise processes are described. Finally, the experimental program and supporting studies of the Transportation Systems Center of the U.S. Department of Transportation are presented.

## INTRODUCTION

An important aspect of any controlled transportation system is the communication link. Over this link, telemetry, command and control signals are sent to the controlled vehicles, and information on vehicular position, passenger load, reports of difficulties, etc., are sent to a central command and control station. Because of the requirements of automatic vehicular monitoring and control and the need for making more effective use of the limited number of available radio channels the trend in urban communication is from voice towards digital communication. Reliable digital data transmission requires more complete knowledge of channel characteristics than does the highly redundant voice transmission. For this reason, the measurement and characterization of the urban communication channel have received an increasing amount of attention in recent years.

In most urban communication systems, information is transmitted to various terminals over links in the VHF band (30-60 MHz and 150 MHz) and UHF band (450-470 MHz). The transmitted signals are subjected to interference consisting of two components: an additive noise component and a time-variant dispersive fading component. The latter is caused by vehicle motion through a continually varying multipath environment. The additive noise in the urban communication channel consists of electromagnetic disturbances generated by other communication equipments, power lines, electrical equipments, automotive ignition systems, etc., as well as Gaussian noise contributed by the receiver itself. It is known that the noise generated unintentionally by the various man-made sources is of an impulsive type with characteristics similar to that of the atmospheric noise which affects the performance of communication systems at lower frequencies.

This report summarizes the available information on the statistical characteristics of the urban communication channel. The techniques used and results obtained in measurements of propagation properties of urban channels are described, together with available data on multipath delay and Doppler spread of the channel. Several statistical models of the urban multipath channel based on these experimental data are discussed. The statistical characteristics of impulse noise in the urban channel are discussed. Models of the noise process are described.

The information summarized here concentrates on characteristics of the urban channel which are relevant to the design of reliable communication systems in the urban environment. It will be evident from this summary that data obtained in measurements made to date on the multipath channel and the additive noise process in the urban environment are inadequate for the

complete characterization of the urban channel and are often misleading for communication system design. We shall point out in this survey areas in which useful work could be done to improve our methods of reliable information transmission in the urban environment. Measurements of the multipath urban channel and the additive man-made noise characteristics which will be made by the Transportation Systems Center of DOT will be described. On the basis of these measurements, working models of the noise process will be constructed and a channel simulator will be built capable of presenting to a candidate communication system the distortion characteristics of the urban channel.

## PROPAGATION PROPERTIES OF THE URBAN CHANNEL

The problem of analyzing the propagation properties of the urban environment and the urban channel characterization has been approached by various investigators on both theoretical and experimental bases. Early work on urban radio propagation has, for the most part, gathered data on fading distributions and Doppler spreads at particular frequencies (1-7). These empirical data obtained by transmitting spectrally pure or narrowband CW signals, are useful in predicting the performance of narrowband systems used in voice communication links. To predict the behaviour of digital communication systems, measurements of the multipath properties of urban channels have been conducted (8-12). Experimental data on multipath propagation of pulse signals have led to several models of the multipath channel. In this section, we shall discuss the results of the measurements made using CW and pulse techniques and the associated theoretical models.

## MEASUREMENTS OF FADING STATISTICS USING CW TECHNIQUES

In a typical mobile-radio system, one station is at a fixed location, while the other is mobile. The received signal is the time-varying super-position of the direct wave and reflected and scattered waves. When the transmitted signal is narrowband, the multipath effects of the propagation medium manifest themselves as fluctuations in signal strength which depend on the relative strengths and phases of the component waves. The amplitude distribution of the received signal, therefore, depends on the characteristics of the propagation path, while the rate of fading is a function also of the speed of the mobile station.

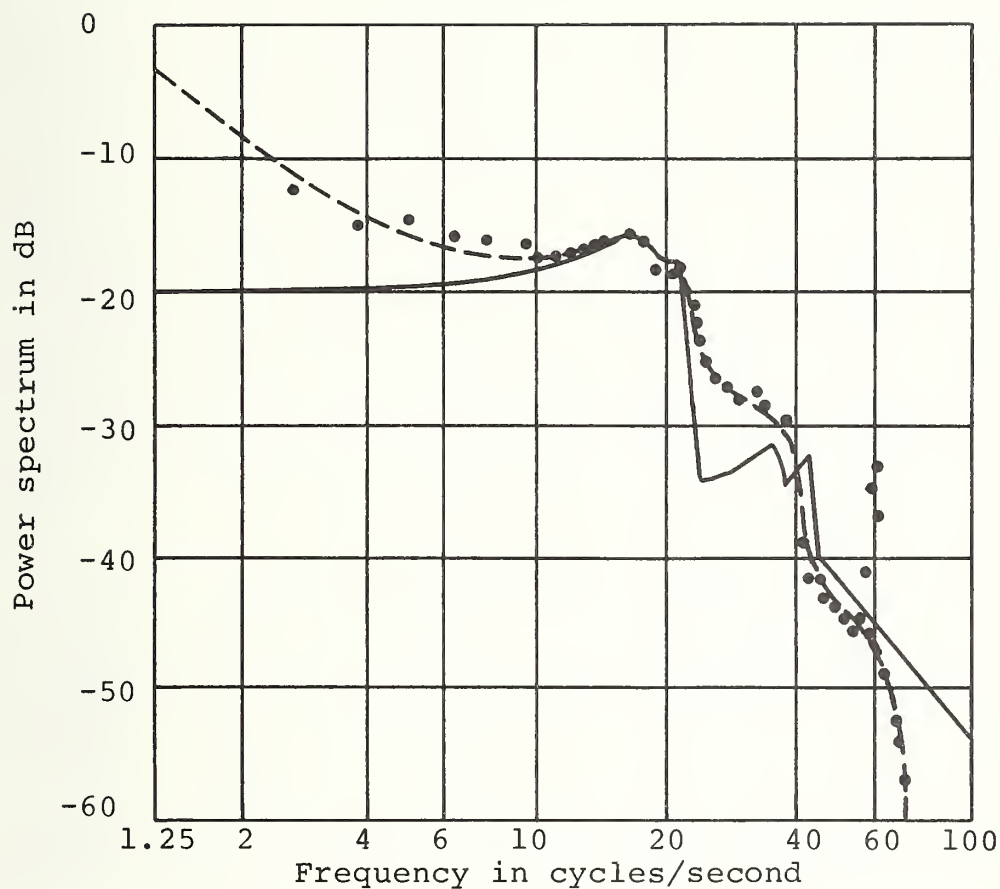
Signal Amplitude Distribution: It has been generally observed that the amplitude distribution of the received signal is independent of the carrier frequency of the transmitted signal over a broad frequency range (6). By transmitting narrowband signals (of approximately 10 KHz bandwidth) at 150, 450 and 900 MHz, Young (13) has found that

the amplitudes of the received signals over small areas (300 ft to 1000 ft in extent) in New York City are Rayleigh distributed when measured with a mobile receiver. The mean values of the received signal amplitudes decrease with the distance between the sample area and the transmitter. Signal amplitudes were also found to be Rayleigh distributed at several other frequencies (14, 15, 7) on suburban streets and in rural areas when the receiver was far from the transmitter (at a distance greater than 4 km). The measured signal amplitude being Rayleigh distributed suggests that the received signals in these experiments are composed of scattered waves of low strengths. For short transmission distance in cities and for transmission over open areas, the received signal amplitude was observed to be Rice distributed (and lognormally distributed (6)). This behaviour of the received signal amplitude distribution suggests the presence of relatively strong direct signal component.

Doppler Power Spectra: By transmitting an 838 MHz CW signal from a fixed based station and recording the fading waveforms of the received signal on a vehicle moving at 15 mph on city streets (New Providence, N.J.), Ossanna (3) calculated the Doppler power spectrum of the received signal. The power spectra obtained on different streets differ somewhat in details. In general, a sharp cut-off in the baseband spectrum at twice the maximum Doppler shift frequency was observed in all measured spectra.

A representative spectrum is shown in Fig. 1. The Doppler power spectrum was also measured at 910 MHz in a suburban environment (1). By plotting the received signal amplitudes as a function of Doppler shift, it is possible to detect distinct propagation paths with different Doppler shifts.

Frequency Correlation of Signals: To determine the maximum usable bandwidth in mobile radio, it is necessary to know the correlation between signals at different frequencies. Since the correlation bandwidth of a channel is inversely related to its multipath spread, by measuring the covariance of two signals as a function of their frequency separation, one can also obtain the distribution of time delays experienced by the component waves of the received signal. The only known empirical data on the covariance of signals were obtained by Ossanna in a measurement at 860 MHz in a suburban environment for carrier frequency separations of 0.1, 0.5, 1.0 and 2.0 MHz (13). The experimental data points fit roughly a theoretical curve corresponding to an exponentially distributed multipath delay with a mean of  $1/4 \mu$  sec.



———— Theoretical spectrum

-·-·-·-·-·-·- Measured spectrum

Speed of the vehicle: 15.8 miles per hour.

Angle between the direction to the fixed station  
and the direction of vehicle travel:  $83.3^\circ$ .

Figure 1. Typical Doppler Power Spectrum  
(Relative Amplitudes are Arbitrary),  
Figure 10 in (37).

Spatial Correlation: Using a space diversity system to receive frequency-modulated signals, Rustako (7) measured the probability distribution of the predetection combined signals of one to four channels with  $1/4$ ,  $3/4$ , and  $5/4$  wavelength antenna spacing. For a single channel, the signal fading was nearly Rayleigh distributed. As more channels were combined, the distribution became different from Rayleigh with noticeable reduction in fading depth. Moreover, the fading was observed to decrease with antenna spacing. The increase in diversity improvement with antenna spacing indicates correlation between received signal and coupling between antennas at these spacings.

Theoretical Models for CW Case: A number of phenomenological models of the urban propagation channels have been proposed to explain the experimentally observed characteristics of the received mobile-radio signals. These models assume that the received field is composed of a number of interfering waves. Fluctuations in received signal amplitude occur because of the motion of the mobile station through the spatial interference pattern. Depending on the properties of the interfering waves, the models can be classified into two types: reflection models and scattering models.

The reflection model was constructed by Ossanna (3) to predict theoretically the Doppler power spectra of the fading waveforms observed in measurements in a suburban environment. The model assumes that reflections occur at the flat sides of houses, modeled as randomly placed vertical plane reflectors. The incident and reflected waves form a standing wave pattern. Using the radio-carrier frequency, vehicle speed, and the angle between the direction of vehicle motion and the direction to the transmitter as parameters, theoretical Doppler power spectra were computed. In general, the theoretical spectra are in good agreement with those obtained in the measurement discussed above except at low frequencies and at frequencies around the maximum Doppler shift frequency. The discrepancies are due to the fact that the theoretical model failed to consider the effects of shadowing by buildings, ground reflection, and non-randomness of the reflectors.

Somewhat better match of the gross behaviours of the theoretical and experimental spectra were obtained by Clarke (4) using a scattering model. The model assumes that the received field is made up of a number of horizontally traveling plane waves, including scattered waves, whose azimuthal angles of arrival and phases are statistically independent. The phases of the component scattered waves are evenly distributed. The probability that a component wave will occur in the azimuthal angular sector  $(\alpha, \alpha + d\alpha)$  and the probability density functions of the time-delays of the component waves can be chosen for different environments. The received field may also contain a direct wave

component whose phase and strength depend on the distance and attenuation of the direct propagation path between the receiver and transmitter.

With this model, it is possible to show that when the strength of the direct wave is weak compared to the scattered waves, the envelope of the total received field is Rayleigh distributed and its phase is evenly distributed, as observed in experiments. When there is a strong direct wave present, the resulting envelope and phase will no longer be, respectively, Rayleigh and uniformly distributed. The phase and amplitude distributions are those derived by Rice for a sine wave plus random noise. Clarke was also able to derive the spatial autocorrelation and covariance functions of the electric and magnetic fields for the particular case in which the arrival angles of the component waves are uniformly distributed. For antennas spaced at  $1/4$ ,  $3/4$ , and  $5/4$  wavelength apart, the spatial correlation coefficients of the signal amplitudes were found to be 0.25, 0.06, and 0.03, respectively. The correlation of signals at different frequency separations may be derived from the probability density function of the time-delays between the component waves.

Gilbert (16) examined several scattering models in which the angles of arrival of the component waves are uniformly distributed. It was shown that when the number of component waves is sufficiently large, all models in which the phases of the component waves are evenly distributed are equivalent, as expected.

Pulse Measurements of Studies of Young and Lacy: To determine the maximum bandwidth or the shortest time interval that may be used satisfactorily in some wideband multi-channel voice communication systems, a measurement of the multipath characteristics of the urban channel was conducted at 450 MHz in New York City by Young and Lacy (19). In the experiment, pulses of  $1/2$   $\mu$ sec duration were transmitted from the base station. The channel response was detected by the receiver on the mobile unit. No information on the absolute time-of-arrival was obtained. Multipaths whose path losses are between 6 and 12 dB more than that of the main path (the path corresponding to the strongest component in the received signal) may occur in a delay spread period of 15 to 20  $\mu$ sec. It was observed that multipaths appear and disappear and their strengths change rapidly as the mobile unit moves at speeds 10 to 15 mph through the city. Unfortunately, no quantitative data were obtained in the experiment.

Schmid Propagation Model: Based on the results of Young and Lacy, Schmid (8) constructed a statistical propagation model

to estimate the probability of occurrence of multipath. The model predicts that for a constant distance between the transmitter and the receiver, the multipath strength decreases with increasing multipath delay. And for a given delay, the probability of occurrence of a multipath increases with the distance between the transmitter and the receiver. That is, the width of the probability of multipath occurrence as a function of excess path delay increases with the distance. (This has not been supported by the experiment results obtained in the Teknekron experiment described next.) Although the Schmid model offers some rough indication of the multipath properties of the channel, it is of little value for communication system design.

Measurement and Theoretical Models of Urban Channel by Teknekron: Recently, for the analysis and design of a wideband radio-location system, Teknekron (9, 17) conducted more extensive measurements of the multipath properties of the urban channel. The measurements were designed to determine the parameters of a statistical model which considers the urban channel as a time-invariant linear filter. The impulse response of the filter was assumed to be of the form

$$y(t) = \sum_{k=0}^{\infty} a_k e^{i\phi_k} \delta(t-t_k)$$

where  $t_0$  is the delay of the direct signal.  $t_k - t_0$ ,  $k = 1, 2$ , represent the excess delays of the multipath signals. The sets of path variable  $\{a_k\}$  and  $\{t_k\}$  are statistically independent of the carrier phases  $\phi_k$  of the paths were assumed to be statistically independent, evenly distributed random variables. Studies of the statistics of the path strengths  $a_k$  in measurements using narrowband signals 4, 6, 8, 2 indicate that over a small, sample reception area the path strengths  $a_k$  have Rayleigh or Rice distributions, while for larger areas the strengths become log-normally distributed. The purpose of the experiment was to determine the statistics of the path variables  $a_k$  and  $t_k$  and their statistical dependence.

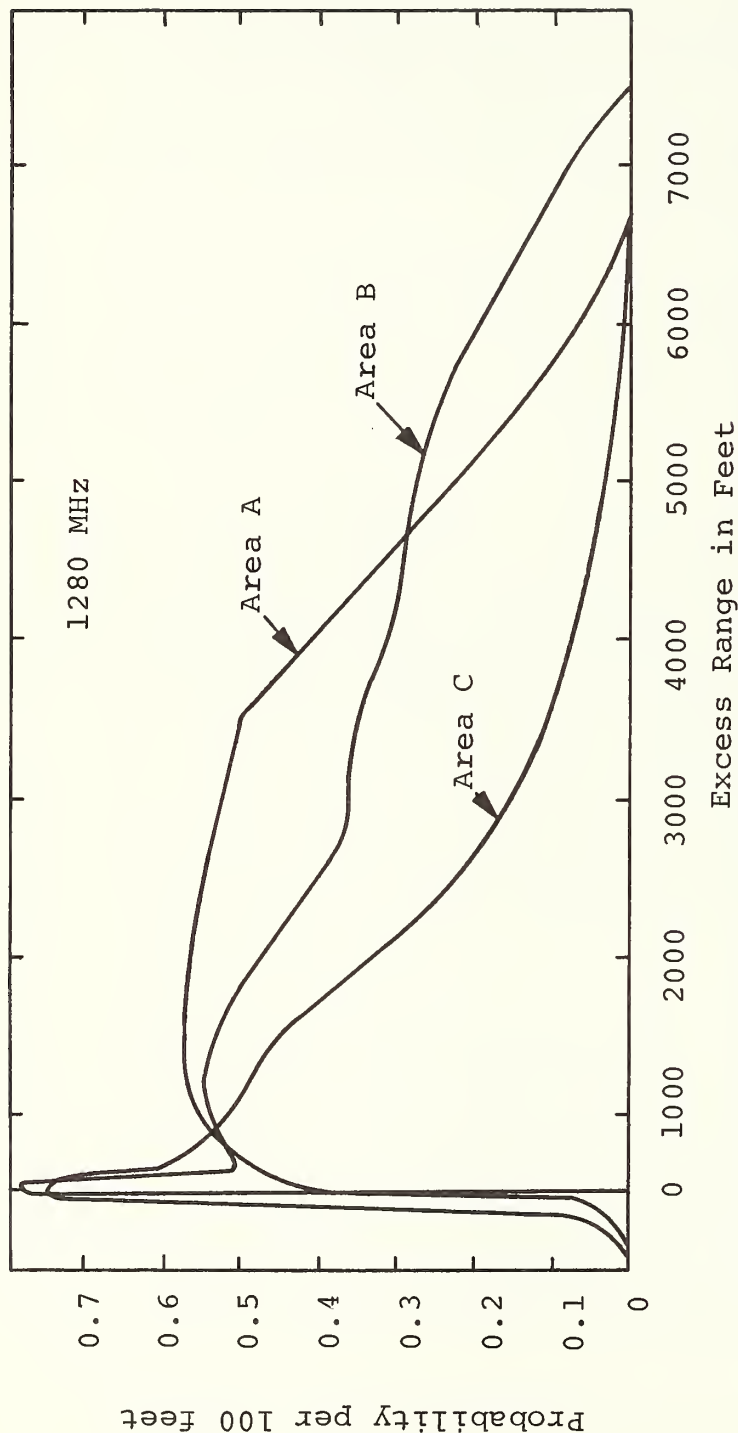
In the experiment, 100 nanosecond pulses at each of the three frequencies 488 MHz, 1280 MHz, and 2920 MHz were transmitted simultaneously from fixed transmitters. The responses of the channel at all three frequencies were received by the mobile unit (not in motion) with the video-detected response displayed on an oscilloscope. The scope was triggered  $\tau$  seconds after the transmitters were pulsed, where  $\tau$  was set to be slightly less than the smallest direct path delay expected in the reception area. The scope traces were photographed and then reduced on an optical scanning - table. Each of the peaks and inflection

points in the video response trace was taken to be a distinct multipath. Its occurrence time, measured with respect to the occurrence time of the first peak or inflection point in the trace, is the excess delay of the path. Its amplitude was taken to be the path strength.

Data obtained in San Francisco in areas of various multipath propagation characteristics indicated that, with minor exceptions, the multipath properties of the urban environment are similar for all three frequencies. Figure 2 shows the probability of occurrence of one or more multipaths within  $\pm 50$  feet of the excess range for various delay ranges at 1280 MHz. This result shows that the multipath spread depends almost totally on the local environment of the receiver contrary to that predicted by Schmid's theoretical model.

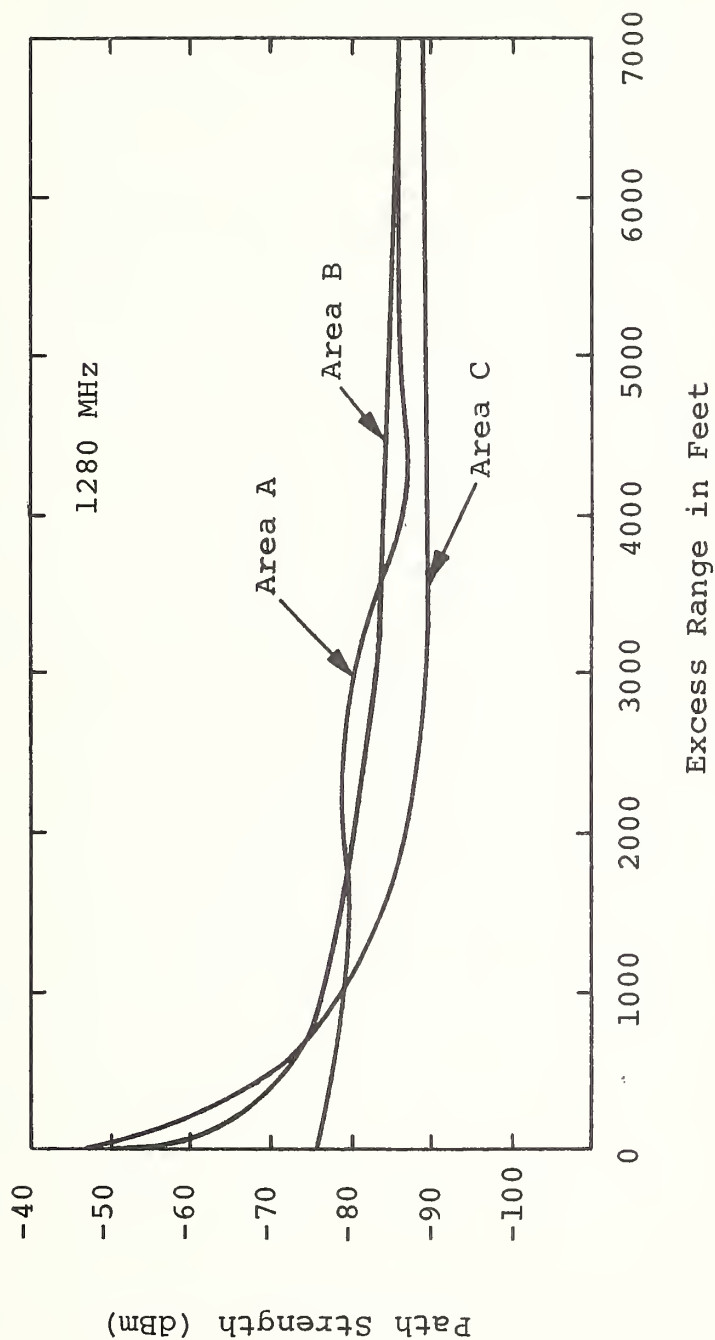
The empirical data on excess delays  $t_k - t_0$ ;  $k = 1, 2, 3$  of the multipath signals indicates that the sequence  $t_k$ ;  $k = 1, 2$ , roughly form a Poisson process. Multipaths with small excess delays tend to be more clustered than a Poisson sequence would dictate. Better fit between the empirical distribution and Poisson distribution was observed for multipaths of larger excess delays.

The multipath strengths  $a_k$  were found to be lognormally distributed with means and standard deviations dependent on the corresponding multipath delay  $t_k$ . Figure 3 shows the dependence of the mean of  $a_k$  as a function of the excess range for different types of environments. The strengths of different paths were found to be correlated. The correlation coefficients of the path strengths are yet to be determined.



Area A: Metropolitan (Transmitter antenna cannot be seen on street at all.)  
 Area B: Medium Cities (Transmitter antenna can be seen on streets at some points.  
 Reception area about 5 1/2 miles from the transmitter.)  
 Area C: Residential (Transmitter antenna can be seen at all points. Reception area  
 about 1 1/2 mile from the transmitter.)

Figure 2. Probability of Given Multipath Occurrence for Various Range. (Fig. 4 in [9]).



For discription of areas see Figure 2.

Figure 3. Dependence of Average Multipath Strength on Excess Range (Fig. 7 in [9]).

## NOISE IN THE URBAN COMMUNICATION CHANNEL

The noise external to the receiving antenna is composed of emissions from natural sources and electromagnetic pollution due to man-made sources. Based on the average noise power levels, the natural noise processes contribute the dominant noise at the extremes of the radio spectrum in urban environment. In addition to the thermal radiation from the local environment, natural noise consists of atmospheric radio noise, galactic radio noise, and sky noise. Most communication systems in the urban environment operate in the VHF and UHF bands. In these systems, the effects of man-made electromagnetic pollution are automotive ignition systems, power lines and electric equipments. Clearly, the contribution of each class of sources depends on the radiation spectrum and the number of sources of that class present in the environment. In urban and suburban environments, at frequencies below 20 MHz, the dominant man-made sources seem to be power lines, and electric equipments (such as r-f stabilized arc welders, brush-type electric motors, large electric contacts, etc.). At frequencies above 20 MHz, the most important noise source is automotive ignition systems.

The characteristics of noise generated by various types of noise sources have been studied extensively (18-26). The relative field strengths, statistical characteristics, frequency and distance dependences of these noise fields have been reported comprehensively in several review papers (26-29), there is no need to describe them in detail here. Generally speaking, incidental man-made noise is impulsive in waveform and aperiodic in occurrence. When recorded with wideband receivers, the waveforms of these noises were observed to be bursts of narrow pulses. (For the power line noise, the durations of the pulses were observed to be in the tens of nanoseconds with the bursts lasting several milliseconds. Automotive ignition noise occurs as nanosecond pulses in bursts lasting for tens of microseconds to several milliseconds.) Since the pulses have very narrow waveforms, the amplitude of the very high frequencies of the spectra remains large even though the rates of occurrence of the noise pulses are low. Figure 4 shows the median operating noise power,  $F_{am}$ , in dB above  $kT_0B$  ( $k$  is Boltzman's constant,  $T_0$  is 288.37 degrees Kelvin and  $B$  is the effective noise bandwidth of the receiving system in Hz) from man-made noise sources together with that from natural noise sources and these values are the levels expected from an omnidirectional, short, lossless, vertical antenna near the surface (29). The composite frequency spectra of major man-made sources are shown in Figure 5. Figures 6 and 7 show the typical values of the average occurrence rates of pulses for power line noise and automotive ignition noise, respectively (30). Figure 8 shows the typical behaviour of the amplitude probability distribution of man-made noise when observed over a narrow band (31).

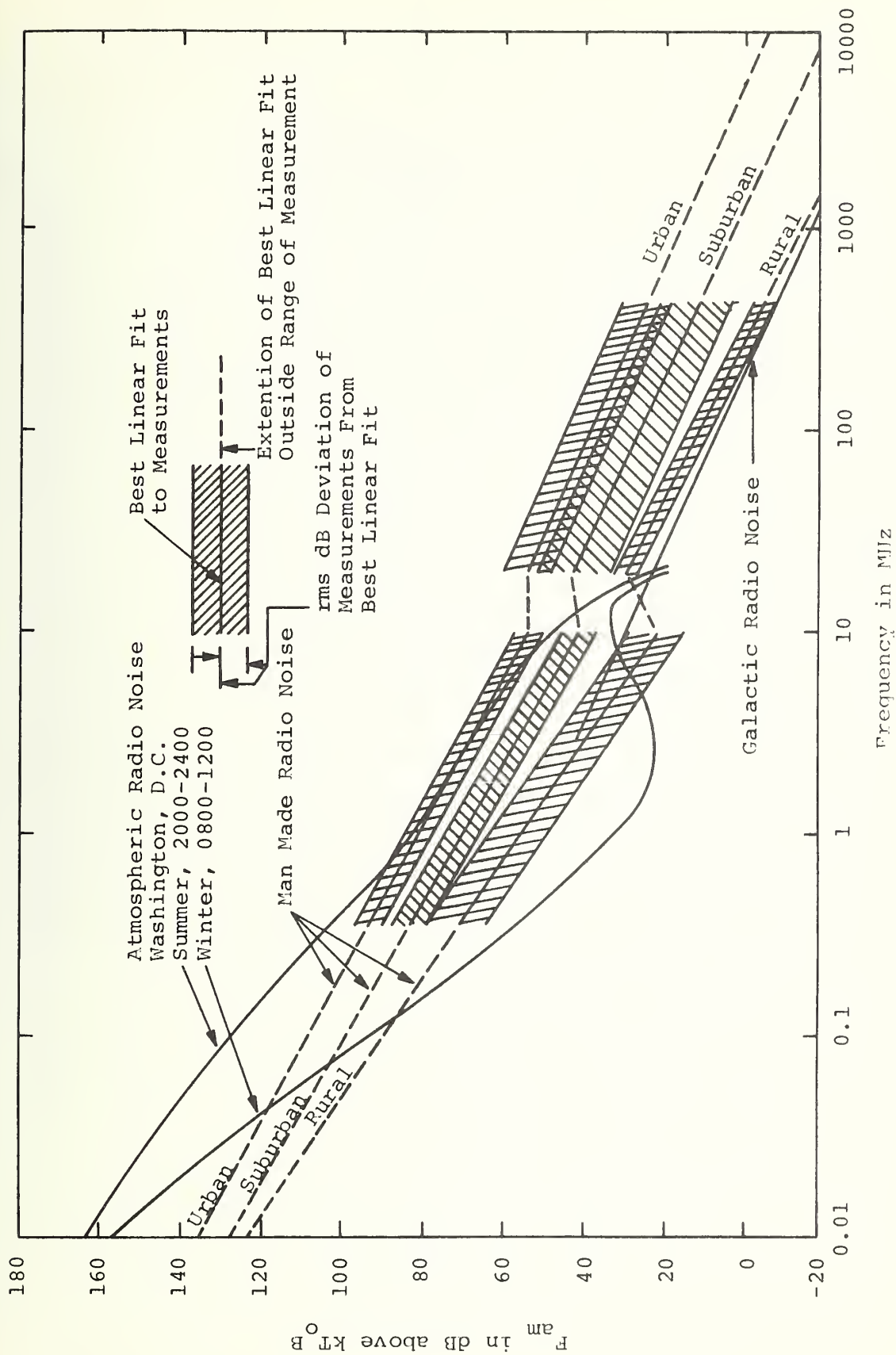


Figure 4. Median Values of Radio Noise Power (Omnidirectional Antenna Near Surface).



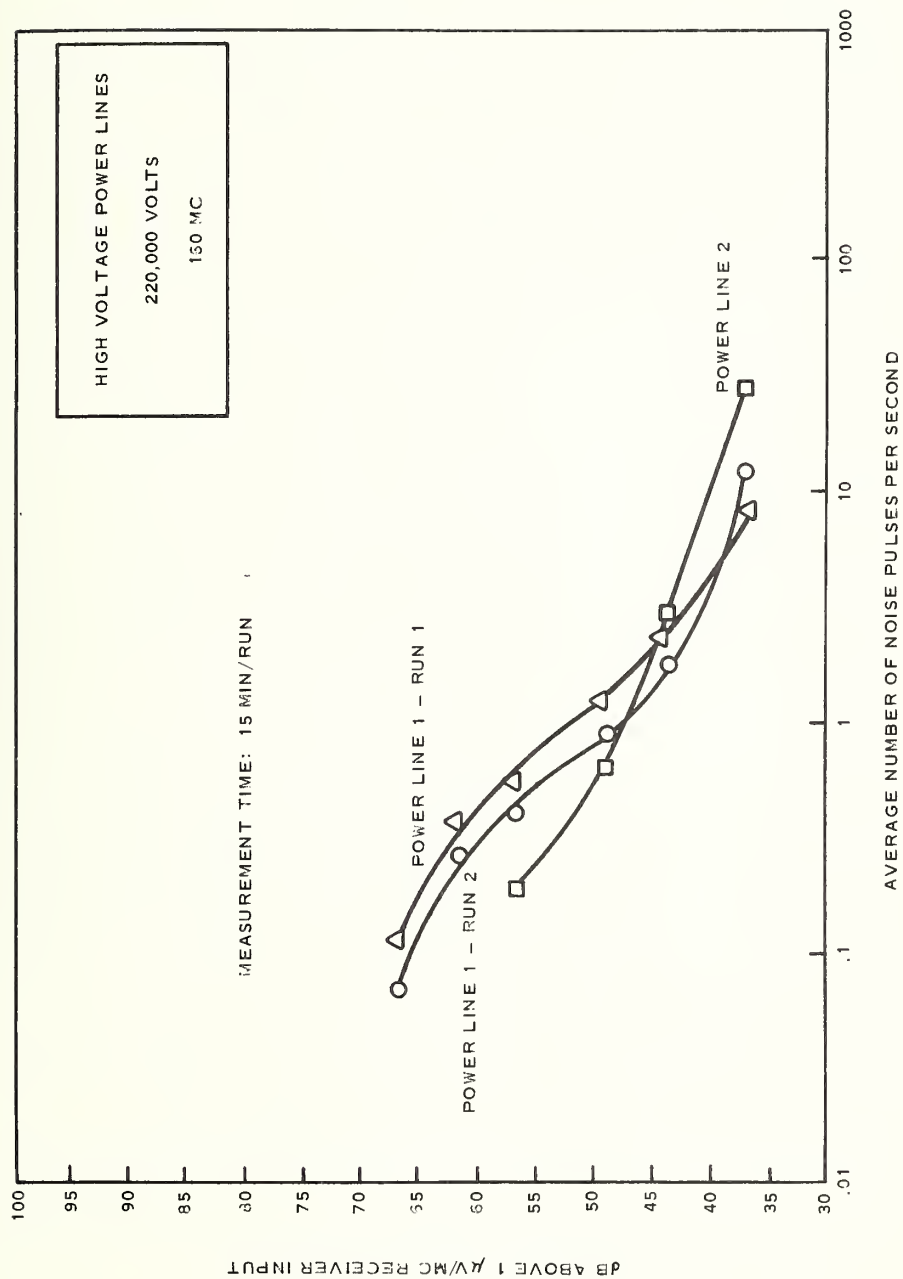


Figure 6. Power Line Noise in Clear Weather. (Graph 3 in [36]).

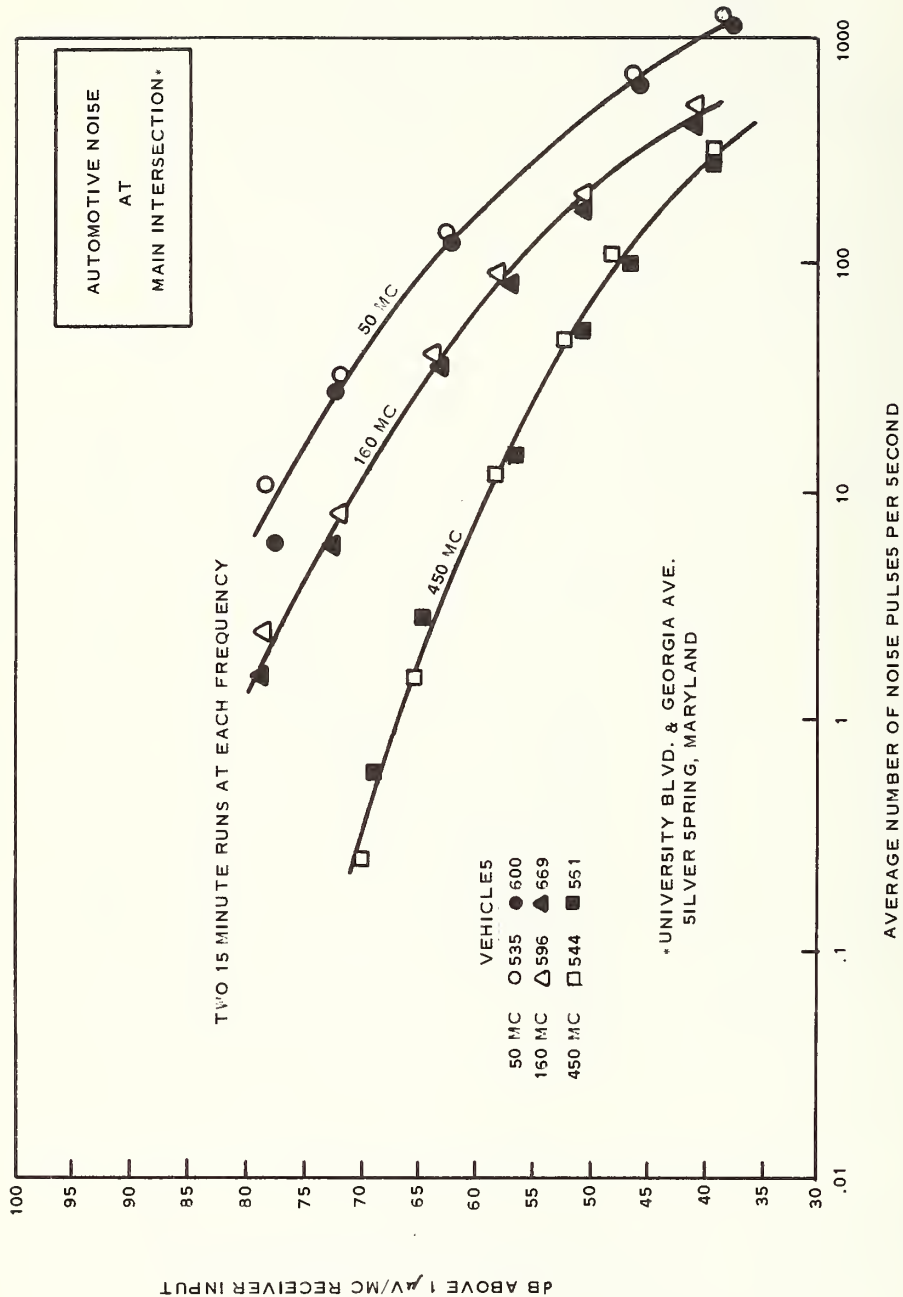


Figure 7. Automotive Ignition System Noise. (Graph 9 in [30]).

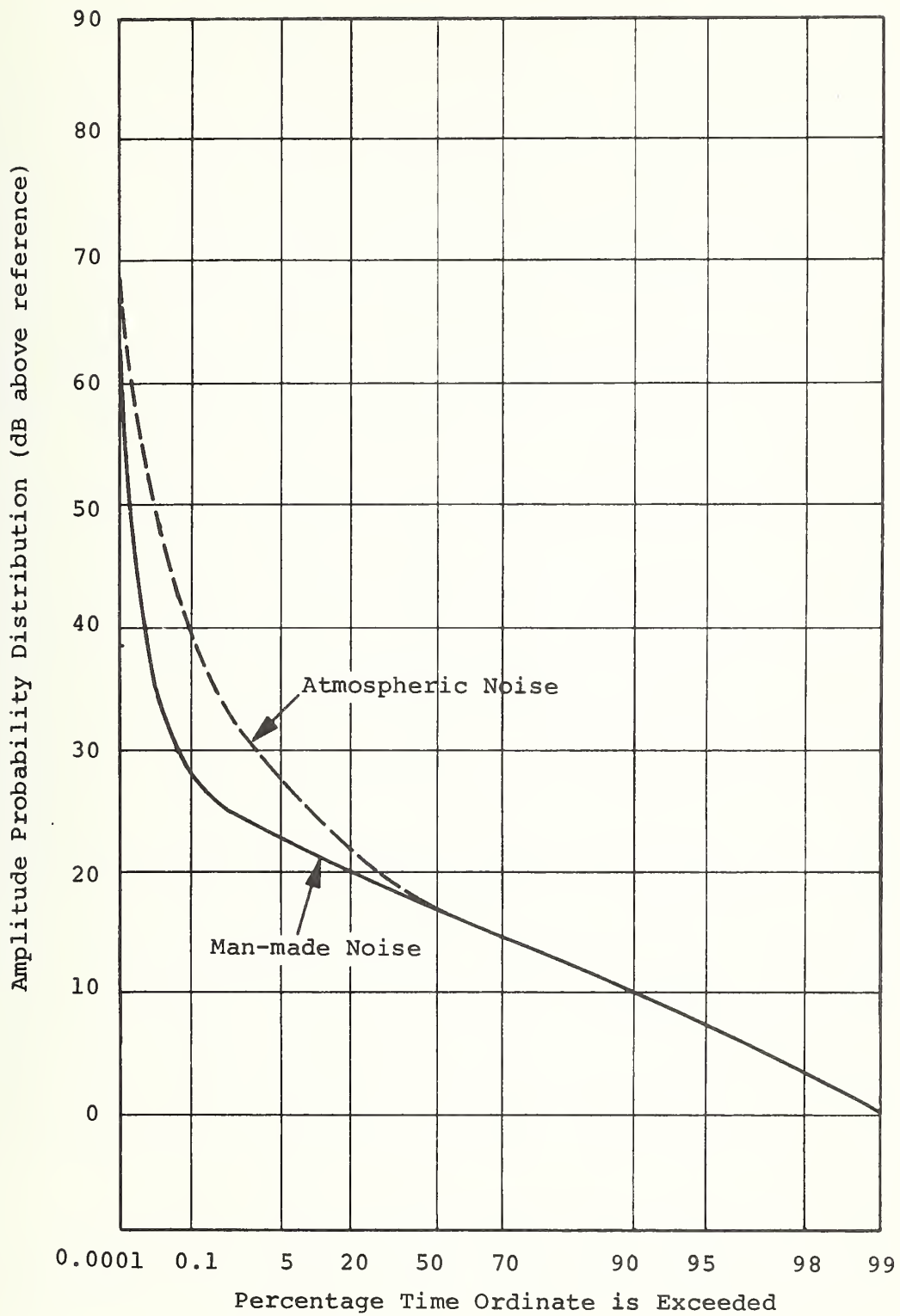


Figure 8. Typical Amplitude Probability Distribution of Man-Made Noise [3].

The amount of published information concerning measurements of man-made noise in the urban environment is truly remarkable. Due to the difference in the scope of the measurements, in the techniques used, and in the detail with which they have been reported, the comparison and characterization of these results is often an impossible task. The report by the Joint Technical Advisory committee of the IEEE, Subcommittee 63.1.3 on unintended radiation (29), represents a good attempt to summarize these results. It contains most of the relevant information on the measurements made on man-made noise prior to 1968. The report also contains some conclusions on the completeness of the available information on man-made noise and some recommendations for future work. Not included in the report are some measurements made in Japan at VHF and UHF with very wideband receivers (32, 33). Few additional measurements have been reported after 1968. Of special interest are the ones made by the Radiotelevisione Italiana at 850 MHz and 12 GHz (34) and the Institute of Telecommunication Science (31).

There is little doubt that man-made urban noise is a problem worthy of serious consideration both for analog and digital communication. Especially in digital communications, even a modest level of impulse noise can seriously degrade the performance of system not designed to withstand this type of interference. (For example, it was reported (35) that an essentially error-free, low data rate (2400 bps) digital system whose performance was degraded to an error rate of  $10^{-2}$  during the interval of time corresponding to the passing by of a single automobile. The theory presented in (36) makes it clear that the problem is especially acute for low data rate systems). Unfortunately, there are very few data and validated models available to adequately describe the wideband characteristics of man-made noise for the purpose of reliable communication systems design. Measurements of man-made noise have been made almost solely with narrow band receivers. Data obtained in the measurements are not sufficient for determining the effects of the noise on the performance of wideband systems. The statistical parameters measured have been very simple ones such as first and second moments, first order probability density functions of the detected noise envelope. Most of the results are presented either as average noise power levels with averaging time on the order of seconds or minutes, or as percentage of the total number of pulses which exceeds a given level. Examples of these results are given in Figures 4-8.

Very little work has been done to date on the problem of modeling the man-made noise process. The only man-made noise models are several simple one- and two-dimensional ones proposed by Ottesen (37). In these models, the field amplitude at any receiver site is the random phasor sum of the field generated by sources scattered randomly in space and overlapping in time.

By adjusting the parameters of the theoretical model, it is possible to match the theoretical amplitude probability distributions of the noise envelope to those obtained experimentally. However, these models are inadequate for characterization of the noise process in the problem of reliable communication system design.

Scientists at ITS have proposed to use some of the models for atmospheric noise to model man-made noise (31). The latter, being of impulsive nature, behaves very similarly to atmospheric noise at least when observed over a narrow band. The atmospheric noise was modeled by Furutsu and Ishida (38) as a Poisson - Poisson process in the sense that bursts of pulses occur at random and the times of arrival of the pulses in the bursts are also Poisson distributed. An explicit method is given in (38) to evaluate theoretical amplitude probability density functions. However, to apply the model to urban man-made noise, more analysis is needed to investigate whether the conditions prevailing in the urban environment allow analytical simplifications of the probability density function. The Hall model (39) is the product of two independent zero mean random processes. One of these processes is Gaussian. A refinement of this model for modeling the man-made noise, which will be discussed in this conference by Middleton (40), is part of the program to be carried out at the Transportation Systems Center.

## PROGRAM OF THE TRANSPORTATION SYSTEMS CENTER

The U.S. Department of Transportation at its Transportation Systems Center in Cambridge, Massachusetts has initiated a program of characterization and measurement of the urban communication channel with the long-range goal of improving the performance of communication systems in the urban environment by establishing a capability for comparative evaluation of competing components, subsystems and systems, on an equal basis, taking into account the effects of the dispersive channel characteristics as well as the additive noise. In addition, supporting theoretical studies are being performed particularly in the area of physical modeling of noise sources. The two main areas of experimental work are the programs of noise measurement and channel characterization and recording. Included in the latter is the fabrication of a channel playback simulator which will allow the comparative evaluations, previously referred to, to be carried out. We will discuss these two areas of experimental work with emphasis on the specification of the equipment and the design of the experiment, as far as present program status allows. Some comments about impulsive noise models will also be made.

Noise Measurement Program: A communication system planner would like to know the detailed characteristics of the background noise in order to evaluate its effects on system performance. This information includes the time and space variation of the noise as well as, for prediction purposes, its correlation with factors such as population density, vehicular traffic, power consumption and topographical characteristics. As has been mentioned the requirements are more stringent for digital communication systems which require a more thorough specification of the statistical characteristics of the noise. By and large this information is not currently available and this lack of design data hampers designers of wideband systems, i.e., systems whose bandwidth exceeds 10 kHz. Therefore, the purpose of the experiment under consideration is to measure broadband, wide dynamic range, impulsive-type noise in selected regions of the VHF and UHF band. The bandwidth of the measuring system has been tentatively selected to be 1 MHz. The predominant noise is expected to be generated by man-made machines such as automobile engines, industrial equipment, etc.

The reasons for this experimental program are the following:

1. To study experimental techniques for the measurement of wideband man-made noise in the VHF-UHF region and establish a capability for the routine performance of such measurements.

2. To identify the major sources of radiation that will interfere with the performance of any transportation system being planned in the frequency region mentioned previously.
3. To determine the information needed for the design and evaluation of any communication or command and control system of mass transit or land, air, water or highway communication. In combination with channel probing measurements this information will provide a complete characterization of the urban and suburban channel.
4. To determine the radiation characteristics of existing and proposed transportation systems such as electric cars, trolley cars, electric trains, etc. Figure 9 gives an overview of the entire program showing the relationships between measurements, data processing and the expected outputs of the program.

Measurement Parameters: One of the first tasks is, of course, the determination of the statistical quantities describing the noise which can be derived by suitable processing of the experimental data. Although a certain amount of data processing can be done in real time the decision has been made to record the IF waveform for later processing and for use in the simulation equipment. This means that most of the processing procedures can be decided upon at a later date. Some initial consideration on what has to be measured is, however, in order. A simple model of the wideband man-made interference is the sum of an impulsive component and of a Gaussian process. Both components can be expected to be nonstationary. It seems necessary to measure at least the following quantities.

1. Average power over each measurement interval
2. Amplitude pdf of the peaks
3. Duration pdf of the impulses at given amplitude levels
4. Pulse spacing pdf
5. Crossing rate pdf

In addition to the above quantities some simpler parameters such as average and rms values after detection can be measured in real time. It is worth pointing out that instrumentation similar to that being studied for the noise measurements can be used in the future for the investigation of channel occupancy. By this we mean the evaluation of the probability that a given

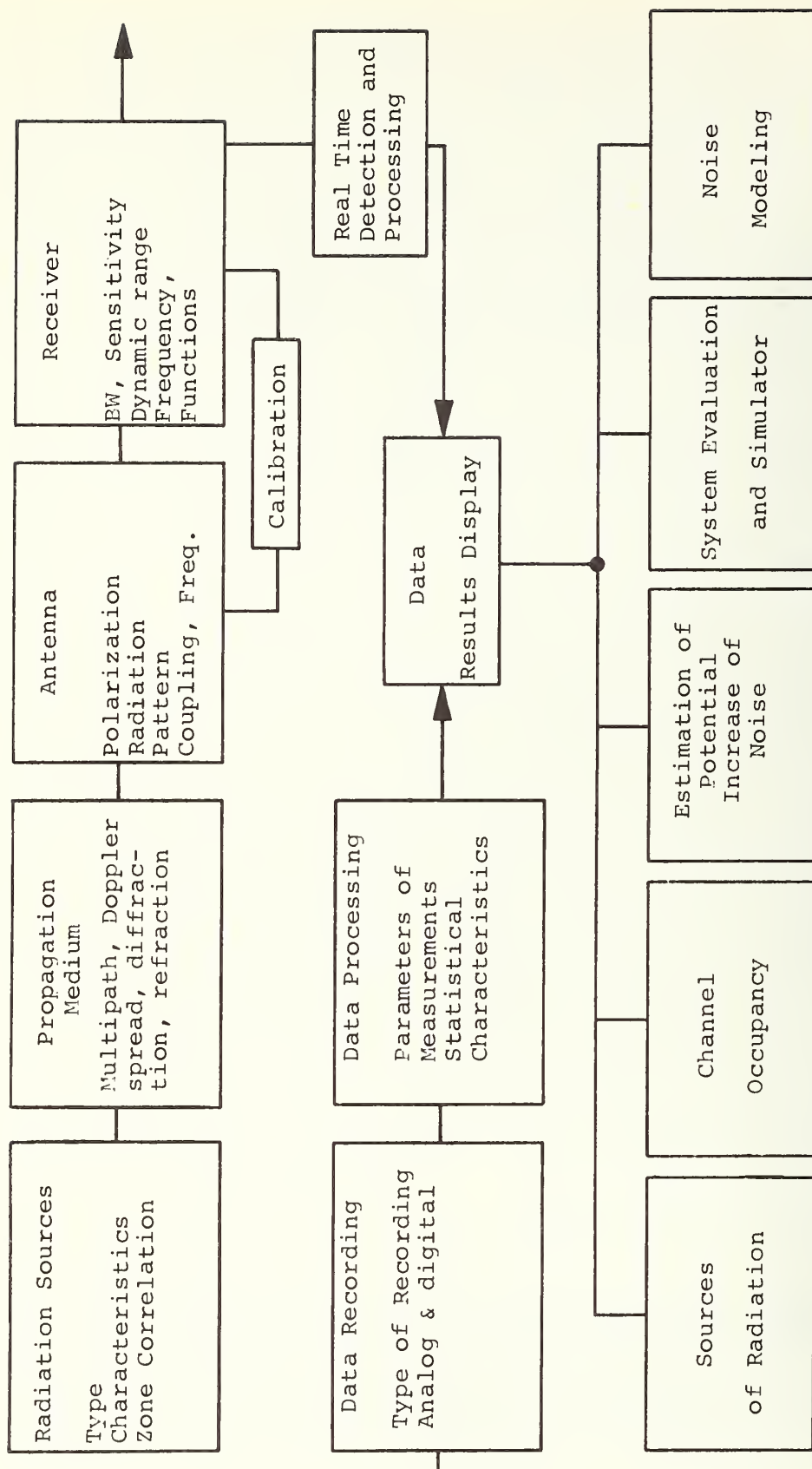


Figure 9. Flow Chart of Major Tasks, Problem Areas and Logical Flow of Data for the Measurement Program.

frequency region be occupied at a certain level, by other transmitters. Because of the limited spectral region available for land mobile communication it is also important to determine the minimum allowed spatial separation of stations transmitting in the same frequency region in order to avoid appreciable cochannel interference. This type of measurement can also be performed by the system under consideration.

A simple block diagram of the noise measuring system is shown in Figure 10.

Design of Noise Measurement Experiment: The characterization of the man-made noise present in the urban environment, and therefore the design of an appropriate experiment to derive such characterization, appears to be, at first a rather hopeless task because of the multifarious variability of that noise with a number of variables such as time, space, hour of the day, traffic conditions etc. In addition, the difficulty of the task is compounded by the fact that some of those variations, for example spatial variations, are seldom smooth owing to occasional sharp discontinuities in the distribution of noise sources and to the presence of standing wave noise patterns. Fortunately, however, a very large number of similar experiments have already been performed by other investigators and we can benefit from their findings and try to improve our knowledge of the urban noise in the iterative fashion that is typical of statistical experimentation.

The first important subdivision of the characterization problem comes from recognizing that there are basically three types of terminals in mobile communication:

1. stationary vehicles
2. moving vehicles
3. base stations

We will thus break the design of our experiment in three categories corresponding to the three types of terminals.

For stationary vehicles we can start with a concept put forward in the FCC study (30), that of "activity zone". The FCC Report divides the total urban and suburban environment into areas characterized essentially by their level of man-made noise. General categories defined in the study were: a) clear areas, b) residences, c) businesses, d) industrial sites, e) transportation areas, f) institutional sites, g) automotive activities. For the purpose of locating most of these zones in a large city like the Greater Boston area use can be made of an

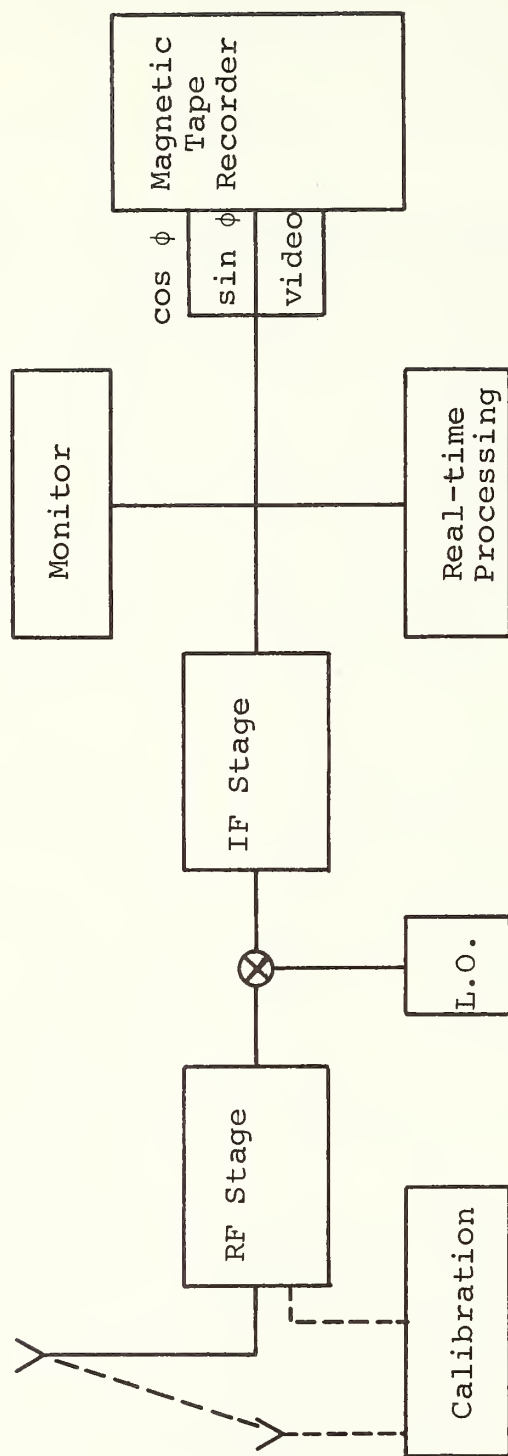


Figure 10. Basic Receiver Block Diagram

Urban Atlas recently published (41). This atlas contains detailed information on the characteristics of 20 large U.S. cities including Boston. Population density is, for example, given with a resolution grid of 250 m x 250 m and the different grids of each city are divided in five categories (50-200, 200-500, 500-1200, 1200-3600 and more people/grid). In the same document the following subdivisions are also identified for a large city: Airport, Institutional, Large Institutional, Park, Industrial, Commercial.

Examination of the FCC measurements and some additional thought suggests the following locations where measurements should be made with a stationary vehicle.

1. Clear areas.
2. Residential - separation between homes 500 ft.
3. Residential - separation less than 30 ft. but detached.
4. Residential - row houses.
5. Apartment buildings - 2 stories.
6. Apartment buildings - 6 stories and higher.
7. Office buildings - 8 stories and more.
8. Industrial plant.
9. High power lines (220 KV).
10. Low power lines (33 KV).
11. Power plant.
12. Hospitals.
13. Main thoroughfare.
14. Busy intersection.
15. Large institution.
16. Airport.

It is expected that these "activity zones" will be sufficiently different in the amount and type of man-made noise present, to justify this subdivision. The experiment will, of course, confirm or modify this assumption. However, even if the noise

characteristics were to be found very similar for two or more categories, the equivalence of different types of sites (say a power line and a congested traffic situation) will certainly constitute important information. It is also expected that for each site there will be at least one "control variable" to take into consideration: for example, the hour of the day in a residential area, the traffic at a busy intersection (smooth versus a traffic jam), weather conditions for a power line, etc. Economy of experimentation suggests the consideration of only two levels for this variable. It seems also advisable to replicate the same experiment at least twice for each type of site in order to gain some insight into the validity of the assumption of similarity. It must also be mentioned that, owing to the fact that automotive noise, whenever present, is an important source of noise, it will be probably impossible, or at least very difficult, to measure the noise characteristics of some of the sites mentioned without including automotive noise. This, however, must be considered a fact of life (office buildings are generally located in areas of high traffic) and it is therefore appropriate and relevant to measure the total noise present at those sites.

The total number of measurements required will in general be

$$N = C \times K \times M$$

C = number of activity areas identified

K = number of levels of the control variable

M = number of replicates for the same activity area

From the above considerations it seems that a minimum of 64 measurements are necessary for stationary vehicles. The number of sites is practically coincident with the number of measurements since, in general, changing the level of the control variable will prevent using a site for more than one measurement.

The characterization of the urban noise for a terminal on a moving vehicle should, in principle, require the duplication of the measurements taken at a stationary site. It seems, however, that the main difference between a moving vehicle and a stationary one arises when the moving vehicle is immersed in traffic. This point of view was implicitly taken in the FCC measurements where the only measurements from moving vehicles were made while riding in downtown traffic and on a busy suburban thoroughfare. These measurements should be duplicated, perhaps adding a few additional ones in other "activity zones" to compare the results with those obtained from a stationary vehicle.

Measurements of urban noise from base stations differ from the ones from stationary vehicles, essentially because of the height of the receiving antenna. Furthermore, most base stations are presently located either downtown or in busy suburban districts. It is suggested that the top of the TSC building be used for a set of such measurements. Two or three additional measurements with antennas located at various heights will probably suffice for the characterization of the base station noise. Remarks similar to the ones made for the accuracy achievable apply here also.

Channel Characterization Experiment: We now consider the experimental work planned for study of the second component of interference caused by the fading dispersive characteristics of the urban channel. This component arises from vehicle motion through a continually changing multipath environment. It is of equal importance to measure these deleterious effects and to analytically model them: measurement is important because it provides a realistic, repeatable replica of the communication channel which can be used in optimizing or refining a system design, or in evaluating contending candidate systems at different times on an equal basis; analytic work in this area is important in defining the form of a channel simulator even when the problem is too complex for a detailed mathematical analysis, and in providing the basic design for suitable transmitter waveforms for use in the fading environment.

Based on extensive research carried out over the last decade in the area of characterization of fading dispersive channels it is now practical to build a channel simulator capable of presenting to a candidate communication system the simulated, stored replica of the distortion characteristics of any desired channel displaying multipath delay, Doppler spread and additive noise. This channel playback approach effectively brings the field conditions into the laboratory and makes possible the comparative evaluation of competing techniques under identical conditions. This stored channel simulation can represent an estimate of the channel characteristics based upon mathematical modeling or can in fact be a faithful reproduction of the channel under operating conditions. The availability of both approaches is desirable for a comprehensive simulator facility.

The proposed technique involves two procedures with corresponding equipment. The first procedure involves field tests employing specially designed transmitter probing signals which cover the frequency bands of interest in the planned program areas. The probing signals are processed in the moving vehicle to extract the time-variant system function of the propagation environment or medium and record it on a multi-channel tape recorder. In addition the additive noise would be recorded. A

tape library could be built up which would adequately cover all environments for which systems are being developed. The replay procedure is carried out using these tape records. The time-varying channel, with the additive noise, would be played back repeatedly to enable tests of various systems to be made under the same field conditions. Basic block diagrams of the signal processing operations carried out in the channel prober and playback systems are shown in Figures 11 and 12.

Figure 11 defines the basic signal processing operations of the probing system. A periodic probing signal with complex envelope  $z(t)$  is filtered at the transmitter by IF and RF filters prior to transmission. All the filtering operations in the transmitter are lumped together as one filter, called the transmitter filter, which has impulse response  $h_T(t)$ . The propagation medium is represented by the complex time-variant impulse response  $h(t, \tau)$ , and the additive noise by the complex process  $\eta(t)$ . All the linear operations in the receiver prior to the correlation operations are lumped together into one receiver filter with impulse response  $h_R(t)$ . The output of the filter is fed to a number of parallel correlators, only one of which is shown in the figure. Complex notation is used to describe the correlation operation as a multiplication of the receiver filter output by the complex conjugate of a shifted probing signal followed by a complex low pass filtering operation.

Channel play back is achieved with a tapped delay line as shown in Figure 12. The complex time-varying multipliers are just equal to the low pass filter outputs of the correlators which yield estimates of the impulse response for uniformly spaced values of delay separated by seconds. Filtering operations necessary to avoid aliasing in the digital realization of the playback channel are shown in dashed lines.

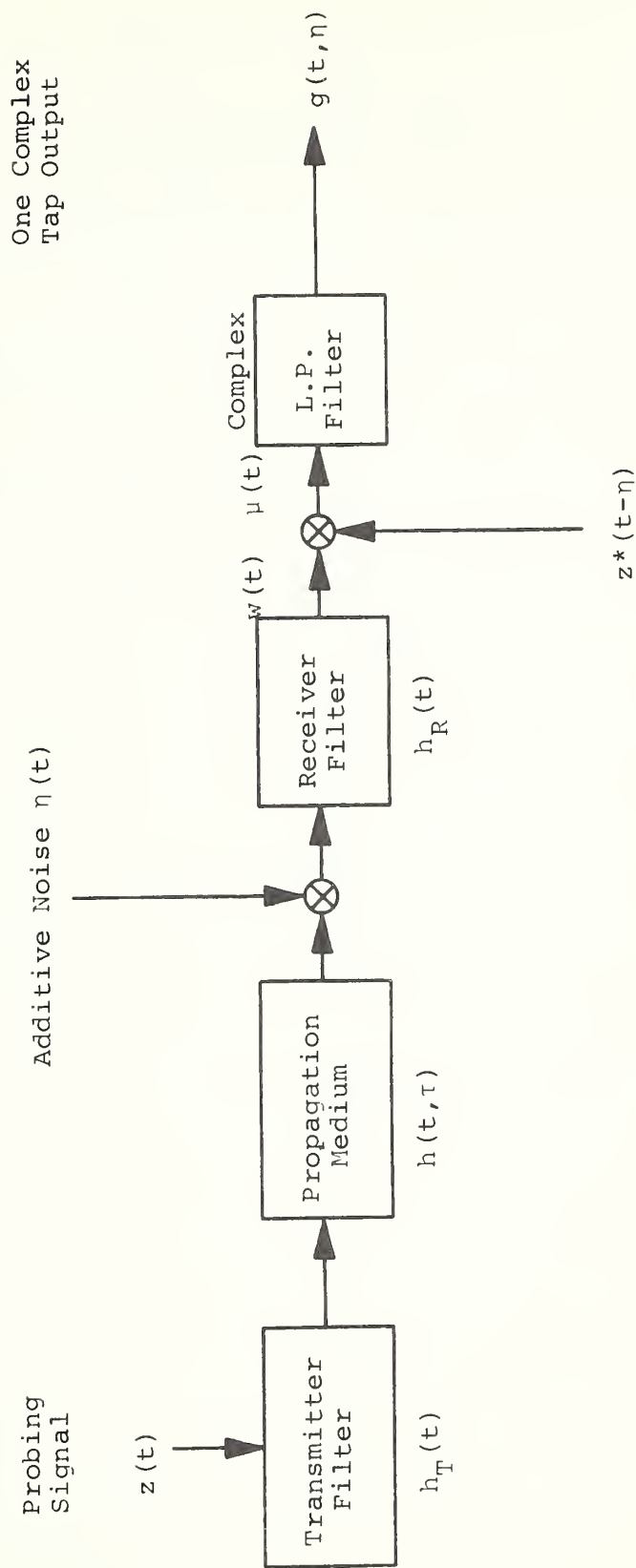


Figure 11. Definition of Basic Signal Processing Operations in Prober System.

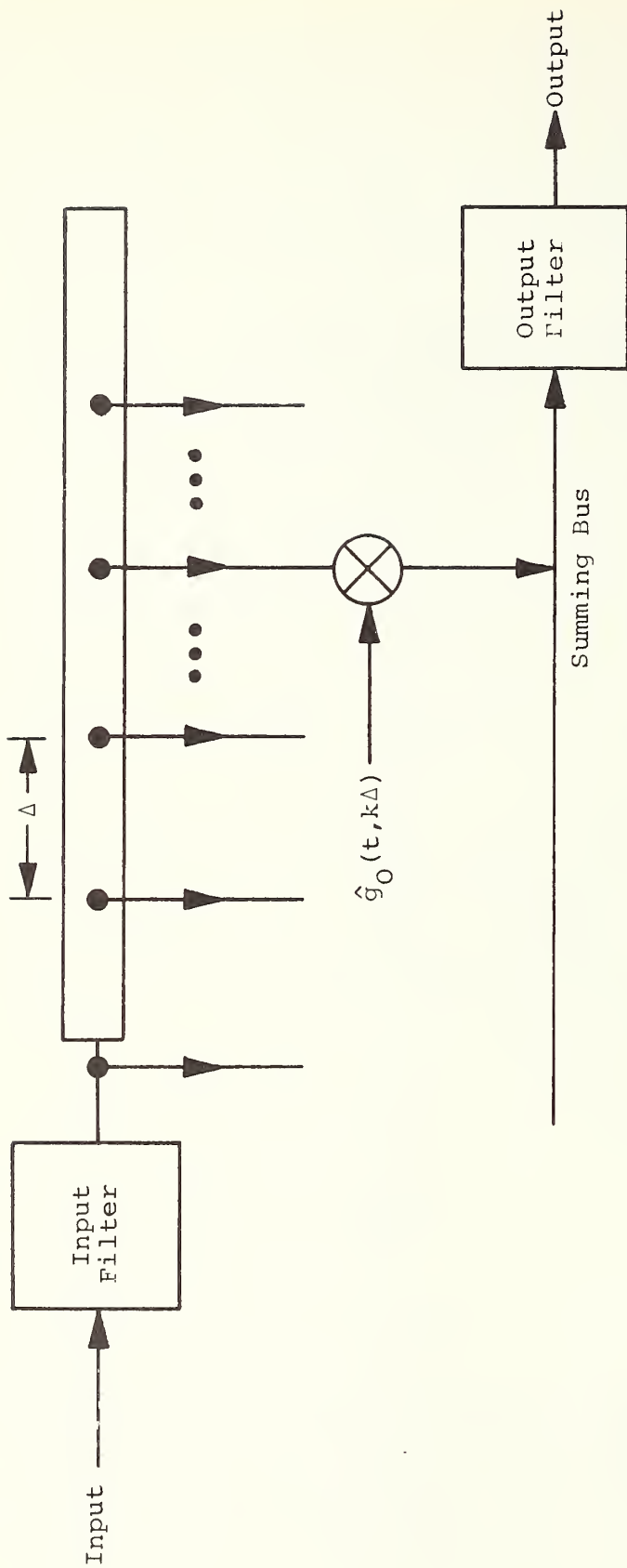


Figure 12. Channel Playback Schematic Diagram.

## REFERENCES

1. Cox, D.C., "Doppler Spectrum Measurements at 910 MHz over a Suburban Mobile Radio Path", Proc. IEEE, 59, pp. 1017-1018, (1971).
2. Gilbert, E.N., "Mobile Radio Diversity Reception," Bell System Technical Journal, 48, pp. 2473-2492, (1969).
3. Ossana, J.F., Jr., "A Model for Mobile Radio Fading Due to Building Reflection: Theroretical and Experimental Fading Waveform Power Spectra", Bell System Technical Journal, 43, pp. 2935-2971, (1964).
4. Clarke, R.H., "A Statistical Theory of Mobile Radio Reception", Bell System Technical Journal, 47, pp. 957-1000, (1968).
5. Bullington, K., "Radio Propagation Variations at VHF and UHF", Proc. IRE, 38, pp. 27-32, (1950).
6. Egli, J.J., "Radio Propagation Above 40 Mc Over Irregular Terrain", Proc. IRE, 45, pp. 1383-1391, (1957).
7. Rustako, A.J., Jr., "Evaluation of a Mobile Radio Multiple Channel Diversity Receiver Using Predetection Combining", IEEE Trans. Vehicular Technology, VT-16, pp. 46-57, (1967).
8. Schmid, H.F., "A Prediction Model for Multipath Propagation of Pulse Signals at VHF and UHF Over Irregular Terrain", IEEE Trans. Antennas and Propagation, AP-18, pp. 253-258, (1970).
9. Turin, G.L., F. Clapp, T.L. Johnston, S. Fine, and D. Lavry, "A Statistical Model of Urban Multipath Propagation", Report on Grant H-1030 Project DC-D6-1, Tekuskion, Inc., Berkeley, CA. (1970).
10. Young, W.R. Jr., and L.Y. Lacey, "Echoes in Transmission at 450 MHz from Land to Car Radio Units", Proc. IRE, 38, pp. 255-258, (1950).
11. Bedsole, W., and J. Lomax, "Propagation Measurements for a Frequency-Time Coded Pulse Communications System," 1964 IEEE International Conference Record, Part 6, pp. 170-181.
12. Heffner, R.W., "A Backscatter-Multipath Model for Ground-Wave Pulse Communication Systems", 1964 IEEE International Conference Record, Part 6, pp. 159-169.

13. Young, W.R., Jr., "Comparison of Mobile Radio Transmission at 150, 450, 950, and 3700 Mc", Bell System Technical Journal, 31, pp 1068-1085, (1952).
14. Trifonov, P.M., V.N. Budko, and V.S. Zotov, "Structure of USW Field-Strength Spatial Fluctuation in a City" (English translation from Russian). Trans. Telecommunications Radio Eng., 9, part 1, pp. 26-30, (1964).
15. Jakes, W.C., Jr., and D.O. Rendink, "Comparison of Mobile Radio Transmission at UHF and X-Band," IEEE Trans. Vehicular Technology, VT-17, pp. 10-14, (1967).
16. Gilbert, E.N., "Energy Reception for Mobile Radio," Bell System Technical Journal, 44, pp. 1779-1803, (1965).
17. Teknekron Inc., Berkeley, CA, "Urban Vehicle Monitoring: Technology, Economics, and Public Policy", Vol. I, Summary, conclusions and recommendations and Vol. II. The Institutional analysis, Report under project DC-D6-1 on Contract No. H-1030. (1970).
18. Eaglesfeld, D.D., "Motor-Car Ignition Interference", Wireless Engineer, 26, pp. 251-255 (1949).
19. Nethercot, W., "Car Ignition Interference", Wireless Engineer, 26, pp 251-255 (1949).
20. Bauer, F., "Vehicular Radio Frequency Interference-Accomplishment and Challenge", IEEE Trans. Vehicular Technology, VT-16, pp. 58-68, (1967).
21. Egidi, C. and E. Nano, "Measurement and Suppression of VHF Radio Interference Caused by Motorcycles and Motor Cars", IRE. Trans Radio Frequency Interference, RF1-3, pp. 30-39. (1961).
22. George, R.W., "Field Strength of Motor Car Ignition Between 40 and 450 WCPS", Proc. IRE, 28, pp. 409-413. (1940).
23. Ellis, A.G., "Site Noise and Its Correlation with Vehicular Traffic Density", Proc. IRE, Australia, 24, pp. 45-52, (1963).
24. Gehig, E.H., A.C. Peterson, C.F. Clark, and I.C. Redmour, "Bonneville Power Administration's 1100KV Direct Current Test Project: II-Radio Interference and Corona Loss, IEEE Trans. Power Apparatus and Systems, PAS-86, pp. 278-290, (1976).

25. Prelissier, M.R., "Les Perturbations Radiophoniques Emises Par Leo Lignes, A Tres Haute Tension", Bulletin le Society Fanacaise Electricians, pp. 409-418, (1953).
26. Skomal, E.N., "Comparative Radio Noise Levels of Transmission Lines, Automotive Traffic, and RF Stabilized Arc Welders", IEEE Transactions on Electromagnetic Compatibility, pp. 73-77, (1967).
27. Herman, J.R., "Survey of Man Made Radio Noise," Report of Lowell Technological Institute Research Foundation, Lowell MA (1969).
28. Skomal, E.N., "The Dimensions of Radio Noise", IEEE 1969, Electromagnetic Compatibility Symp. Record, pp. 18-28 (1969).
29. Spectrum Engineering -- the Key to Progress, A Report of the Joint Technical Advisory Committee of the IEEE, Supplement 9. Unintended Radiation (1968).
30. Advisory Committee for Land Mobile Radio Services, Technical Committee, Man-Made Noise, Working Group 3 report (1966 and 1968).
31. Disney, R.T. and A.D. Spaulding, "Amplitude and Time Statistics of Atmospheric and Man-Made Radio Noise", ESSA Technical Report ERL 150-ITS 98, Research Laboratories, Boulder, CO, and Final Report Vol. 6, "Interference Measurements and Analysis; Contract FO701-68-F-0072, ITS ESSA. (1968).
32. Nakamura, T., M. Inoue, H. Suzuki, and K. Endo, "Characteristics of City Noise in the VHF Band", the Technical Journal of Japan Broadcasting Corporation, 41 (1959).
33. Suzuki, H. "Characteristics of City Noise in the UHF Band", Journal Institute of Electrical Communication Engineers of Electrical Communication Engineers of Japan, 46, pp. 186-194, (1963).
34. Pacini, G.P., R. Giandio and F.R. Donia, "Indagine Sperimentale sul Disturbo Industriale nelle Gamme d: Frequenza 850 MHz 12 GHz," Relazione Tecnica No. 701291, RAI, Radio-televisione Italiana, (1970).
35. Motorola Inc., "Data Transmission Investigation", Final Report Contract DA 36-039-SC-90728, AD457527 (1964).

36. Bello, P.A. and R. Esposito, "A New Method for Calculating Probabilities of Enon due to Impulsive Noise" IEEE Trans. in Communication Technology, COM-17, No. 3, pp. 368-379 (1969).
37. Ottesen, M., "Electromagnetic Compatibility of Random Man-Made Noise", Ph.D Dissertation, University of Colorado, (1968).
38. Furutsu, K. and T. Ishida, "On the Theory of Amplitude Distribution of Impulsive Random Noise," J. Radio Res. Labs., Japan, 7, No. 32, pp. 279-307. (1960).
39. Hall, H.M. "A New Model for Impulsive Phenomenona; Application to Atmospheric Noise Communication Channels" Reports No. 3412-8 and 7050-7 Stanford Electronics Labs, Stanford, Co. (1966).
40. Middleton, D., "Statistical Physical Models of Urban Radio Noise Environments" Report prepared for TSC, April 1971, also to be presented at International Conferences on Communication, at Montreal, Canada. (June 1971).
41. J.R. Passoneau and R.S. Warman, "Urban Atlas: 20 American Cities," (1968).

# **REPRINT OF SPECIAL CONTRACTOR REPORT:**

STATISTICAL-PHYSICAL MODELS OF URBAN  
RADIO-NOISE ENVIRONMENTS

ERRATA FOR D. MIDDLETON'S DOT REPORT (JAN. 31, 1971):  
DOT-TSC-70:

- p.12. 4 lines after Eq. (3.1):  $\tilde{R}'_j = \tilde{R}_j - \tilde{R}'$ .
- p.22. Eq. (3.28): insert  $A_T(\xi, f')$  directly before  $Y_I$ .
- p.26. Eq. (3.39): coefficient of  $-i\omega'$  should be  $T_0 - \hat{c}_R \cdot 3/c$   
 Before the words "The double.." on line  
 below Eq. (3.39), insert "With electrically  
 small apertures, so that  $\hat{c}_R \cdot \xi/\mu c$  is negligible  
 in the term  $T_0 - \hat{c}_R \cdot \xi/c$ ,  
 line just before Eq. (3.41): add ", for  
 sufficiently small apertures again,".
- p.42. Eq. (4.42a): insert a constant, "C", as multiplier of  
 last term.  
 2 lines above Eq. (4.43): delete exponent  
 2 on  $\chi$ .
- p.43. (Eq. 4.48): replace  $\gamma-2$  in  $\Gamma\left(\frac{\gamma-2}{2}\right)$  by  $\gamma-1$ .
- p.44. Eqs. (4.49a,b): multiply by  $1/2\pi$ :  
 Eq. (4.49b): insert  $\sigma_0$  as factor of  $|\xi|^{\nu/2}$ .  
 Eq. (4.50): close bracket as  $[(3-\gamma)/2]_k$ .  
 Eq. (4.51): replace  $|a|$  by  $a^2$ .  
 Line below Eq. (4.51):  $W_1(0)$  replaced by  
 $W_1(a)$ .  
 Eq. (4.52): replace  $\gamma$  by  $\gamma+$ .  
 Eq. (4.52a): delete and write  $C\gamma = (\gamma-1)\sigma_0^{\gamma-1}$ .

p.44. Eq. (4.53): delete right hand side,  $\gamma > k+2$ , and  
(cont'd): replace by

$$\frac{(\gamma-1)}{2} \sigma_0^k \frac{\Gamma\left(\frac{k}{2}+1\right) \Gamma\left(\frac{\gamma-k-1}{2}\right)}{\Gamma \frac{\gamma+1}{2}}, \gamma > k+1 .$$

pg.45. Eq. (4.53a): insert  $\sigma_0^{-1-\gamma}$  before  $C_\gamma$ , 1st line,  
and delete 2nd relation and second line.

2 Lines below Eq. (4.53):

delete "p.d." and insert "form;  
at end of sentence, add: ",for small  
amplitudes".

p.46: Eq. (4.56): right hand should be:  $\sigma_0^2 / (\gamma-3) \sigma_Z^2$ .

D. Middleton

10/1/71

# STATISTICAL-PHYSICAL MODELS OF URBAN RADIO-NOISE ENVIRONMENTS

## I. FOUNDATIONS \*

by

David Middleton \*\*

[Jan. 31, 1971]

### ABSTRACT

Theoretical foundations for an analytical model of urban radio-noise environments are presented, at a level of generality broad enough to include the pertinent physical and statistical elements which critically influence the temporal and statistical character of such interference in radio receivers. The control rôles of geometry, directionality (beam patterns), waveforms (from the interfering sources), motion (doppler), source density and distribution, and secular variations of source parameters, as well as the radiation mechanism, are specifically developed. The basic statistical model involves independent sources, in space (and in time), leading to Poisson radiation fields and a Poisson process  $X(t)$  in a typical receiver. This received process  $X(t)$  can be considered the sum of a Gauss process (by the Central Limit Theorem), representing the cumulative effects of a large number of sources, none of which is very large vis-à-vis the rest, and a Poisson process, produced by those few strong transients, which when present, dominate the background. The process

---

\* Work supported on Contract DOT-TSC-70 [Oct. 15, 1970], from the Transportation Systems Center (Dept. of Transportation), 55 Broadway, Cambridge, Mass. 02142.

\*\* Consulting Physicist and Contractor [Physics and Applied Mathematics], 35 Concord Avenue, Cambridge, Mass. 02138.

$X(t)$  is essentially stationary for periods comparable to the secular period of changes in traffic intensity and flow, which permits the construction of usefully large experimental ensembles from which to estimate the process statistics.

An equivalent, semi-empirical, but more analytically tractable model, similar to that introduced by Hall for impulsive atmospheric noise, but used here for independent sources, is constructed. This model is represented by  $X(t) = a(t) Z(t)$ , where  $a, Z$  are independent processes, both zero-mean, and  $Z$  is regarded as gaussian. The first-order p.d. of  $X(t)$  is determined empirically for large  $|X|$  (i.e.,  $|a| \rightarrow \infty$ ), which in turn specifies the parameters of the first-order p.d. of  $a$ . The equivalent model is postulated to have the same moments (of first- and higher-order) as the basic Poisson model, which now permits us to include explicitly the details of the governing physical mechanisms in the formulation. The present study serves also as a guide for the experimentation needed to establish the model.

## TABLE OF CONTENTS

	<u>Page</u>
ABSTRACT . . . . .	ii
TABLE OF CONTENTS . . . . .	iv
1. INTRODUCTION . . . . .	1
2. STEPS IN THE FORMULATION . . . . .	5
3. AMBIENT FIELDS AND WAVEFORMS . . . . .	12
A. General Development . . . . .	12
B. Stochastic Fields $N_I(t, R)$ and Random Process $X(t)$ . . . . .	17
C. Generalities and Modifications . . . . .	19
(1) Doppler . . . . .	20
(2) Generalized Sources and Signals . . . . .	22
(3) Narrow-band Sources; An Example . . . . .	25
D. Summary Remarks . . . . .	28
4. STATISTICAL MODELS . . . . .	28
A. The (BSM) Poisson Process, $X(t)$ . . . . .	28
(1) Characteristic Function, $F_n$ . . . . .	29
(2) Two Independent Poisson Processes . . . . .	30
(3) Moments . . . . .	31
(4) Behavior of $X(t)$ at Large Amplitude . . . . .	32
(5) The Process Density $\rho$ . . . . .	33
(6) Poisson Noise Fields . . . . .	35
(7) Special Results . . . . .	35
(8) Macrostationarity . . . . .	38
B. The Equivalent Model for $X(t)$ . . . . .	41
5. CONCLUDING REMARKS . . . . .	46
REFERENCES and FOOTNOTES . . . . .	48
GLOSSARY OF PRINCIPAL SYMBOLS . . . . .	52
LIST OF FIGURE CAPTIONS . . . . .	55

# STATISTICAL-PHYSICAL MODELS OF URBAN RADIO-NOISE ENVIRONMENTS

## I. FOUNDATIONS \*

by

David Middleton \*\*

[Jan. 31, 1971]

### 1. INTRODUCTION

The present paper is the first of a series of technical studies whose ultimate aim is to provide a joint analytical and experimental treatment of radio-noise interference occurring in the urban environment. The purpose of this treatment is to determine quantitatively the physical character of such electromagnetic noise, its primary sources, its effects on the reception of desired signals, and methods of improving the design and performance of receiving systems, in order to mitigate, minimize, or remove, this class of electromagnetic pollution. This is, of course, not a new problem.<sup>1,2</sup> However, in order to achieve these desired results, and to take advantage of the many advances in communication theory and technology of recent years, much more fully developed physical and analytical models of these noise processes appear

---

\* Work supported on Contract DOT-TSC-70 [Oct. 15, 1970], from the Transportation Systems Center (Dept. of Transportation), 55 Broadway, Cambridge, Mass. 02142.

\*\* Consulting Physicist and Contractor [Physics and Applied Mathematics], 35 Concord Avenue, Cambridge, Mass. 02138.

necessary on the one hand, and more sophisticated and sensitive criteria and experiments are needed, on the other, with theory and experiment reinforcing each other at each appropriate stage.

The aims of this proposed series of papers may now be stated in more detail. We wish to construct an analytical model of typical urban radio-noise environments, which will include the following critical features:

- (i) the geographical (i.e., geometric) distribution of the various interfering sources vis-à-vis a typical receiver;
- (ii) the physical character of the noise fields generated by these sources;
- (iii) the conversion of these noise fields into waveforms upon reception by a typical receiver;
- (iv) a statistical model which is phenomenologically broad enough to account for the principal observed interference effects, and which has sufficient physical structure to enable us to identify and incorporate the pertinent, individual interference mechanisms;
- (v) analytical evaluation of the "statistical parameters" of (iv), which incorporate the physical structure of the model. By "statistical parameters" here we mean not only those structural parameters of the fields and waveforms which may in our ensemble model have statistical distributions, e.g., amplitudes, frequency, phases, epochs, signal duration, etc., but, principally, the "statistics" of the noise model. These are the intensity, the covariance functions of the process (and their associated intensity spectra), moments of higher-order and higher degree<sup>3</sup>, first-order probability distributions, and where possible, higher-order distributions.
- (vi) various special features, such as doppler (sources and receiver in relative motion; directionality effects (beam patterns); mixed classes of interference, i.e., a variety of different interference mechanisms; the effects of buildings, traffic patterns, diurnal and seasonal changes, weather, etc.

The noise mechanisms we are considering here are, of course, man-made, and as such must be identified and classified as to their relative importance as

interfering agents. Broadly speaking, we may say that these man-made processes consist of a mixture of impulsive and background noise, with the former a markedly impulsive component consisting of a few, discrete signals. For the present, we shall focus our attention on ignition noise, which appears to be the most common culprit where communication involving land-mobile transportation systems, at VHF and UHF, are concerned.

Two principal approaches are indicated:

- (I) measurement of, and model-building for, the wide-band noise, as it actually occurs, and
- (II) measurement and modelling of this interference, after it has been corrected to comparatively narrow-band noise in a typical receiver.

In the former case (I), essentially nothing adequate appears to have been done,<sup>4</sup> while for the latter (II), the modelling and data need to be extended to include and establish the validity and specific rôle of many of the physical elements cited in (i) - (vi) above. In both instances more sophisticated models and criteria are needed.

Collateral aims of this series of studies are:

- (1) To provide structure and guidance for the experimental investigations that must be undertaken to give us the desired empirical knowledge of urban radio noise. This is needed, in order to relate our models to reality and to make the kind of measurements which will enable us to predict the effects of this electromagnetic pollution on receiver performance and design.
- (2) To provide a framework for simulation, wherever and whenever the analytic results are intractable and/or the reservoir of data is incomplete or too expensive or impracticable to obtain.
- (3) Once adequate noise models have been constructed and tested, to apply the results to the design of optimal (or near-)optimal receivers for maximum immunity against this class of interference. This includes the calculation and measurement of receiver performance in:
  - (a) urban radio-noise, without the desired signals;
  - (b) urban radio-noise, with desired signals.

The new results of this study (Part I) are:

- A. The construction of a primarily physical model of the propagation fields arising from the spatially and temporally distributed noise sources. This provides us with the explicit waveforms at the receiver, and allows us to include the necessary factors of geometry, source characteristics, and so on. Earlier approaches have not usually made this anatomization of their models. We emphasize that it is essential to include the waveforms of the interference, since it is ultimately waveform, i.e., a time-phenomenon, which registers upon the observer as interference.
- B. The development of the so-called "Basic Statistical Model" (abbreviated "BSM"), which provides the framework for incorporating quantitatively the principal mechanisms and features noted above in (i) - (vi). This model consists of the sum of two independent noise fields. The first is a high density Poisson field, with (asymptotically) normal statistical properties, representing the general interference background. The second is a low density Poisson field, which represents the few but distinct and effectively high level sources of impulsive noise interference. From the physical description of this composite ambient field we can derive the detailed structure of the mean intensity and covariance functions (and higher-order moments,<sup>3</sup> and in principle, the probability densities as well), which constitute the "statistical parameters" of the statistical model [cf. (iv), (v) above].
- C. The use of a modified version of Hall's atmospheric noise model,<sup>5</sup> which we shall call here the "Equivalent Statistical Model" (ESM). This is a plausible, quasi-empirical model, which is used to replace the exact, but generally intractable Basic Model in the analytic determination of probability densities. In essence, it replaces the sum of a Gauss and Poisson process by a process equivalent to it, at least in the first-order distribution.<sup>6</sup> This equivalent process is postulated (and later justified) to be a Gaussian process in product with a relatively slowly-varying process, whose first-order distribution is asymptotically matched at large amplitudes to the observed, empirical distribution (at these large levels) of the urban noise in question.

The key innovation here is that we now determine the moments of higher degree<sup>3</sup> of this quasi-empirical, equivalent process directly from the corresponding moments of the Basic Model (BSM). Thus, for example, the covariance function of the former is specified by that of the latter, which is itself explicitly structured according to the underlying physics of the actual, ambient interference field. And this field, in turn, we have ab initio determined, according to (A) above. [Certain important differences between this Equivalent Statistical Model (ESM) and Hall's Atmospheric Model<sup>5</sup> will be discussed more fully in the following sections.]

The approach described in (A) - (C) above is in part based on recent work of the author<sup>7,8</sup>, with appropriate modifications and extensions (see Sections 3 & 4 below). The organization of this paper (Part I) is accordingly: Section 2 outlines the principal steps in the general formulation of our models; Section 3 is devoted to the physical aspects, and Section 4, to the statistical features, of both the BSM and ESM. Section 5 concludes with a brief discussion of the principal results and indicates some of the next steps to be taken. In Part I here, our presentation is what might be called a "detailed summary," where we reserve to later papers (Parts II, III, etc.) any desired developments in depth. Finally, although we consider only ignition noise specifically here, it will be clear from Secs. 2 - 4 that this in no fundamental way restricts the generality of our treatment.

## 2. STEPS IN THE FORMULATION:

We next outline the principal stages in the construction of our statistical model. A somewhat more detailed account is given in Sections 3 and 4, following. Our intent here is to provide a general overview before developing the analytical structure.

We begin with the determination of the interference field  $N_I(t, \underline{R})$  and the waveform  $X(t)$  of the received interference, after it has been processed by the receiving aperture (antenna), whose beam pattern is  $\mathcal{Q}_R(\underline{v}, f)$ . Letting  $\underline{T}_M^{(N)}$ ,  $\underline{T}_{AR}$  be the general operators<sup>9</sup> representing respectively the effects of the

medium — here the set of interfering noise ( $\equiv$  signal) sources  $\{S_I(t, \underline{R})_j\}$ , and the receiving aperture — we may write generally

$$X(t) = \underline{T}_{AR} \underline{T}_M^{(N)} \{S_I(t, \underline{R})\} \quad (2.1)$$

for the received, "ambient" noise entering the subsequent linear (and nonlinear) stages  $\underline{T}_{R_0}^{(N)}$  of the receiver. Thus, the observed interference is

$$N_I(t) = \underline{T}_{R_0}^{(N)} \{X(t)\} = \underline{T}_{R_0}^{(N)} \underline{T}_{AR} \underline{T}_M^{(N)} \{S_I(t, \underline{R})\} \quad (2.2)$$

In this way we can link the various stages in the generation and propagation of the interference field to the final observed effect. For the present, however, our attention is directed toward the waveform  $X(t)$ .

We proceed as follows: we consider a typical  $j^{\text{th}}$  source of ambient radio noise  $S_I(t, \underline{R})_j$  and calculate its field at some point  $P(\underline{R})$ . We assume, for the time-being here to simplify the analysis, a scalar source, i.e., one that effectively represents that particular component of the actual, vector field that the receiving aperture principally responds to, so that the resulting field is a scalar quantity.<sup>12</sup> Next, we additively combine a number  $K$  ( $j=1, \dots, K$ ) of the fields of these sources to produce the composite field that impinges upon our receiver. These sources are independently operative and distributed in space — for our purposes of mobile-land transportation (e.g., ignition noise) — on a surface, namely the streets of the urban region in question. Knowing  $\underline{T}_{AR}$ , we then have the desired resultant waveform,  $X(t)$ , cf. (2.1). By suitable attention to the form and structure of  $S_I(t, \underline{R})_j$ , and to the relative locations of these sources, in the particular region and under the conditions appropriate to the traffic state at the time (of day, week, year, etc.), we can incorporate the governing physical and geometrical characteristics of the interference situation.

This completes the first major step in the construction of the model. The second major step is to introduce a statistical mechanism. This is done by postulating that the sources have a Poisson distribution in space.<sup>8</sup> Moreover, each source represents an "event" in time: the generation of a noise field whose

physical character is basically transient and impulsive,<sup>13</sup> the epoch of initiation of the transient being a random parameter vis-à-vis the receiver. Other random parameters may be introduced: amplitude, frequency, duration, for example, which allow us to treat a variety of ambient sources, which may be operating concurrently, but which may arise from different mechanisms. In any case, the result is that the interference field  $N_I(t, \underline{R})$  is a Poisson stochastic field, and that  $X(t)$  is correspondingly a Poisson random process, since the aperture  $(\sim T_{AR})$  operates linearly on the incident field.

A further structure can be imposed. From our experience so far, it is reasonable to classify the noise sources into two groups: those that are not resolvable in the receiver and which together form a "background" noise field, and those that are sufficiently strong to appear individually and discretely. The former are very numerous, of all signal strengths and locations, but none such that anyone dominates the others vis-à-vis the receiver. The resultant is then essentially a "high-density" Poisson process,<sup>14</sup> whose statistics are asymptotically gaussian. The latter few, however, retain their individual character and remain a Poisson process, of low-density,<sup>14</sup> and may exhibit the very large amplitude excursions, when "on," of typical impulse noise. Thus, we have a sum of gauss and Poisson fields and processes:

$$N_I(t, \underline{R}) = G(t, \underline{R}) + P(t, \underline{R}) \quad , \quad (2.3a)$$

$$\{X(t)\} = G(t) + P(t) \quad , \quad (2.3b)$$

respectively.

The key assumption here is the independence of the various sources with respect to one another. [This is entirely reasonable for the urban noise model, where one ignition acts independently of another, but is generally not the case for atmospheric noise, where the interference tends to come in clusters of impulses,<sup>15</sup> so that the purely Poisson assumption is no longer valid.] If we let  $U_j$  ( $j=1, \dots, K$ ) be the  $j^{\text{th}}$  waveform, attributable to the  $j^{\text{th}}$  source, as it appears in the receiver following the aperture, we can accordingly divide  $X(t)$  into these

two components:

$$X(t) = \sum_j^K U_j = \sum_j^{K_B} U_{Bj} + \sum_j^{K_D} U_{Dj} , \quad (2.4)$$

where the first is the sum of the large number  $(K_B \rightarrow \infty)$  of relatively weak and comparable sources producing the gaussian background, and the second represent the few  $(K_D = 0, 1, 2, 3, \text{ say})$ , strong sources which discretely impinge on the receiver, and which belong to the low-density Poisson process. This, then, is the essence of our "Basic Statistical Model" (BSM), which we shall regard as the fundamental model, by which all other equivalent and approximate models are to be calibrated, as we shall indicate presently. Statistically, the BSM [for  $X(t)$ ] is described as the sum of independent Gauss and Poisson processes.

Although the BSM appears to be the correct form of noise model here, it presents a fundamental technical disadvantage: it is analytically complex, when we attempt to develop explicit, closed-form expressions for the probability densities describing the process, densities which are needed not only in estimating and predicting its properties, but also, ultimately, in determining the performance of receiving systems subject to such interference.

One approach, which we shall consider in the course of the investigation, is directly to employ simulation, based on the general expressions developed below (Sec. 4) for the BSM. A second approach, which is very attractive analytically, is to use an "equivalent," mixed-process model (the ESM), of the type suggested by Hall's Atmospheric Noise model,<sup>5</sup> but differing from it in a number of basic assumptions. Specifically, we replace (2.3a,b) by the mixed (or "modulated") process

$$\{X(t)\} = \{a(t) Z(t)\} , \quad (2.5)$$

where  $a(t)$  is a slowly-varying, comparatively broad-band random process, which effectively sets the unit, or scale, of  $X(t)$ , and whose statistical properties are to be determined empirically. To begin with, this is done by choosing  $W_1(a)$ , the first-order p.d. of  $a$ , so that it gives the same first-order p.d. of  $X$  for large

amplitudes ( $|X| \rightarrow \infty$ ), as is observed empirically. Higher-order densities are to be similarly constructed, from whatever higher-order statistical information can be obtained, in conjunction with the physically derived moments of the Poisson process.

Here  $Z(t)$  is a (zero-mean) gaussian random process, independent of  $a(t)$ , whose statistical character is to be found from the basic Gauss-plus-Poisson model (BSM) above, and whatever empirical data are required to relate that model to specific noise situations. As we shall show presently (Sec. 4), at least the expected first-order p.d. of  $X$  is gaussian for small amplitudes, which supports our postulate of the gaussian character<sup>16</sup> of  $Z(t)$ . For the important first- and second-order moments we have

$$\langle X \rangle = \langle a(t) \rangle \cdot \langle Z(t) \rangle = 0 ; \quad \langle Z(t) \rangle = 0 , \quad \langle a(t) \rangle = 0 \quad (2.6)$$

for the mean values (this last from physical considerations, Sec. 4), and for the covariance functions,

$$K_X(t_1, t_2) = \langle X(t_1) X(t_2) \rangle = K_a(t_1, t_2) K_Z(t_1, t_2) = K_X(t_1, t_2)_{\text{BSM}} , \quad (2.7)$$

( $\langle X \rangle = 0$ ) ,

where  $K_{X\text{-BSM}}$  is the covariance function of the BSM, whose detailed structure is determined by the Poisson form of the process and which explicitly incorporates the basic waveform,  $U$  (e.g., the physics) of the interfering noise, e.g.,<sup>17</sup>

$$K_X(t_1, t_2)_{\text{BSM}} = \int_{\Lambda_I} \rho(\underline{\lambda}) \left\langle U(t_1; \underline{\lambda}, \underline{\theta}) U(t_2; \underline{\lambda}, \underline{\theta}) \right\rangle_{\underline{\theta}} d\underline{\lambda} . \quad (2.8)$$

Here,  $\rho$  is a "density" function which measures the number of (independent) contributing noise sources in the domain,  $\Lambda_I$ , of possible sources, which, in turn, is determined by the particular urban environment we are considering. The  $\underline{\lambda}$  ( $= t, \theta, \varphi$ ) are a set of coördinates with respect to a convenient (at rest) reference system, and  $d\underline{\lambda}$  is a volume, or surface element  $[dt d\varphi, dt d\theta d\varphi]$ , cf. Sec. 4 - (5) below. The  $\underline{\theta}$  are a set  $\underline{\theta} = [\theta_1, \theta_2, \dots]$  of (time-invariant) statistical

parameters which can govern the shape and strength of the basic waveform  $U$ . In view of (2.4), we see that (2.8) can be further anatomized:

$$K_X(t_1, t_2)_{BSM} = \int_{\Lambda_B} \rho_B(\underline{\lambda}) \left\langle U_B(t_1; \underline{\lambda}, \underline{\theta}) U_B(t_2; \underline{\lambda}, \underline{\theta}) \right\rangle d\underline{\lambda} \\ + \int_{\Lambda_D} \rho_D(\underline{\lambda}) \left\langle U_D(t_1; \underline{\lambda}, \underline{\theta}) U_D(t_2; \underline{\lambda}, \underline{\theta}) \right\rangle d\underline{\lambda} , \quad (2.9)$$

where  $\rho_B, \rho_D$  are the respective Poisson densities for the background (limiting gaussian) process, and the low-density, transient interference; (it may be that  $U_D = U_B$  without loss of generality), and  $\Lambda_B \cup \Lambda_D$ . Accordingly, if we can determine  $K_a$ , we obtain  $K_Z$ , cf. (2.7).

Note that the statistical independence of  $a(t)$  and  $Z(t)$  requires, at least, that their (intensity) spectra<sup>18</sup> do not noticeably overlap. Actually, here  $a(t)$  will be quite low-frequency, i.e., slowly-varying, while  $Z(t)$  is comparatively narrow-band, centered about some carrier frequency  $f_0$ , even when apertures and RF stages of the receiver, broad compared to the usual communication practice, are used, e.g.,  $O(1,2 \text{ Mc/sec.})$  vs.  $O(10 \text{ kc/sec.})$ . The process  $X(t)$  is, therefore, "narrow-band," and can be expressed as

$$X(t) = a(t)x(t) \cos \omega_0 t + a(t)y(t) \sin \omega_0 t = |a(t)| e(t) \left[ \cos \omega_0 t - \varphi(t) \right] , \quad (2.10a)$$

$e \geq 0$

$$= E(t) \cos \left[ \omega_0 t - \varphi(t) \right] , \quad (2.10b)$$

where  $E(t) = |a(t)| e(t)$  ( $\geq 0$ ) is the envelope of  $X(t)$ , and  $\varphi(t) = \tan^{-1} [a(t)y(t)/a(t)x(t)] = \tan^{-1} [y(t)/x(t)]$ , is the phase. From (2.5), we have

$$Z(t) = x(t) \cos \omega_0 t + y(t) \sin \omega_0 t , \quad (2.10c)$$

and it is clear that since  $Z(t)$ , and  $\therefore x(t), y(t)$ , are gaussian processes, the phase  $\varphi(t)$  must, in the first-order be uniformly distributed over  $2\pi$ . The envelope  $e(t)$  will likewise have a Rayleigh distribution in the first-order, but the envelope  $E(t)$

will, in general, not. Even if the bandwidth of  $Z$  is comparable to, say,  $f_0/2$ , this model applies, but, of course, it is then physically meaningless to speak of  $X(t)$  as having an envelope and phase in the customary sense, cf. Eqs. (2.10).

So far, we have neglected system noise (which is symbolically indicated in  $\underline{T}_{R0}^{(N)}$ ). This is permissible as long as the background ambient field of the interference is strong enough to dominate the system noise in the receiver, which may often be the case. However, if the background contribution is excessively weak, and only the transient interference is significant, then we must include the system noise. Since this is gaussian (and stationary), with a spectrum determined essentially by the frequency response of the RF(-IF) stages of the receiver, we have again our Basic Model, but now only the impulsive interference belongs to a Poisson process. Equation (2.9) is accordingly modified to

$$K_X(t_1, t_2)_{BSM} = K_S(|t_1 - t_2|) + \int_{\Lambda_D} \rho_D(\lambda) \left\langle U_D(t_1; \lambda, \theta) U_D(t_2; \lambda, \theta) \right\rangle_{\theta} d\lambda, \quad (2.11)$$

with the covariance of the system noise becoming

$$K_S(\tau) = \frac{W_0}{2} \int_{-\infty}^{\infty} h_{RI}(x) h_{RI}(x + \tau) dx, \quad \tau = t_2 - t_1, \quad (2.12)$$

cf. Eq. (3.86), Ref. 10, where  $W_0$  is the spectral intensity density of the ("white") system noise initially, and  $h_{RI}$  is the combined weighting function (impulsive response of the RF- and IF-stages of the receiver<sup>19</sup>).

We have now the beginnings of a quantitative theory of urban radio-noise interference. Two major steps follow:

- (1) we must develop the analytical details of our models; and
- (2) we must verify, and modify the theory where necessary, by appropriate experimentation.

For the former we sketch the development in Secs. 3 and 4 below; for the latter a program of experiments is now underway at the Transportation Systems Center (TSC).

### 3. AMBIENT FIELDS AND WAVEFORMS:<sup>20</sup>

Here we shall indicate the principal steps in determining the interference field incident upon the receiver and the resulting noise waveform following the receiver's aperture. The present approach is based mainly on the methods of Ref. 7 [cf. Sec. III B).

#### A. General Development:

We begin by observing that the principal component  $\mathcal{L}_j^{21}$  of the electromagnetic field produced by a typical  $j^{\text{th}}$  source  $S_j$  obeys the (scalar) wave equation (in rectangular coördinates and for an assumed homogenous, isotropic, and non-conducting medium here)

$$\left. \begin{aligned} \nabla^2 \mathcal{L}(t, \underline{R}_j) - \frac{1}{c^2} \frac{\partial^2 \mathcal{L}(t, \underline{R}_j)}{\partial t^2} &= -G_I(t, \underline{\xi} | \underline{R}_j) , & (\underline{\xi} \in V_I) \\ &= 0 , & \text{elsewhere} \end{aligned} \right\} \quad (3.1)$$

where  $G_I$  is the source function, and  $c$  ( $= 3 \cdot 10^8$  m/sec.) is the velocity of propagation;  $V_I$  denotes the region occupied by the source and is generally a volume. The geometry is shown in Fig. 3.1;  $P(R')$  is some point in space, a vector distance  $\underline{R}' = -\underline{R}' - \underline{R}_j$  from the source's origin  $O_S$ , and here  $\underline{R}_j$  is the vector joining the origins of the  $j^{\text{th}}$  source and the receiver, with  $\underline{R}_j = \hat{i}'_x x' + \hat{i}'_y y' + \hat{i}'_z z' = \hat{i}_x x + \hat{i}_y y + \hat{i}_z z$ , etc.;  $\underline{\xi}$  and  $\underline{\eta}$  are radiating and receiving elements in their respective apertures, and similarly oriented rectangular coördinate systems are used for convenience. Letting  $A_I(\underline{\xi}, f)_j$  be the (frequency form) of the source's aperture, we have

$$G_I(t, \underline{\xi} | \underline{R}_j) = \int_{-\infty}^{\infty} A_I(\underline{\xi}, f)_j S_I(f, \underline{\xi} | \underline{R}_j)_j e^{i\omega t} df , \quad (\omega = 2\pi f) , \quad (3.2)$$

where

$$S_I(f, \underline{\xi} | \underline{R}_j)_j = \int_{-\infty}^{\infty} S_I(t, \underline{\xi} | \underline{R}_j)_j e^{-i\omega t} dt \quad (3.2a)$$

is the amplitude spectrum of the  $j^{\text{th}}$  source  $S_I(t, \underline{\xi} | \underline{R}_j)_j$ , which in generality is



position-dependent and unless otherwise indicated, is a real quantity. An alternative form for  $A_{I_j}$  is

$$A_I(\underline{\xi}, f)_j = \int_{-\infty}^{\infty} \alpha_I(\underline{\xi}, \tau)_j e^{-i\omega\tau} d\tau, \quad (3.3)$$

so that (3.2) is also written

$$G_I(t, \underline{\xi} | R_j) = \int_{-\infty}^{\infty} \alpha_I(\underline{\xi}, t-\tau)_j S_I(\tau, \underline{\xi} | R_j)_j d\tau. \quad (3.4)$$

Thus, the source's aperture  $A_I$  (or  $\alpha_I$ ) is a linear filter, which also depends in magnitude on location ( $\underline{\xi}$ ). The spatial Fourier transform of the aperture is the beam pattern  $\mathcal{A}_I$ , e.g.,

$$\mathcal{A}_I(\underline{v}, f)_j = \int_{V_I} A_I(\underline{\xi}, f)_j e^{2\pi i \underline{v} \cdot \underline{\xi}} d\underline{\xi}, \quad (3.5)$$

where  $\underline{v}$  is a (vector) spatial frequency:

$$\underline{v}(\hat{i}) = \hat{i}_x \underline{v}_x + \hat{i}_y \underline{v}_y + \hat{i}_z \underline{v}_z = k/2\pi = \hat{i}_x \lambda_x^{-1} + \hat{i}_y \lambda_y^{-1} + \hat{i}_z \lambda_z^{-1}, \quad (3.6)$$

with  $\lambda_x^{-1}$ , etc. wavenumbers, for the direction  $\hat{i}$  of  $P(R)$ , e.g.,  $\hat{i}_R \equiv R/|R|$ , where  $P(R)$  is some point in space, outside  $V_I$ . Applying (3.3), we see that the beam pattern is alternatively given by

$$\mathcal{A}_I(\underline{v}, f)_j = \int_{V_I} e^{2\pi i \underline{v} \cdot \underline{\xi}} d\underline{\xi} \int_{-\infty}^{\infty} \alpha_I(\underline{\xi}, \tau)_j e^{-2\pi i f\tau} d\tau. \quad (3.7)$$

Note that like the aperture function  $A_I$ , the beam-pattern  $\mathcal{A}_I$  is frequency-dependent.<sup>23</sup>

We assume, safely, that  $P(\underline{R}_j)$ ,  $P(\underline{R}'_j)$  are always in the far-field, so that the solution of (3.1) becomes<sup>22</sup>

$$\mathcal{L}\left(t, \underline{R}'_j\right) \doteq -\frac{1}{4\pi R'_j} \int_{-\infty}^{\infty} \mathcal{A}'_I\left(\underline{\hat{i}}'_j f/c, f | S_I\right)_j e^{i\omega\left(t-R'_j/c\right)} df, \quad (3.8a)$$

or

$$= \frac{1}{4\pi R'_j} \int_{V_I} d\underline{\xi} \int_{-\infty}^{\infty} \alpha_I\left(\underline{\xi}, t-\tau-R'_j/c + \underline{\hat{i}} \cdot \underline{\xi}/c\right)_j S_I\left(\tau, \underline{\xi} | R_j\right)_j d\tau, \quad (3.8b)$$

or

$$= \frac{1}{4\pi R'_j} \int_{V_I} d\underline{\xi} \int_{-\infty}^{\infty} A_I(\underline{\xi}, f)_j S_I\left(f, \underline{\xi} | R_j\right)_j e^{i\omega\left(t-R'_j/c + \underline{\xi} \cdot \underline{\hat{i}}'_j/c\right)} df, \quad (3.8c)$$

where  $\mathcal{A}'_I$  is a generalized beam pattern:

$$\mathcal{A}'_I\left(\underline{\hat{i}}'_j f/c, f | S_I\right)_j \equiv \int_{\underline{\xi}} \left\{ A_I(\underline{\xi}, f)_j S_I\left(f, \underline{\xi} | R_j\right)_j \right\}. \quad (3.9)$$

The spatial frequency  $\underline{\nu}(\underline{\hat{i}}'_j)$  is  $\underline{\hat{i}}'_j f/c = (\underline{R}'_j/R'_j) f/c$ ,  $R'_j = |\underline{R}'_j|$ , etc. In the rectangular coördinates of the source we have

$$\underline{\hat{i}}'_j = \underline{\hat{i}}'_x \cos \varphi_S \sin \theta_S + \underline{\hat{i}}'_y \sin \varphi_S \sin \theta_S + \underline{\hat{i}}'_z \cos \theta_S. \quad (3.9a)$$

Reception is handled in an analogous fashion.<sup>24</sup> We have for the typical waveform,  $U_j$ , after processing by the receiving aperture,  $A_R(\underline{\eta}, f)$ , with  $\underline{R}'_j \rightarrow \underline{r}_j(\underline{\eta})$ :

$$U_j(t) = \int_{V_R} d\underline{\eta} \int_{-\infty}^{\infty} \alpha_R(\underline{\eta}, t-\tau) \mathcal{L}\left[\tau, \underline{r}_j(\underline{\eta})\right]_j d\tau, \quad (3.10a)$$

or in frequency form

$$U_j(t) = \int_{V_R} d\underline{\eta} \int_{-\infty}^{\infty} A_R(\underline{\eta}, f) S_{\mathcal{L}}\left[f | \underline{r}_j(\underline{\eta})\right] e^{i\omega t} df, \quad (3.10b)$$

where  $S_{\mathcal{L}}$  is the Fourier transform of the field  $\mathcal{L}$ , (3.8), in which  $\underline{r}_j(\underline{\eta}) = \underline{R}_j - \underline{\eta}$ , cf. Fig. 3.1. As in (3.3), (3.4), (3.8b),  $\alpha_R$  is the spatio-temporal form of the receiving aperture, and  $V_R$  is its physical domain. Inserting (3.8) into (3.10) gives us a variety of equivalent expressions for the waveform of the interfering

noise entering the time-processing portion of the receiver,  $\underline{T}_{R0}^{(N)}$ , cf. (2.2). These are, for this far-field state (when there is ignorable mutual coupling from receiver to source):

$$U_j(t) \doteq \frac{1}{4\pi R_j} \int_{V_R} d\underline{\eta} \int_{-\infty}^{\infty} \alpha_R\left(\underline{\eta}, t - \tau - \frac{\hat{\underline{i}}_{Rj} \cdot \underline{\eta}}{c}\right) d\tau$$

$$\times \int_{V_I} d\underline{\xi} \int_{-\infty}^{\infty} \alpha_I\left(\underline{\xi}, \tau - \tau' - R_j/c + \frac{\hat{\underline{i}}_{Rj} \cdot \underline{\xi}}{c}\right) S_I\left(\tau', \underline{\xi} | R_j\right)_j d\tau' \quad (3.11a)$$

or

$$\doteq \frac{1}{4\pi R_j} \int_{-\infty}^{\infty} \mathcal{A}_R\left(-\frac{\hat{\underline{i}}_{Rj}}{c} f/c, f\right) \mathcal{A}'_I\left(\frac{\hat{\underline{i}}_{Rj}}{c} f/c, f | S_I\right)_j e^{i\omega(t - R_j/c)} df, \quad (3.11b)$$

this last in terms of the beam patterns, where we have used  $\hat{\underline{i}}' \rightarrow \hat{\underline{i}}_R$ ,  $r_j = |\underline{R}_j - \underline{\eta}| \doteq R_j + \hat{\underline{i}}_R \cdot \underline{\eta}/c$  in this far-field approximation, along with the definitions (3.5), (3.9). [We remember that  $\hat{\underline{i}}_{Rj}$  here is the unit vector directed outward along  $\underline{R}_j$  toward  $O_R$  of the receiver.]

Note that the operators for the  $j^{\text{th}}$  source and for the receiver, on comparing (3.10), (3.11) with (2.1), can be written now explicitly

$$\underline{T}_{AR}\{\ }_j = \int_{V_R} d\underline{\eta} \int_{-\infty}^{\infty} \alpha_R\left(\underline{\eta}, t - \tau - \frac{\hat{\underline{i}}_{Rj} \cdot \underline{\eta}}{c}\right) ( )_{\tau,j} d\tau, \quad (3.12a)$$

or

$$= \int_{-\infty}^{\infty} \mathcal{A}_R\left(-\frac{\hat{\underline{i}}_{Rj}}{c} f/c, f\right) ( )_{f,j} e^{i\omega(t)} df, \quad (3.12b)$$

and<sup>25</sup>

$$\underline{T}_M^{(N)}\{\ }_j \doteq \frac{1}{4\pi R_j} \int_{V_I} d\underline{\xi} \int_{-\infty}^{\infty} \alpha_I\left(\underline{\xi}, t - \tau - R_j/c + \frac{\hat{\underline{i}}_{Rj} \cdot \underline{\xi}}{c}\right) ( )_{\tau,j} d\tau \quad (3.13a)$$

or

$$\doteq \frac{1}{4\pi R_j} \int_{-\infty}^{\infty} e^{i\omega(t - R_j/c)} df \int_{V_I} A_I(\underline{\xi}, f)_j ( )_{f,j} e^{2\pi i f \frac{\hat{\underline{i}}_R \cdot \underline{\xi}}{c}} d\underline{\xi}$$

$$= \frac{1}{4\pi R_j} \int_{-\infty}^{\infty} \mathcal{A}'_I\left(\frac{\hat{\underline{i}}_{Rj}}{c} f/c, f | ( )_f\right)_j e^{i\omega(t - R_j/c)} df. \quad (3.13b)$$

Equations (3.12), (3.13) are the associated far-field (Fraunhofer) operators. The condition

$$\left( \pi L_{\max}^2 / \lambda_{\min} \right)_j \ll R_j \quad (3.14)$$

must be obeyed here [and for (3.8), (3.11)], where  $L_{\max}$  is the largest physical dimension of the interfering source's aperture  $A_I$ , and  $\lambda_{\min}$  is the shortest wavelength of the significant radiation from the source. For example, at  $f_0 \approx 100$  mc/sec. and  $L_{\max} = 1$  meter, we have  $\pi \cdot 1^2/3 \ll R$ , or  $R \gg 1$  meter for far-field operation.

#### B. Stochastic Field $N_I(t, R)$ and Random Process $X(t)$ :

The stochastic field representing the total effect of all interfering sources, considered over all possible representations of such sources in space, time, and parameter space, is simply the sum of the individual contributions

$$N_I(t, R) = \left\{ \sum_j \mathcal{L}(t, \underline{r}_j)_j \right\} ; \quad \left[ \mathcal{L}_j \text{ given by Eqs. (3.8)} \right] . \quad (3.15)$$

Again, for the far-field, (3.8) is used, where now  $\underline{r}_j = \underline{R} - \underline{R}_j$ , is the vector distance between the  $j^{\text{th}}$  source and some point  $P(R)$  in the field [here  $\underline{R}$  and  $\underline{R}_j$  are both directed toward the origin,  $O_R$ , cf. Fig. 3.1]. In operator notation (3.15) becomes

$$N_I(t, R) = \sum_j T_{Mj}^{(N)}(S_{Ij}) \equiv T_M^{(N)}(S_I) ; \quad T_M^{(N)}\{ \} \equiv \sum_j T_{Mj}^{(N)}\{ \} ; \quad (3.16a)$$

$$\equiv \sum_j \mathcal{L}_I(t, \underline{r}_j)_j = \sum_j \frac{1}{4\pi R_j} \int_{-\infty}^{\infty} \mathcal{A}'_I(\hat{i}_{Rj} f/c, f | S_I(f, \tau)) e^{i\omega(t - r_j/c)} df . \quad (3.16b)$$

Here  $\hat{i}_{Rj}$  is the unit vector -  $(\underline{R} - \underline{R}_j)/|\underline{R} - \underline{R}_j|$ , directed toward  $P(R)$ . Figure 3.2 illustrates the situation schematically, for a given configuration of sources during any short period of time.

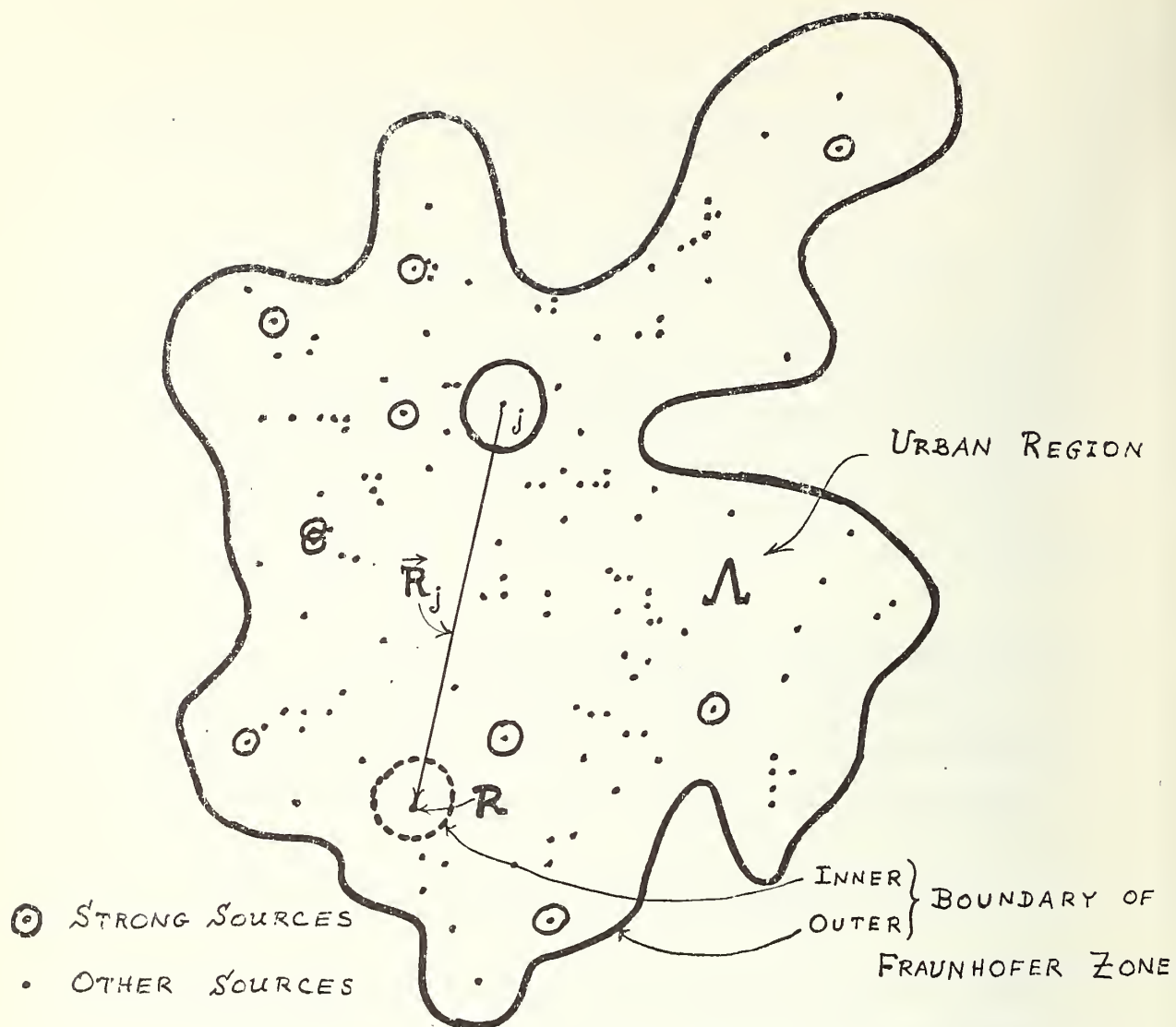


Figure 3.2. Schema of a typical distribution of urban noise sources and a receiver (R)

As mentioned in Sec. 2, we may divide the interference field into a background, or gaussian field  $G(t, \underline{R})$  (as the limit of a Poisson field), and the added field  $P(t, \underline{R})$  of a small number of strong, discrete sources, cf. Eq. (2.3a). The statistics of  $N_I(t, \underline{R})$  may then be determined by the methods outlined in Sec. 4 following. The important thing to observe here is that the physics and structure of the source enter explicitly through  $\mathcal{L}_j$  and  $S_{Ij}$  above.

Our principal interest, however, at this stage of the study is the interference process  $X(t)$  in the receiver. This is directly the sum

$$X(t) = \left\{ \sum_j U_j(t) \right\} ; \quad \left[ U_j \text{ given by Eqs. (3.11)} \right] , \quad (3.17)$$

which in operator formalism becomes [cf. (3.12), (3.13) in (2.1)]

$$\begin{aligned} X(t) &= \sum_j \underline{T}_{AR_j} \left\{ N_I(t, \underline{R}) \right\} \equiv \sum_j \underline{T}_{AR_j} \left\{ \mathcal{L}(t, \underline{R}_j) \right\} \\ &= \sum_j \int_{V_R} d\underline{\eta} \int_{-\infty}^{\infty} \alpha_R \left( \underline{\eta}, t - \tau - \frac{\hat{\underline{i}}_{Rj} \cdot \underline{\eta}}{c} \right) \mathcal{L} \left[ \tau, \underline{R}_j(\underline{\eta}) \right] d\tau, \end{aligned} \quad (3.18a)$$

or

$$= \sum_j \int_{-\infty}^{\infty} \alpha_R \left( -\frac{\hat{\underline{i}}_{Rj}}{c} f, f \right) \underline{\mathcal{F}}_t \left\{ \mathcal{L}_j \right\} e^{i\omega t} df , \quad (3.18b)$$

with  $\mathcal{L}_j$  once more given by (3.8),  $\underline{R}'_j \rightarrow \underline{R}_j$ , etc. As Eq. (2.4) indicates, we may divide  $X(t)$  into two processes, corresponding to the gaussian background,  $G(t)$ , and low-density Poisson process,  $P(t)$ , of the few, interfering sources, strong in the receiver, cf. Fig. 3.2. Again, the physics and the structure of the source enter explicitly here, through  $\mathcal{L}_j$  and  $S_{Ij}$ .

### C. Generalities and Modifications:

We need next to develop the model somewhat further, and to include such features as doppler due to relatively moving sources and receiver, narrow-bandedness, transient signal structures, and generalizations of the source mechanism. We include, also, an Example.

(1) Doppler:

Because of the possible relative motion between a typical interfering source and the receiver, a doppler distortion in the received waveform is introduced; (this, of course, affects desired, as well as undesired signals). We may calculate this doppler by a direct adaptation of the procedure of Sec. 4.4, Ref. 8. Letting:

$t_R$  = time at which leading edge of the wavefront (from source  $j$ ) reaches the receiver;

$t_S$  = time at which leading edge of the wavefront (from source  $j$ ) is emitted from the source,

we find that here, after modifying the Eqs. (4.22a-e) in Ref. 8 appropriately,

$$t_R = \frac{R/c + (1 - \beta_{SR}) t_S}{1 + \beta_{RS}} . \quad (3.19)$$

The delay between source and receiver is, therefore,

$$t_R - t_S \equiv R(t_R, t_S)/c = \frac{R/c - t_S(\beta_{SR} + \beta_{RS})}{1 + \beta_{RS}} . \quad (3.20)$$

Since  $t_S = t - \tau$ , where  $t$  is the "now" at the receiver, and  $\tau$  is the elapsed time since transmission, we get

$$\underline{\text{delay:}} \quad R_j(\tau, t)/c = \left[ \frac{R/c + (\beta_{SR} + \beta_{RS})(\tau - t)}{1 + \beta_{RS}} \right] \equiv a_j + (\tau - t)b_j , \quad (3.21)$$

for the now time-dependent delay  $R_j/c$  appearing in (3.11a). Here we have the normalized doppler velocities

$$\beta_{SR} \equiv \underline{v}_S \cdot \underline{\hat{r}}_R / c ; \quad \beta_{RS} \equiv -\underline{v}_R \cdot \underline{\hat{r}}_R / c , \quad (3.22)$$

where  $\underline{v}_S, \underline{v}_R$  are respectively uniform velocities of the source and receiver with respect to a stationary coordinate system (the same in which the velocity  $c$  is measured);  $\underline{v}_S$  and  $\underline{v}_R$  need not be coplanar, but they must be uniform. For the small platform and receiver velocities encountered in practise<sup>26</sup> (3.21)

reduces to:

$$\underline{\text{(small doppler):}} \quad R_j(\tau, t)/c \doteq T_{0j} + \left( \beta_{SR} + \beta_{RS} \right)_j (\tau - t) ; \quad (3.23)$$

$$T_0 \equiv R_j/c \left( 1 + \beta_{RS} \right) \doteq R_j/c .$$

It is convenient to define

$$\begin{aligned} \beta &\equiv \frac{\beta_{SR} + \beta_{RS}}{1 + \beta_{RS}} \left( \doteq \beta_{SR} + \beta_{SR} \right) ; \\ \mu &\equiv 1 + \epsilon \equiv (1 - \beta)^{-1} = \frac{1 + \beta_{RS}}{1 - \beta_{SR}} \doteq 1 + \left( \beta_{RS} + \beta_{SR} \right) \\ \therefore \quad \epsilon &\doteq \beta_{RS} + \beta_{SR} \doteq \beta \quad \therefore \quad 1 + \beta \doteq \mu \end{aligned} \quad (3.24)$$

for each  $j^{\text{th}}$  source vis-à-vis the receiver.

Let us now "dopplerize" our expressions (3.11) and (3.12). For (3.11a) we simply replace  $R_j/c$  therein by  $R_j(\tau', \tau)/c = T_{0j} + (\tau' - \tau) \beta_j$ , and the temporal argument of  $\alpha_I$  becomes  $(\tau - \tau') \left( 1 + \beta_j \right) - T_{0j} + \frac{1}{R_j} \cdot \xi/c$ . For (3.11b) we get

$$U_j(t) \doteq 4\pi R_j \left\{ \int_{-\infty}^{\infty} \mathcal{Q}_R \left( \frac{1}{R} (1 + \beta) f/c, (1 + \beta) f \right) \mathcal{Q}'_I \left( \frac{1}{R} f/c, f \mid S_I[(1 + \beta) f, \xi] \right) e^{-i\omega T_0 + i(1 + \beta)\omega t} df \right\}_j \quad (3.25)$$

and the operators (3.12b), (3.13b) become

$$\underline{T}_{AR} \{ \}_j = \left\{ \int_{-\infty}^{\infty} \mathcal{Q}_R \left( \frac{1}{R} (1 + \beta) f/c, (1 + \beta) f \right) ( )_f e^{i(1 + \beta)\omega t} df \right\}_j \quad (3.26a)$$

and

$$\underline{T}_M^{(N)} \{ \}_j \doteq \left\{ \frac{1}{4\pi R} \int_{-\infty}^{\infty} \mathcal{Q}'_I \left( \frac{1}{R} f/c, f \mid (1 + \beta) f \right) e^{i\omega[(1 + \beta)t - T_0]} df \right\}_j . \quad (3.26b)$$

With no relative motion,  $\beta = 0$  ( $\mu = 1$ ,  $\epsilon = 0$ ),  $T_0 \rightarrow R/c$  and (3.25), (3.26) reduce as expected to our previous results (3.11) - (3.13). [In the usual case of small

doppler, with comparatively narrow-band  $S_{Ij}$ , we may set  $\beta=0$  in  $\mathcal{Q}_R$ .]

## (2) Generalized Sources and Signals:

While the class  $\{S_I(t, \xi)\}$  of sources is probably adequate to account for many of the source mechanisms that produce the urban noise interference field, we can generalize it to include a much broader class, by making  $S_I$  time-variable, i.e., setting  $S_I = S_I(\tau, t; \xi | R_j)$ , etc. Here, the convention is to regard " $\tau$ ", the first variable, as the "memory" and " $t$ ", the second variable, as the time-variation of the waveform. Thus, the source function  $G_I$ , (3.4), now becomes

$$G_I(t; \xi | R_j)_j = \int_{-\infty}^{\infty} \alpha_I(\xi, t-\tau)_j S_I(\tau, t; \xi | R_j)_j d\tau \quad (3.27a)$$

$$= \int_{-\infty}^{\infty} A_I(\xi, f)_j S_I(f, t; \xi | R_j)_j e^{i\omega t} df, \quad (3.27b)$$

where  $S_I$  now [in (3.27b)] is the time-variable amplitude spectrum of  $S_I(\tau, t; \dots)_j$ . The relations (3.8), (3.9), (3.10), (3.11a) are formally unchanged, except that  $\mathcal{Q}'_I$  is now time-dependent, and  $S_I$  depends on  $t$ . The alternative form (3.11b), however, is modified, as is (3.25) when there is a doppler. The result for (3.25) becomes

$$U_j(t) \doteq \frac{1}{4\pi R_j} \left\{ \int_{-\infty}^{\infty} \mathcal{Q}_R\left(\frac{\hat{i}_R}{\sim} f/c, f\right) e^{i\omega t} df \int_{V_I} d\xi A_T(\xi, f') \int_{-\infty}^{\infty} \mathcal{Y}_I[(1+\beta)f'; f-(1+\beta)f'; \xi | R] \right. \\ \left. \times c^{2\pi i f' \hat{i}_R \cdot \xi / c} \cdot e^{-i\omega' T_0} df' \right\}_j \quad (3.28)$$

where  $\mathcal{Y}_I$  is the bi-frequency function<sup>27</sup> of the time-varying source  $S_I$ , viz.

$$\mathcal{Y}_I(f, \nu; \xi | R) \equiv \mathcal{F}_t \left\{ S_I(f, t; \xi | R) \right\} \equiv \mathcal{F}_t \mathcal{F}_\tau \left\{ S_I(\tau, t; \xi | R) \right\}. \quad (3.29)$$

[When  $S_I$  is not time-variable, then  $\mathcal{V}_I[(1+\beta)f'; f - (1+\beta)f', \underline{\xi} | \underline{R}] = S_I[(1+\beta)f'; \underline{\xi} | \underline{R}] \delta[f - (1+\beta)f']$ , and (3.28) then reduces directly to (3.25); with no doppler,  $\mathcal{V}_I = \mathcal{V}_I(f', f - f'; \underline{\xi} | \underline{R})$ .] The operators (3.26a,b) are readily obtained from (3.28) by inspection.

To facilitate handling of the general class of transient signals  $(S_{Ij})$ , we may replace the various Fourier integrals over frequency in (3.2) - (3.28) by suitable contour integrals, e.g.,

$$G_I(t; \underline{\xi} | \underline{R}_j) = \int_{-\infty i + d}^{\infty i + d} A_I(\underline{\xi}, s/2\pi i)_j S_I(s/2\pi i, t; \underline{\xi} | \underline{R}_j)_j \frac{ds}{2\pi i}, \quad (3.30)$$

etc., where  $(-\infty i + d, \infty i + d)$  is a Bromwich contour.<sup>28</sup>

When instead of the distributed sources assumed above we may use the approximation of a point source, then we have

$$S_I(\tau, \underline{\xi} | \underline{R}) = S_I(\tau | \underline{R}) \delta(\underline{\xi} - 0), \quad (3.31a)$$

or

$$S_I(\tau, t; \underline{\xi} | \underline{R}) = S_I(\tau, t | \underline{R}) \delta(\underline{\xi} - 0) \quad (3.31b)$$

for the time-varying sources above. The (far-) field  $\mathcal{L}_j$ , (3.8), is accordingly

$$\mathcal{L}(t, \underline{R}'_j) \doteq \frac{1}{4\pi \underline{R}'_j} \int_{-\infty}^{\infty} A_I(0, f)_j S_I(f | \underline{R}_j)_j e^{i\omega(t - \underline{R}'_j/c)} df, \quad (3.32)$$

and is thus omni-directional:  $\mathcal{Q}_I(0, f) = A_I(0, f)_j$  here. Similarly, we obtain for the received wave (3.11b)

$$\begin{aligned} \text{(pt. source): } U_j(t) &\doteq \frac{1}{4\pi \underline{R}_j} \int_{-\infty}^{\infty} \mathcal{Q}_R(\hat{i} \underline{R}_j f/c, f) \\ &\times \mathcal{Q}_I(0, f)_j S_I(f | \underline{R}_j)_j e^{i\omega(t - \underline{R}_j/c)} df, \end{aligned} \quad (3.33)$$

with corresponding, obvious modifications of the Eqs. (3.12), (3.13). Extending the point-source assumption to the cases of doppler and time-variable sources,

(3.31b), we find at once that the desired waveform (3.28) in the receiver becomes

$$\begin{aligned}
 \text{(pt. source): } U_j(t) &\doteq \frac{1}{4\pi R_j} \int_{-\infty}^{\infty} \mathcal{Q}_R \left( \frac{\hat{\epsilon}_j}{R_j} f/c, f \right) e^{i\omega t} df \\
 &\times \int_{-\infty}^{\infty} A_I(0, f')_j \mathcal{Y}_I \left[ (1+\beta)f'; f - (1+\beta)f' \right]_j e^{-i\omega' T_0} df'
 \end{aligned} \tag{3.34}$$

with corresponding forms for the operators  $\underline{T}_{AR_j}, \underline{T}_{MJ}^{(N)}$ , cf. (3.26a, b). [Note from (3.24) that for small doppler,  $1+\beta \doteq \mu$ .]

Finally, there remains the structuring of  $S_I(\tau, \xi | R)$ . While the details remain for verification by experiment, a plausible model of ignition noise is (for point sources here) the deterministic waveform

$$S_I(t | R)_j = A_{0j} \cos \omega_{0j} \left( t - \hat{\epsilon}_j \right), \quad t_0 < t < t_0 + T_S; \quad = 0, \text{ elsewhere} \tag{3.35}$$

where  $A_{0j}, \omega_{0j}, \hat{\epsilon}_j$  are time-invariant. The epoch  $\hat{\epsilon}_j$  (with respect to a cycle of the carrier  $f_0$ ) indicates a time relationship between the initiation of the ignition transient (3.35) and the time scale of the observer at the receiver. The time-delay between reception and the emission of the transient field from the  $j^{\text{th}}$  source is given by  $T_{0j}$ , cf. (3.23). This latter converts a distance  $(R_j)$  into a time-delay  $(T_{0j})$  by virtue of a finite velocity of propagation ( $c$ ), while the former  $(\hat{\epsilon}_j)$  establishes the coherence or incoherence of the ignition waveform with the observer's time-scale. Generally, we do not have to worry about  $\hat{\epsilon}_j$ : we include it, in effect in  $T_{0j}$ . [From the point of view of the ensemble,  $\{S_{Ij}\}$ ,  $A_0, \omega_0$ , also  $^{29} T_0$  and doppler  $1+\beta (\doteq \mu)$ , can be considered as independent random parameters, with some appropriate p.d.'s, ultimately to be established empirically.] Other plausible waveforms are:

$$\begin{aligned}
 S_I(\tau, R)_j &= A_{0j} e^{-\alpha_{0j} (t - t_1)} \cos \omega_{0j} \left( t - \hat{\epsilon}_j \right); \quad t_0 < t < t_0 + T_S \rightarrow \infty; \\
 &= 0, \text{ elsewhere} .
 \end{aligned} \tag{3.36}$$

For some other types of interference  $S_{I_j}(\tau, R)_j$  might belong to a (gaussian) noise process, or  $S_{I_j}$  might effectively persist for a long time ( $-\infty < t < \infty$ ), and so on. One task of the general study is to determine the  $S_{I_j}$  and study their statistical properties.

### (3) Narrow-band Sources; An Example:

For practical consideration most of the interfering sources are narrow-band: in this definition the bandwidth  $\Delta f_S$  of the source emission is  $O(10^{-1} f_0)$ , or smaller, where  $f_0$  is the carrier or central frequency of the band. Even in the so-called "wide-band" situations of measurement,  $\Delta f_S$  is only the order 1 or 2 megacycles, at carriers  $O(50 \text{ mc})$ ,<sup>4</sup> in part because of the great dynamic range required of the receiver to measure signals of such bandwidths without serious distortion.

The narrow-band (n.b.) condition, in conjunction with far-field operation, enables us to simplify our preceding, general relations considerably. In place of the real signal sources  $S_{I_j}$  used heretofore, it is convenient to employ the complex n.b. signal

$$S_I(\tau, t; \underline{\xi} | R) = \hat{S}_0(\tau, t; \underline{\xi}) e^{i\omega_0 \tau}; \quad \hat{S}_0 = A_0(\tau, t; \underline{\xi}) e^{i\varphi_0(\tau, t; \underline{\xi})}, \quad (3.37)$$

where  $\hat{S}_0$  is a complex envelope;  $A_0, \varphi_0$  are real envelopes and phases. Then (3.29), as it appears in (3.28), becomes

$$(\mathcal{V}_I)_0 = \int_{-\infty}^{\infty} S_0[(1+\beta)(f'-f_0), t; \underline{\xi}] e^{-2\pi i [f - (1+\beta)f'] t} dt, \quad (3.38)$$

where  $S_0$  is  $\mathcal{F}_{\tau} \left\{ \hat{S}_0 \right\}$ .

Next, if the apertures are essentially frequency-insensitive to changes in frequency in the region  $f_0 + \Delta f_S$ , where the n.b. source has any significant output, we can rewrite (3.28) with the help of (3.38) for distributed sources  $S_{I_j}$ , as

$$\begin{aligned}
 U_j(t) \doteq & \frac{e^{-i\omega_0 T_{0j}}}{4\pi R_j} \mathcal{Q}_R\left(\hat{\underline{\underline{i}}}_{R_j} f_0/c, f_0\right) \int_{-\infty}^{\infty} e^{i\omega t} df \int_{V_T} d\underline{\underline{\xi}} A_I(\underline{\underline{\xi}}, f_0) e^{i\omega_0 \hat{\underline{\underline{i}}}_{R_j} \cdot \underline{\underline{\xi}}/c} \\
 & \times \int_{-\infty}^{\infty} df' e^{-i\omega' T_0} \mathcal{Y}_I[(1+\beta) f'; f - (1+\beta) f_0 - (1+\beta) f'; \underline{\underline{\xi}} | R]_0, \quad (3.39)
 \end{aligned}$$

where now  $(\mathcal{Y}_I)_0$  is given by (3.38), with the appropriate arguments. The double integration over  $f$  and  $f'$ , in that order, gives us finally (with  $1+\beta \doteq \mu$  here):

$$U(t)_j \doteq \left\{ \frac{e^{i\mu\omega_0(t-T_0/\mu)}}{4\pi\mu R} \mathcal{Q}_R\left(\hat{\underline{\underline{i}}}_{R_j} f_0/c, f_0\right) \mathcal{Q}_I''\left[\hat{\underline{\underline{i}}}_{R_j} f_0/c, f_0 \middle| \hat{S}_0\left(t-T_0/\mu, t; \underline{\underline{\xi}} | R\right)\right] \right\}_j \quad (3.39a)$$

where  $\mathcal{Q}_I'' \equiv \mathcal{F}_{\underline{\underline{\xi}}} \left\{ \Lambda_I(\underline{\underline{\xi}}, f_0) \hat{S}_0\left(t-T_0/\mu, t; \underline{\underline{\xi}} | R\right) \right\}$  is another generalized beam pattern, cf. (3.9).

Now, if the drive  $S_I(\underline{\underline{\xi}} | R)_j$  at each element  $d\underline{\underline{\xi}}$  of the source's aperture is the same, i.e.,  $S_{Ij}$  is independent of  $\underline{\underline{\xi}}$ , Eq. (3.39) takes the still simpler form (with  $1+\beta \doteq \mu$ )

$$\begin{aligned}
 U_j(t) \doteq & \frac{e^{-i\omega_0 T_{0j}}}{4\pi R_j} \mathcal{Q}_R\left(\hat{\underline{\underline{i}}}_{R_j} f_0/c, f_0\right) \mathcal{Q}_I\left(\hat{\underline{\underline{i}}}_{R_j} f_0/c, f_0\right) \int_{-\infty}^{\infty} e^{i\omega t} df \\
 & \times \int_{-\infty}^{\infty} e^{-i\omega' T_0} \mathcal{Y}_I(\mu f', f - \mu f_0 - \mu f' | R)_0 df', \quad (3.40)
 \end{aligned}$$

wherein the beam-patterns are now factored out. Following the same steps used to obtain (3.39a), we integrate next over  $f$ , to get

$$\begin{aligned}
 U_j(t) \doteq & \frac{e^{-i\omega_0 T_{0j}}}{4\pi R_j} \mathcal{Q}_R\left(\hat{\underline{\underline{i}}}_{R_j} f_0/c, f_0\right) \mathcal{Q}_I\left(\hat{\underline{\underline{i}}}_{R_j} f_0/c, f_0\right) \\
 & \times \int_{-\infty}^{\infty} e^{-i\omega' T_0} Y_I(\mu f'; t)_0 e^{i\mu(\omega_0 + \omega')t} df' \quad (3.41)
 \end{aligned}$$

where  $Y_I(\underline{\underline{\xi}}; t)_0$  is the time-varying system function of the source (envelope), c.g.,

$$Y_I(f, t)_0 = \int_{-\infty}^{\infty} \hat{S}_0(\tau, t) e^{-i\omega\tau} d\tau = \hat{\mathcal{F}}_f^{-1} \left\{ \left( \mathcal{Y}_I \right)_0 \right\}, \quad \text{in (3.40).} \quad (3.41a)$$

Carrying out the integration over  $f'$  gives us finally the desired result

$$U_j(t) \doteq \left\{ \frac{e^{i\mu\omega_0(t-T_0/\mu)}}{4\pi\mu R} \hat{S}_0(t-T_0/\mu, t) \mathcal{A}_R\left(\frac{\hat{f}_0}{c}, 0\right) \mathcal{A}_I\left(\frac{\hat{f}_0}{c}, f_0\right) \right\}_j. \quad (3.42)$$

With the small doppler in force in all our applications, we can set  $\mu=1$  everywhere, except in  $\mu\omega_0$ , so that our narrow-band, complex waveform from the  $j^{\text{th}}$  source becomes finally the expected result<sup>30</sup>

$$U_j(t) \doteq \left\{ \frac{e^{i\mu\omega_0(t-T_0)}}{4\pi R} \hat{S}_0(t-T_0, t) \mathcal{A}_R\left(\frac{\hat{f}_0}{c}, f_0\right) \mathcal{A}_I\left(\frac{\hat{f}_0}{c}, f_0\right) \right\}_j. \quad (3.43)$$

If a point-source is assumed, then  $\mathcal{A}_T \rightarrow \mathcal{A}_I(0, f_0) = A_I(0, f_0)$ , a real constant, representing an omni-directional radiator. Also, if the source is not time-varying, we replace  $\hat{S}_0(t-T_0, t)$  by  $\hat{S}_0(t-T_0)$  in (3.43).

#### Example:

As a simple example, let us consider the ignition transient (3.35), with a point-source emitter, and a duration long enough so that  $S_{I_j}$  is narrow-band vis-à-vis the receiver's beam-pattern  $\mathcal{A}_R$ . In terms of the complex signal (3.37) we have

$$S_{I_j} = \begin{pmatrix} A_0 e^{-i\omega_0 \hat{\epsilon}} & e^{i\omega_0 \tau} \end{pmatrix}_j; \quad \therefore \hat{S}_{0j} = A_{0j} e^{-i\omega_0 \hat{\epsilon}_j}. \quad [t \in T_S]. \quad (3.44)$$

Equation (3.43) applies here, and with (3.44), is

$$U_j(t) \doteq \left\{ \frac{A_0 e^{i\mu\omega_0(t-T_0-\hat{\epsilon}_j)}}{4\pi R} A_I(0, f_0) \mathcal{A}_R\left(\frac{\hat{f}_0}{c}, f_0\right) \right\}_j, \quad [t_0 < t < t_0 + T_S] \quad (3.45)$$

= 0, elsewhere

including spreading loss, doppler, and receiving beam-pattern. Other examples are readily constructed in a similar way. Observe, of course, that the physical signal is always  $\Re U_j(t)$  here.

#### D. Summary Remarks:

In Section 3, we have shown how to determine the (scalar) interference field  $N_I(t, R)$  and more particularly, the typical waveform  $U_j$  into the receiver, following the receiving aperture. This has been done at both the general level and the specialized level. The former is needed for two reasons:

- (1) we will require a general model, in order to handle all the possible types of interference at some future stage of the study;
- (2) we need the general approach in order to establish the specific approximations and assumptions required for the special cases.

In all cases we include doppler, spreading loss, waveform structure, and pertinent geometric features, i. e., beam-patterns. At the specialized level, we have focussed on a typical example, characteristic of the kind of interference we may expect.

#### 4. STATISTICAL MODELS:

Here we shall derive the pertinent statistics for the Basic Statistical Model (BSM) described in Sec. 2. We shall also develop expressions for the first-order p.d., covariance function, and a variety of other moments of the equivalent model (ESM), based on the relations (2.5) - (2.10) presented earlier. Our principal interest here is in the received process,  $X(t)$ , whose physical structure is specified by Eqs. (3.17), (3.18) generally, and by Eqs. (3.25), (3.28), (3.33), (3.34), (3.39a), (3.42), (3.43), (3.45), in particular.

##### A. The (BSM) Poisson Process, $X(t)$ :

Let us express  $X(t)$  in somewhat more statistical detail than is indicated in Sec. 3: we write

$$X(t) = \sum_j U\left(t; \underline{\lambda}_j, \underline{\theta}_j\right)_j, \quad (4.1)$$

where the  $U_j$  are the typical waveforms derived in Sec. 3;  $\underline{\lambda}$  is a set of coördinate variables, and  $\underline{\theta}$  are a set of (time-independent) statistical parameters,

e.g., scale (amplitude), epoch, doppler frequency, etc., cf. the Example, (3.45), for instance. Then,  $U_j$  is the basic waveform of each random "event," as indexed by  $j$  — the "event" here is the generation of an ignition transient — and  $\lambda_j = (t_j, \theta_j, \varphi_j)$  are the coördinates of the point in space where the event takes place. This point is randomly located, in a small spatial element  $\Delta S_j$ , such that  $P(1|\Delta S_j) = \sigma_S(\lambda_j) \Delta S_j$  is the probability that exactly one such event occurs in  $\Delta S_j$ . With the requirement that  $P(N|\Delta S_j) \ll P(1|\Delta S_j)$ ,  $N \geq 2$ , for sufficiently small  $\Delta S_j$ , and the condition that in non-overlapping regions the number of events associated with the physical density,  $\sigma_S$ , of points where these events can occur, is independent for each region, a Poisson process of the number of events is defined, e.g.,

$$P_1(N|\Delta S_j) = (\sigma_S \Delta S_j)^N e^{-\Delta S_j \sigma_S} / N! \quad (N \geq 0) . \quad (4.2)$$

This, in turn, defines a Poisson process for  $X(t)$ . The key point here is that the "events" are all independent. The details of the derivation are given in Secs. (2.1), (3.1), Ref. 8; we present the results here only:

- (1) It is found that the  $n^{\text{th}}$  order characteristic function (c.f.) for  $X(t)$ , considered at the time  $t_1, \dots, t_n$ , is

$$\begin{aligned} F_n(i\xi_1, t_1; i\xi_2, t_2; \dots; i\xi_n, t_n | \Lambda) \\ = \exp \left[ \int_{\Lambda} \rho(\underline{\lambda}) \left\langle \exp i \left( \sum_{\ell=1}^n \xi_{\ell} U(t_{\ell}; \underline{\lambda}, \underline{\theta}) \right) - 1 \right\rangle_{\underline{\theta}} d\underline{\lambda} \right], \quad n \geq 1 . \end{aligned} \quad (4.3)$$

The corresponding  $n^{\text{th}}$  order p.d.,  $W_n$ , is the  $n$ -fold Fourier transform of (4.3). Here the process "density"  $\rho$  is a non-negative function, and the operator  $\hat{\rho} \equiv \int_{\Lambda} \rho(\underline{\lambda}) ( ) d\underline{\lambda}$  is a counting functional, which adds up all the contributions of the individual sources, without regard to their magnitude;  $\Lambda$  is the region in which the sources lie, for example, as indicated in Fig. 3.2.

The first-order c.f. is, directly:

$$F_1(i\xi_1, t_1) = \exp \left\{ \int_{\Lambda} \rho(\lambda) \left\langle e^{i\xi_1 U(t_1; \lambda, \theta)} - 1 \right\rangle_{\theta} d\lambda \right\}, \quad (4.4)$$

with higher-order c.f.'s similarly obtained from (4.3).

The chief difficulty with (4.3) and its transform is their analytic complexity. Although this is an "exact" model of the urban radio noise environment under the basic assumptions presented earlier (in Sec. 2), it is not practically amenable to closed-form results in the distributions, which severely limits its analytic usefulness whenever these are directly required (i.e., in system design, etc.). However, in the case of the moments, and particularly those of the first- and second-order, closed forms are readily obtained, and in this respect our model is practically useful, particularly in conjunction with the equivalent model (ESM) (Sec. 2). Finally, note that in general, because of the distributed nature and secular variation of the sources (with time)  $X(t)$  is not strictly a stationary process. (Sec. 4-(8) below, however.)

(2) As we pointed out in Sec. 2, we can express  $X(t)$  as the sum of two independent Poisson processes,  $X_B + X_D$ , with densities  $\rho_B$  and  $\rho_D$ . The former represents a high-density process, which is asymptotically gaussian. Rewriting (4.3), since  $\rho \equiv \rho_B + \rho_D$  here, we have

$$\begin{aligned} (F_n)_{G+P} &= \exp \left[ \int_{\Lambda_B} \rho_B \left\langle \exp \left( i \sum_{\ell} \xi_{\ell} U_{B\ell} \right) - 1 \right\rangle_{\theta} d\lambda \right] \\ &\quad \times \exp \left[ \int_{\Lambda_D} \rho_D \left\langle \exp \left( i \sum_{\ell} \xi_{\ell} U_{D\ell} \right) - 1 \right\rangle_{\theta} d\lambda \right] \end{aligned} \quad (4.5a)$$

$$= (F_n)_G \cdot (F_n)_P. \quad (4.5b)$$

Furthermore, expanding  $(F_n)_G$  in an Edgeworth series<sup>31</sup> gives us

$$\left(F_n\right)_G \cong \exp \left[ -\tilde{\xi} \tilde{K}_B \tilde{\xi} / 2 + i \tilde{\xi} \langle X_B \rangle \right], \quad (4.6)$$

where  $\tilde{\xi} = [\xi_1, \dots, \xi_n]$  is a row vector,  $\langle X_B \rangle = \langle X_B \rangle, \dots, \langle X_{nB} \rangle$  a (row) vector of mean values, and

$$\tilde{K}_B = \left[ \langle X(t_k) X(t_\ell) \rangle - \langle X(t_k) \rangle \cdot \langle X(t_\ell) \rangle \right]_B, \quad [k, \ell = 1, \dots, n], \quad (4.6a)$$

is an  $(n \times n)$  covariance matrix of the process,  $X_B$ . The process  $X_P$  remains Poisson, with a low-density.

(3) The moments of  $X(t) = X_B(t) + X_D(t)$  [ $= G(t) + P(t)$ , cf. (2.3b)] are readily found from (4.3), or (4.5), in the usual way by differentiating the characteristic function. We have specifically,

$$\langle X(t) \rangle = -i \frac{d}{d\xi_1} F_1 \Big|_{\xi_1=0} = \int_{\Lambda} \rho(\lambda) \left\langle U(t_1; \lambda, \theta) \right\rangle_{\theta} d\lambda \quad (4.7a)$$

$$= \int_{\Lambda_B} \rho_B(\lambda) \left\langle U_B(t_1; \lambda, \theta) \right\rangle_{\theta} d\lambda + \int_{\Lambda_D} \rho_D(\lambda) \left\langle U_D(t_1; \lambda, \theta) \right\rangle_{\theta} d\lambda; \quad (4.7b)$$

and

$$\begin{aligned} K_X(t_1, t_2)_{(BSM)} &\equiv \left[ -\frac{\partial^2}{\partial \xi_1 \partial \xi_2} F_2 - \left( \frac{\partial}{\partial \xi_1} F_1 \right) \left( \frac{\partial}{\partial \xi_2} F_1 \right) \right]_{\xi_1, \xi_2=0} \\ &= \int_{\Lambda} \rho(\lambda) \left\langle U(t_1; \lambda, \theta) U(t_2; \lambda, \theta) \right\rangle_{\theta} d\lambda = K_X(t_1, t_2)_B + K_X(t_1, t_2)_D, \end{aligned} \quad (4.8)$$

cf. (2.9), for the covariance function. For the mean intensity, we have

$$\begin{aligned} \langle X(t_1)^2 \rangle &= \left[ -\frac{\partial^2}{d\xi_1^2} F_1 \right]_{\xi_1=0} = \int_{\Lambda_B} \rho_B(\lambda) \left\langle U_B(t_1; \lambda, \theta)^2 \right\rangle_{\theta} d\lambda \\ &+ \int_{\Lambda_D} \rho_D(\lambda) \left\langle U_D(t_1; \lambda, \theta)^2 \right\rangle_{\theta} d\lambda, \end{aligned} \quad (4.9)$$

and we proceed similarly for the higher moments of all orders and degrees.

[We shall need to examine the higher-order, higher-degree moments in our later studies, when we seek to develop the equivalent model (ESM) more fully.]

- (4) The behavior of  $X(t)$ , in the BSM, for large amplitudes is not at all easy to determine from (4.3) or its Fourier transform. However, for small amplitudes [i.e., values of  $X$  small compared to the occasional large values of  $X$  when the impulsive part,  $X_D$ , dominates], which occur most of the time and which are attributable to the general background portion,  $X_B$ , we can show the expected gaussian character.

Here we shall consider only the first-order density ( $n=1$ ) with zero mean, as an illustration: from (4.4) and (4.5) we can write

$$\left(F_1\right)_{G+P} = e^{-\xi_1^2 \sigma_B^2 / 2 - \xi_1^2 \sigma_D^2 / 2} \sum_{m=2}^{\infty} \left[ \left(\Gamma_{2m}\right)_B + \left(\Gamma_{2m}\right)_D \right] \xi_1^{2m} (-1)^m / (2m)! , \quad (4.10)$$

where

$$\left(\Gamma_{2m}\right)_{B,D} = \int_{\Lambda_{(B,D)}} \rho_{B,D}(\lambda) \left\langle U_{B,D}^{2m}(t_1; \lambda, \theta) \right\rangle_{\theta} d\lambda ; \quad (4.11)$$

$$\sigma_{B,D}^2 = \int_{\Lambda_{(B,D)}} \rho_{(B,D)}(\lambda) \left\langle U_{B,D}^2 \right\rangle_{\theta} d\lambda .$$

Now the summation in (4.11) can be replaced by the finite series, with remainder, of the expansion of  $\exp(-\xi_1^2 \sigma_G^2 / 2)$ , since (4.11) can be alternatively written

$$\left(F_1\right)_{G+P} = e^{-\xi_1^2 (\sigma_B^2 + \sigma_D^2) / 2} \cdot \exp \left[ \frac{\xi_1^4}{4!} \Gamma_4 \left( \frac{d^4}{d\xi_1^4} F_G \right)_{\theta \xi_1} \right] ; \quad 0 < \theta = \theta(\xi_1) < 1 . \quad (4.12)$$

Now  $\lim |\xi_1| \rightarrow \infty$  corresponds to  $|X| \rightarrow 0$ , and here we have

$$\lim_{|\xi_1| \rightarrow \infty} \exp \frac{\xi_1^4}{4!} \Gamma_4 \left( \frac{d^4}{d\xi_1^4} F_G \right)_{\theta \xi_1} = \lim_{|\xi_1| \rightarrow \infty} \exp \left[ \frac{\xi_1^4}{4!} H_4(\theta \xi_1) e^{-\theta^2 \xi_1^2 \sigma_G^2 / 2} \right] \rightarrow 1 , \quad (4.13)$$

(with  $H_4$  an Hermitian polynomial), so that

$$\lim_{|\xi_1| \rightarrow \infty} \left( F_1 \right)_{G+P} = \lim_{|\xi_1| \rightarrow \infty} e^{-\xi_1^2 \sigma_{G+P}^2 / 2}, \quad \sigma_{G+P}^2 \equiv \sigma_G^2 + \sigma_P^2 \quad (4.14)$$

which is the expected gaussian behavior at small values of  $X (= X_B + X_P)$ .

- (5) The process density  $\rho$  now needs to be established from the controlling geometry. Here we shall assume first that all the interfering sources lie on a single surface (not necessarily flat), which reflects the fact that vehicular traffic moves on the streets of the urban region in question. The receiver, however, may be on or above this surface. The process density  $\rho$  is accordingly specified by

$$\rho_{S_{\sim}}(\lambda) d\lambda = \sigma_{S_{\sim}}(\lambda) dS, \quad (4.15)$$

and since  $d\lambda = dt d\varphi$ , ( $ct = R$ ), cf. Fig. 4.1, and  $\lambda = [t, \theta(t, \varphi), \varphi]$  are the coördinates of a point in the surface  $\Lambda$  that is available to the receiver at  $O_R$ . Thus, the shaded region in Fig. 4.1 is that portion of the overall urban region within the beam  $\mathcal{A}_R$  of the receiver. Accordingly, from (4.15) we can write

$$\rho_{S_{\sim}}(\lambda) = \sigma_S \left[ t, \theta_R(t, \varphi_R), \varphi_R \right] dS / dt d\varphi_R. \quad (4.16)$$

Following the analysis of Sec. 3.1, Ref. 8, with  $L=0$  therein, we find that

$$\rho_{S_{\sim}}(\lambda) = \sigma_S(t, \theta_R, \varphi_R) t c^2, \quad ct \geq h_R, \quad (4.17)$$

with

$$\cos \theta_R = h_R / R = h_R / ct. \quad (4.18)$$

[If the receiver is in the same surface as the sources (and that surface is flat, cf. Fig. 4.1), then  $\theta_R = \pi/2$ , ( $h_R = 0$ ).] Here  $\sigma_S$  is the physical density of the radio noise sources, i. e., the number per unit area, a quantity which needs to be determined for different urban regions and different times of day, week, etc., as part of the experimental portion of the study.

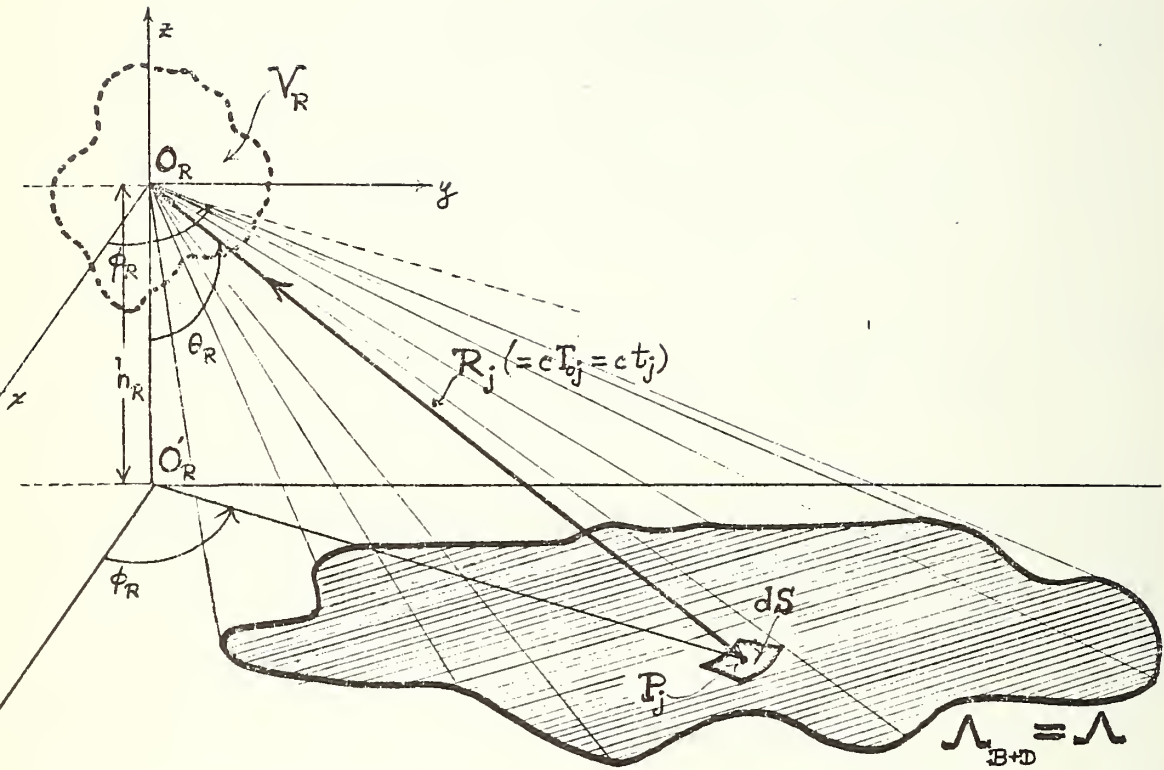


Figure 4.1. Geometry of an interfering source (at  $P_j$ ) and a receiver at height ( $h_R \geq 0$ ), for an urban region  $\Lambda$  containing independent radio noise sources. (Exaggerated in the vertical direction.)

Fields

- (6) The Poisson Noise  $N_I(t, \underline{R}) = G(t, \underline{R}) + P(t, \underline{R})$ , cf. (2.3a) are determined in similar fashion. The  $n^{\text{th}}$  order c.f. of  $N_I(t, \underline{R})$ , cf. (3.16), analogous to (4.3), becomes here

$$F_n(i\zeta_1, t_1, \underline{R}_1; \dots; i\zeta_n, t_n, \underline{R}_n | \Lambda_S) = \exp \left[ \int_{\Lambda_S} \rho(\underline{\lambda}) \exp \left\langle i \left( \sum_{\ell=1}^n \zeta_{\ell} \mathcal{L}(t_{\ell}, \underline{R}_{\ell}; \underline{\lambda}, \underline{\theta}) \right) - 1 \right\rangle_{\underline{\theta}} d\underline{\lambda} \right], \quad (4.19)$$

where now  $\mathcal{L}$  plays the rôle of  $U$  earlier, with  $\underline{R}'_j$  therein replaced by  $\underline{r}_j = \underline{R} - \underline{R}_j$ , for each  $\ell=1, \dots, n_S$ , cf. (3.8), and  $\Lambda_S$  is the domain of all the sources, not just those "viewed" by the receiver, as is the case in (1) - (5).

We may proceed as in (2) - (5) above. For instance, the lower-order moments of this ambient noise field are

$$\left\langle N_I(t, \underline{R}) \right\rangle = \int_{\Lambda_S} \rho(\underline{\lambda}) \left\langle \mathcal{L}(t, \underline{R}; \underline{\lambda}, \underline{\theta}) \right\rangle_{\underline{\theta}} d\underline{\lambda}, \quad (\underline{R}'_j \rightarrow \underline{r}_j = \underline{R}_1 - \underline{R}_j), \quad (4.20)$$

for the mean, and for the covariance function of the field, we have

$$K_{N_I}(t_1, \underline{R}_1; t_2, \underline{R}_2) = \int_{\Lambda_S} \rho(\underline{\lambda}) \left\langle \mathcal{L}(t_1, \underline{R}_1; \underline{\lambda}, \underline{\theta}) \mathcal{L}(t_2, \underline{R}_2; \underline{\lambda}, \underline{\theta}) \right\rangle_{\underline{\theta}} d\underline{\lambda}, \quad (4.21)$$

with  $\underline{R}'_{1j} \rightarrow \underline{r}_{1j} = \underline{R}_1 - \underline{R}_j$ , etc. in  $\mathcal{L}$ . The mean intensity at  $P(\underline{R})$  is likewise

$$\left\langle N_I(t, \underline{R})^2 \right\rangle = \int_{\Lambda_S} \rho(\underline{\lambda}) \left\langle \mathcal{L}(t, \underline{R}; \underline{\lambda}, \underline{\theta})^2 \right\rangle_{\underline{\theta}} d\underline{\lambda}, \quad (4.22)$$

and so on for the other moments. We can parallel the analysis of (2) - (4) for  $X(t)$ , here for  $N_I$ , in similar fashion; the details are left to a later study. For the surface distribution of ambient sources sketched in Fig. 4.1, the process density  $\rho$  is given by (4.17), (4.18).

(7) Some Special Results; The Narrow-band Process:

Let us assume narrow-band sources, small doppler, a non-time-varying

signal, and far-field reception, so that (3.43) applies for  $U_j$ . Furthermore, we have

$$\langle U_j \rangle = 0, \quad (4.23)$$

since the epoch  $\hat{\varepsilon}_j$  [cf. (3.45) and comments following (3.35)] is assumed randomly and uniformly distributed  $(0, 2\pi)$ . In fact, all odd, first-order moments of  $U_j$  vanish, e.g.,  $\langle U_{(t)}^{2m+1} \rangle = 0$ , not unexpectedly here. However, the covariance function  $K_X(t_1, t_2)$  is non-vanishing. For narrow-band processes here we have,<sup>32</sup> generally [for real  $X(t)$ ]:

$$K_X(t_1, t_2) = \langle X(t_1) X(t_2) \rangle = R_X(t_1, t_2) \cos \omega_0 \tau + \Lambda_X(t_1, t_2) \sin \omega_0 \tau \quad (4.24a)$$

$$= \mathcal{R}e \left\{ \left( R_X - i \Lambda_X \right) e^{i \omega_0 \tau} \right\}, \quad \tau \equiv t_2 - t_1 \quad (4.24b)$$

$$= \frac{1}{2} \mathcal{R}e \left\{ B_X(t_1, t_2)^* e^{i \omega_0 \tau} \right\} \quad (4.24c)$$

where  $B_X(t_1, t_2)$  is defined by

$$B_X(t_1, t_2) \equiv 2 \left( R_X + i \Lambda_X \right), \quad (4.25)$$

with

$$R_X = \frac{1}{2} \mathcal{R}e B_X; \quad \Lambda_X = -\frac{1}{2} \mathcal{I}m B_X.$$

Specifically, for the present Poisson cases we have, now for the complex  $U$  of Sec. 3C-3 above,

$$B_X(t_1, t_2) = e^{i \omega_0 \tau} \int_{\Lambda} \rho(\underline{\lambda}) \left\langle U(t_1; \underline{\lambda}, \underline{\theta}) U(t_2; \underline{\lambda}, \underline{\theta})^* \right\rangle_{\underline{\theta}} d\underline{\lambda}. \quad (4.26)$$

Now using (3.43), (4.17), and  $\underline{\lambda} = (\underline{\lambda}, \varphi_R)$ ,  $d\underline{\lambda} = d\underline{\lambda} d\varphi_R$ , with  $\lambda = R/c$  here, we get for (4.26)

$$B_X(t_1, t_1 + \tau) = \frac{1}{(4\pi)^2} \int_{\Lambda} |\mathcal{A}_R|^2 |\mathcal{A}_I|^2 \frac{\sigma_S(\lambda, \varphi_R)}{\lambda} \\ \times \left\langle e^{i\omega_0 \varepsilon \tau} \hat{S}_0(t_1 - \lambda; \underline{\theta}) \hat{S}_0(t_1 + \tau - \lambda; \underline{\theta})^* \right\rangle_{\underline{\theta} = \varepsilon, \omega_0, \dots} d\lambda d\varphi_R, \quad (4.27)$$

with  $\hat{\mathbf{i}}_R$  in  $\mathcal{A}_R$ ,  $\mathcal{A}_I$ , cf. (3.43) given by

$$\hat{\mathbf{i}}_R = - \left[ \hat{\mathbf{i}}_X \cos \varphi_R \sin \theta_R + \hat{\mathbf{i}}_Y \sin \varphi_R \sin \theta_R + \hat{\mathbf{i}}_Z \cos \theta_R \right]; \quad (4.28)$$

$$\theta_R = \cos^{-1} (h_R / c\lambda) .$$

Here the averages indicated by  $\langle \rangle_{\underline{\theta}}$  are over doppler ( $\varepsilon$ ), cf. (3.24), over "carrier" frequency  $f_0$ , which also appears in the beam patterns, cf. (3.43) again, over epoch ( $\hat{\varepsilon}$ ) and amplitude ( $A_0$ ), contained implicitly in the complex envelope  $\hat{S}_0$  [cf. (3.45) in a particular instance]. As is evident from (4.24) - (4.27),  $X(t)$  is not in general a wide-sense stationary process, since  $K_X(t_1, t_2) \neq K_X(|t_2 - t_1| = \tau)$  here, unless certain conditions, readily met in practice are obeyed [vide 4-(8) below].

With a uniform beam in the receiver and point sources  $[\mathcal{A}_I \rightarrow A_I(0, f_0)]$ , both insensitive to frequency over a band  $\pm \Delta f$  about  $\bar{f}_0$ , the average carrier frequency, Eq. (4.27) may be simplified to

$$B_X(t_1, t_1 + \tau) = \frac{|\mathcal{A}_R|^2}{(4\pi)^2} |A_I(0, \bar{f}_0)|^2 \int_{\Lambda} \frac{\sigma_S(\lambda, \varphi_R)}{\lambda} \\ \times \left\langle e^{i\omega_0 \varepsilon \tau} \hat{S}_0(t_1 - \lambda; \underline{\theta}) \hat{S}_0(t_1 + \tau - \lambda; \underline{\theta})^* \right\rangle_{\varepsilon, f_0, \dots} d\lambda d\varphi_R, \quad (4.29)$$

with proper attention to the domain  $\Lambda$  implied by the nonvanishing of  $|\mathcal{A}_R|$ .

If  $U_B \neq U_D$ , cf. (2.9), and certainly  $\rho_B \neq \rho_D$ , then  $B_X$  becomes

$$B_X(t_1, t_2) = B_X(t_1, t_2)_B + B_X(t_1, t_2)_D, \quad (4.30)$$

where each  $B_X$  in (4.30) is a term of the form (4.27);  $\sigma_S = \sigma_B + \sigma_D$ , as well, with  $\sigma_B \gg \sigma_D$ . In this way, by an anatomization of the waveform we arrive at a corresponding anatomization of the statistics. From an experimental point of view the covariance function is also an important descriptor of the noise process.

Finally, we mention that there is a spectral statistic associated with  $K_X$  here. This is the cointensity spectrum [Ref. 8, Sec. 8.5], defined by the double Fourier transform

$$\mathcal{K}_X(f_1, f_2) \equiv \lim_{T \rightarrow \infty} \frac{1}{T} \int_{-T}^T \int_{-T}^T \left\langle K_X(t_1, t_2) \right\rangle e^{i\omega_1 t_1 - i\omega_2 t_2} dt_1 dt_2. \quad (4.31)$$

This quantity measures the amount of statistical correlation between components of  $X(t)$  at frequency  $f_1$  and frequency  $f_2$ . If  $X(t)$  is stationary (as it can be approximated in many important cases [vide 4-(8) following]), then (4.31) reduces to

$$\mathcal{K}_X(f_1, f_2) = \mathcal{K}_X(f_1) \delta(f_2 - f_1), \quad (4.32)$$

where  $\mathcal{K}_X(f)$  is the familiar (auto-) spectral (intensity) of the (now stationary) process  $X(t)$ . The auto- and cointensity spectra are also quantities of experimental interest in building workable models of this class of radio noise.

- (8) Macrostationarity: The interfering radio noise process  $X(t)$  is not strictly or even wide-sense stationary, because of (a), the finite duration of the emitted signals, and (b), the secular variation of source density ( $\rho$ ) and signal level with geography ( $\Lambda$ ) and time of day, week, etc. However, in most instances  $X(t)$  can be regarded as effectively stationary in the wide sense at least, from the viewpoint of the usual observer, whose receiving system is influenced by this noise. This is because (1), the number of such sources in  $\Lambda$  is large enough that there is always at least one or more emissions going on at any given time, and (2), the average emission,  $S_I$ , has a duration long compared to the time it takes to propagate over the maximum effective distance  $\lambda_{\max}$  between source and receiver in the domain of possible sources,  $\Lambda$ . Beyond

this distance we say that the spreading loss ( $\sim \lambda^{-2}$  in energy) is so great that the source projects negligible interfering energy into the receiver. Thus, if the maximum effective dimension is  $O(30 \text{ km, i.e., } \lambda_{\max} = 30 \text{ km/}$  ( $c = 3 \cdot 10^5 \text{ km/sec.}) = 0.1 \text{ msec.}$ , or less, a dimension very probably on the large side in practice, a 1 msec. emission will persist for ten times the time it takes the wavefront to cover  $\lambda_{\max}$ . The result is what we call here a macrostationary process, i.e., one that is not truly stationary in the analytical sense but which can be treated as such for time periods during which the secular changes in the source conditions are small. Thus, in a period of heavy traffic, say 4-6 p.m. of a city weekday, we may expect that the secular time scale is  $O(\frac{1}{2} \text{ hr.} - 1 \text{ hr.})$ , much longer than a typical signal period, and certainly much longer than any one (non-zero) signal duration and  $\lambda_{\max}$ .

Mathematically, the conditions for macrostationarity may be established as follows: we start with (4.27), for the usual narrow-band signals, and expand the signal envelope  $\hat{S}_0$ , viz.  $\hat{S}_0(t-\lambda; \underline{\theta}) \doteq \hat{S}_0(t; \underline{\theta}) - \lambda \dot{\hat{S}}_0(t; \underline{\theta})$ , so that a typical condition for neglecting  $\dot{\hat{S}}_0$  during the time  $\lambda_{\max}$  is

$$\left[ \left\langle \hat{S}_0(t; \underline{\theta})^2 \right\rangle \right]^{1/2} \gg \lambda_{\max} \left[ \left\langle \dot{\hat{S}}_0(t; \underline{\theta})^2 \right\rangle \right]^{1/2} ; \quad (4.33)$$

this defines our characteristic, interfering signal of "long duration" here. Accordingly, we can now replace  $\hat{S}_0(t_{1,2} - \lambda; \underline{\theta})$  by  $\hat{S}_0(t_{1,2}; \underline{\theta})$  in (4.27), which in (4.24c) in turn, allows us to write for the covariance of the process

$$K_X(t_1, t_1 + \tau) \doteq C_\Lambda \mathcal{R}e \left\{ F_1^* (i\omega_0 \tau)_\epsilon e^{i\omega_0 \tau} \left\langle \hat{S}_0(t_1; \underline{\theta})^* \hat{S}_0(t_1 + \tau; \underline{\theta}) \right\rangle_{\underline{\theta}} \right\} , \quad t_2 = t_1 + \tau , \quad (4.34)$$

with  $(F_1)_\epsilon \equiv \left\langle \exp(i\omega_0 \tau \epsilon) \right\rangle_\epsilon$  the characteristic function of the doppler,  $\epsilon$ , where it is assumed that  $f_0$  is known,<sup>33</sup> and where

$$C_\Lambda = \frac{1}{2(4\pi)^2} \int_\Lambda |\mathcal{A}_R|^2 |\mathcal{A}_I|^2 \sigma_S(\lambda, \varphi_R) d\lambda d\varphi_R / \lambda , \quad (4.34a)$$

a (real) constant ( $> 0$ ), depending only on the geometry of the receiver vis-à-vis

the interfering sources. Next, if the epochs of initiation of the  $S_I$  are uniformly distributed in time, over a period comparable to or larger than the mean duration of a typical interfering source, a situation entirely reasonable in practice, we see that

$$\begin{aligned} \left\langle \hat{S}_0(t_1; \underline{\theta})^* \hat{S}_0(t_1 + \tau; \underline{\theta}) \right\rangle_{\varepsilon; \underline{\theta}} &= \frac{1}{T_S} \int_{-\infty}^{\infty} \left\langle \hat{S}_0(t_1; \underline{\theta}')^* \hat{S}_0(t_1 + \tau; \underline{\theta}') \right\rangle_{\underline{\theta}} dt \\ &\equiv K_{S_0}^*(\lambda) , \end{aligned} \quad (4.35)$$

the (complex) covariance of the source envelope; then  $\underline{\theta} = (\varepsilon, \underline{\theta}')$ ,  $\underline{\theta}'$  = amplitude, durations, etc. Thus, we have for (4.34)

$$K_X(t_1, t_1 + \tau) \doteq C_\Lambda \mathcal{R}e \left\{ F_1^*(i\omega_0 \tau) e^{i\omega_0 \tau} \hat{K}_{S_0}(\tau)^* \right\} \doteq K_X(\tau) , \quad (4.36)$$

which is a function of  $\tau$  only, and hence,  $X$ , in the above sense, is "macrostationary." With ignorable doppler, (4.36) reduces to the still simpler form

$$\text{(no doppler):} \quad K_X(t_1, t_1 + \tau) \doteq C_\Lambda \mathcal{R}e \left\{ e^{i\omega_0 \tau} \hat{K}_{S_0}(\tau)^* \right\} . \quad (4.37)$$

For a typical interfering signal like (3.35), we get at once

$$K_X(t_1, t_1 + \tau) \doteq A_0^2 C_\Lambda \left\langle \cos \omega_0 (1 - \varepsilon) \tau \right\rangle_\varepsilon \doteq A_0^2 C_\Lambda \cos \omega_0 \tau , \quad (4.38)$$

this last for ignorable doppler. The covariances for other, more complex interfering signals are readily found in similar fashion.

Finally, this property of macrostationarity is very important for experimental measurement, for it allows us to construct an experimental data ensemble directly from a continuous record of the output of a single receiver subject to this mixed-process (Gauss and Poisson) interference. The procedure is to divide the record up into equal intervals long compared to the reciprocal of the bandwidth of the interference (as observed in the receiver), but short compared to the (much longer) period during which secular variations in the traffic intensity,

and hence ignition noise level and character, begin to manifest themselves. Before we calculate from these ensemble data the various desired statistics (moments, p.d.'s, etc.), it is necessary to establish the validity of the data, e.g., we must verify that we have a valid ensemble — one where the member functions are independent and constitute a homogeneous set. For these purposes various statistical tests are available; illustrative applications have been discussed, for example, by Middleton<sup>34</sup> in connection with ocean reverberation, and by Plemons,<sup>35</sup> in an experimental study of the scattering of acoustic waves from lake surfaces. Applications of these concepts to our present problem is immediate and direct.

### B. The Equivalent Model for X(t):

As we noted in Sec. 2, the equivalent statistical model (ESM) is postulated to have the form

$$X(t) = a(t) Z(t) , \quad (4.39)$$

cf. (2.5), where  $Z(t)$  is gaussian ( $\langle Z \rangle = 0$ ), and  $a(t)$  is slowly-varying vis-à-vis  $Z(t)$ , which is narrow-band about some carrier frequency  $f_0$ , determined by the receiver. The process  $a(t)$  is also zero-mean, i.e.,  $\langle a \rangle = 0$ . Both  $a$  and  $Z$  are statistically independent.

First, let us show that for small amplitudes of  $X$ ,  $X$  is gaussian, at least in the first-order, as it must be to be consistent with the Basic Model [cf. A, (4) above]. Since  $Z(t)$  is normal, we can write the first-order p.d. of  $X$  as

$$W_1(X)_{aZ} = \int_{-\infty}^{\infty} \left\langle e^{-\xi^2 a^2 \sigma_Z^2 / 2} \right\rangle_a e^{-i\xi X} \frac{d\xi}{2\pi} , \quad (\langle Z \rangle = \langle a \rangle = 0) . \quad (4.40)$$

Let  $b = 1/a$ ,  $[-\infty < a < \infty$ , and  $\therefore -\infty < b < \infty]$ ; then (4.40) becomes

$$W_1(X)_{aZ} = \left\langle \frac{e^{-X^2 / 2a^2 \sigma_Z^2}}{\sqrt{2\pi\sigma_Z^2 a^2}} \right\rangle_a = \left\langle \frac{|b| e^{-b^2 X^2 / 2\sigma_Z^2}}{\sqrt{2\pi\sigma_Z^2}} \right\rangle_b . \quad (4.41)$$

Since  $X$  is small, we expand (4.41) and get (with  $K$  a normalizing constant)

$$W_1(X)_{aZ} = K \left\langle \left[ \langle |b|^{-1} \rangle - |b| X^2 / 2\sigma_Z^2 + \dots \right] \right\rangle_b \doteq \frac{e^{X^2/2A^2}}{\sqrt{2\pi A^2}} , \quad (4.42a)$$

$$A^2 = \sigma_Z^2 / \langle |b| \rangle \langle |b|^{-1} \rangle^{-1} , \quad (4.42b)$$

which shows the expected normality for small amplitudes.

For large amplitudes ( $|X| \rightarrow \infty$ ) it is known empirically that  $W_1(X)$  falls off much more slowly than if  $X(t)$  were gaussian only. This is because of the more or less discrete, large impulsive transients, that greatly exceed the background, and which tend to take on the amplitude distributions of the impulses themselves. To generate a class of first-order p.d.'s in  $\underline{a}$  that yields the proper behavior at large amplitudes in  $X$ , we follow the procedure suggested by Hall [Ref. 5, pp. 13-15] for his model of atmospheric noise, except that here the impulsive events are all independent, unlike the situation occurring in the lightning discharges which generate atmospheric noise. Accordingly, we consider the reciprocal process  $b(t) = a(t)^{-1}$ , and require it to have a first-order  $\chi^2$ -p.d. of  $\nu$  degrees of freedom, with scale parameter  $\sigma_b$ , viz:

$$w_1(b) = \frac{(\nu/2)^{\nu/2} |b|^{\nu-1}}{\Gamma(\nu/2) \sigma_b^\nu} e^{-\nu b^2/2\sigma_b^2} , \quad (-\infty < b < \infty) ; \quad (4.43)$$

$$\sigma_b > 0 ; \quad \nu > 0 .$$

Then one readily shows that for  $a = 1/b$ ,

$$W_1(a) = \frac{(\nu/2)^{\nu/2}}{\Gamma(\nu/2) \sigma_b^\nu} |a|^{-\nu-1} e^{-\nu/2\sigma_b^2 a^2} , \quad (-\infty < a < \infty) , \quad (4.44)$$

and

$$\lim_{|a| \rightarrow \infty} W_1(a) = \lim_{|a| \rightarrow \infty} A_\nu |a|^{-\nu-1} , \quad (\nu > 0) , \quad (4.44a)$$

which is the desired form of large-amplitude dependence for  $X$ , since  $|a| \rightarrow \infty$  implies  $|X| \rightarrow \infty$  and from (4.41), we have (remembering that  $|dZ/dX| = 1/a$ )

$$W_1(X)|a| \rightarrow \infty = \lim_{|X| \rightarrow \infty} \frac{A_\nu \langle Z^{\nu+1} \rangle}{|X|^{\nu+1}} = \lim_{|X| \rightarrow \infty} \frac{B_\nu}{|X|^{\nu+1}} . \quad (4.44b)$$

Our next step is to obtain  $W_1(X)$  explicitly. For this we use (4.44) in (4.41),

$$W_1(X) = \int_{-\infty}^{\infty} e^{-1/2a^2 \left[ \nu/\sigma_b^2 + X^2/\sigma_Z^2 \right]} |a|^{-\nu-2} \frac{A_\nu}{\sqrt{2\pi\sigma_Z^2}} da ; \quad (4.45)$$

$$A_\nu \equiv \frac{(\nu/2)^{\nu/2}}{\Gamma(\nu/2)} \sigma_b^{-\nu} ,$$

and get finally

$$W_1(X) = \frac{\Gamma[(\nu+1)/2]}{\Gamma(\nu/2)} \frac{(\sqrt{\nu} \sigma_Z/\sigma_b)^\nu}{\sqrt{\pi}} \frac{1}{(X^2 + \nu\sigma_Z^2/\sigma_b^2)^{(\nu+1)/2}} , \quad \nu > 0 . \quad (4.46)$$

Letting

$$\sigma_0 \equiv \sqrt{\nu} \sigma_Z/\sigma_b \quad \text{and} \quad \nu+1 \equiv \gamma (>1) , \quad (\sigma_Z^2 > 0) , \quad (4.47)$$

we can express  $W_1(X)$  in the somewhat more compact form

$$W_1(X) = \frac{\Gamma(\gamma/2)}{\Gamma\left(\frac{\gamma-2}{2}\right)} \cdot \frac{\sigma_0^{\gamma-1}}{\sqrt{\pi}} \cdot (X^2 + \sigma_0^2)^{-\gamma/2} . \quad (4.48)$$

Note that (4.44b) is indeed the behavior as  $|X| \rightarrow \infty$ , and, in particular, that

$$B_\nu = \frac{\Gamma[(\nu+1)/2]}{\Gamma(\nu/2)\sqrt{\pi}} \sigma_0^\nu . \quad (4.48a)$$

The characteristic function (c.f.) for  $W_1(X)$  is

$$F_1(i\xi)_{X=aZ} = B_\gamma \int_{-\infty}^{\infty} \frac{e^{i\xi X}}{(X^2 + \sigma_0^2)^{[(\gamma+1)/2]}} dX = \frac{2\pi B_\gamma \sqrt{\pi}}{\Gamma[(\gamma+1)/2]} \left( \frac{|\xi|}{2\sigma_0} \right)^{\gamma/2} K_{\gamma/2}(\sigma_0 |\xi|), \quad (4.49a)$$

$$= \frac{\pi 2^{2-\gamma/2}}{\Gamma(\gamma/2)} |\xi|^{\gamma/2} K_{\gamma/2}(\sigma_0 |\xi|) \Big|_{\gamma=\gamma-1}, \quad (4.49b)$$

where  $K_{\gamma/2}$  is a modified Bessel function of the second kind.<sup>36</sup> The various moments  $\langle X^{2k} \rangle$ , when they exist,<sup>37</sup> are found most easily from

$$\left\langle X^{2k} \right\rangle = B_\gamma \int_{-\infty}^{\infty} \frac{X^{2k} dX}{(X^2 + \sigma_0^2)^{\gamma/2}} = \frac{(-1)^k \Gamma(k+1/2) (\sigma_0)^{2k}}{[(3-\gamma)/2]_k \sqrt{\pi}}, \quad \left. \begin{array}{l} \gamma > 2k+1 \\ \gamma \leq 2k+1 \end{array} \right\} \rightarrow \infty; \quad (4.50)$$

In a similar fashion we can readily obtain the first-order statistics of the envelope  $E = |a(t)| e(t)$  [cf. Sec. 2, Eqs. (2.10)]. We have

$$W_1(E) = \left\langle w_1(E|a) \right\rangle_a; \quad w_1(E|a) = \frac{E e^{-E^2/2a^2 \sigma_Z^2}}{|a| \sigma_Z^2}, \quad (4.51)$$

which from (4.44) for  $W_1(0)$  is found to be

$$W_1(E) = C_\gamma E / (E^2 + \sigma_0^2)^{\gamma/2}, \quad 0 \leq E < \infty, \quad (4.52)$$

where

$$C_\gamma \equiv 2\Gamma(\gamma/2) \sigma_0^{\gamma-2} / \Gamma(\gamma/2 - 1). \quad (4.52a)$$

As already noted in Sec. 2, cf. remarks following Eqs. (2.10), the first-order p.d. of the phase,  $\varphi$ , is uniform on  $2\pi$ . The various first-order moments of the envelope are also easily obtained. We have directly

$$\left\langle E^k \right\rangle = C_\gamma \int_0^\infty \frac{E^{k+1} dE}{(E^2 + \sigma_0^2)^{\gamma/2}} = \frac{\sigma_0^k \Gamma(k/2 + 1) \Gamma(\gamma/2 - k/2 - 1)}{\Gamma(\gamma/2 - 1)}, \quad \left. \begin{array}{l} \gamma > k+2 \\ \gamma \leq k+2 \end{array} \right\} \rightarrow \infty, \quad (4.53)$$

Finally, note that for small amplitudes

$$W_1(E) \doteq C_Y E \doteq 2 \left( E / \langle E^2 \rangle \right) e^{-E^2 / \langle E^2 \rangle}, \quad E \geq 0, \quad \left. \begin{array}{l} \\ \langle E^2 \rangle = 2/C_Y \end{array} \right\}, \quad (4.53a)$$

which shows the expected Rayleigh form for the envelope [analogous to the gaussian p.d. for the instantaneous amplitude, cf. (4.42)].

The parameters  $\sigma_0$  and  $\nu$  are to be determined empirically. We expect that they will show secular variations with the time of day, week, etc. They may also vary with the urban region chosen for study. They will certainly depend on the bandwidth and frequency allocation of the receiver used. In any case, they are a part of the experimental data to be investigated in the overall study.

The higher-order statistics of  $X=aZ$  need to be studied theoretically in conjunction with the basic model (BSM) developed here [Secs. 3, 4A]. As noted in Sec. 2, for example, and with the aid of (2.7), (2.9), and the results of Sec. 4A-7 above, we have

$$K_{X=aZ}(t_1, t_2) = K_a(t_1, t_2) K_Z(t_1, t_2) = K_X(t_1, t_2)_{\text{BSM}} \quad (4.54)$$

where  $K_{X\text{-BSM}}$  is given explicitly by (4.27) or (4.29). Moreover, because  $X(t)$  may be expected to be macrostationary [Sec. 4A-8], we may replace (4.54) by

$$K_X(t_1, t_1 + \tau) \doteq K_a(\tau) K_Z(\tau), \quad (4.54a)$$

with considerable simplification of the higher-order statistics of  $X$ .

Because of the independence of the basic interference "events" in the urban model, in contradistinction to the atmospheric situation,<sup>5</sup> we may expect that  $a(t)$  may be quite slowly varying over reasonable observation intervals,  $(t_0, t_0 + T)$ , so that during such periods  $T$ ,  $a(t)$  is effectively constant. If this is the case in conjunction with macrostationarity, calculation of the higher-order statistics of the equivalent statistical model (ESM) is greatly simplified. For example, we have

$$K_{X=aZ}(t_1, t_2) = \langle a^2 \rangle K_Z(\tau) = K_X(\tau)_{\text{BSM}} \quad , \quad [\text{Eq. (2.9) and Sec. 4A-3, 8}], \quad (4.55)$$

which determines  $K_Z$  and, therefore, all orders of p.d.'s for  $Z$ , since  $Z(t)$  is postulated to be zero-mean and gaussian. From (4.50) we have

$$\langle a^2 \rangle = \sqrt{\pi} \sigma_0^{(5-\gamma)/2} / (\gamma-3) \sigma_Z^2 \quad , \quad (\gamma > 3) \quad . \quad (4.56)$$

The relative invariance of  $a(t)$  with time is accordingly a very important question, to be tested experimentally.

Finally, even though it may be established empirically that  $\gamma$  is 3 (or less), and consequently  $\langle a^2 \rangle$  and  $\langle X^2 \rangle \rightarrow \infty$ , our ESM may still be used.<sup>38</sup> Physically, of course,  $\langle X^2 \rangle$  must be finite. What probably occurs in reality is that not one, but two laws for  $a(t)$  are required at large amplitudes: one with a value  $\gamma (\leq 3)$ , say, for large amplitudes, up to some very high level, at and above which there is not only possible saturation at the front-end of the receiver, but also a modification of  $\gamma$ , now larger than 3, to insure the necessary finiteness of  $\langle X^2 \rangle$ .

## 5. CONCLUDING REMARKS:

In this first paper (Part I), we have laid the foundations for a workable analytical model of urban radio-noise interference. Although attention here has been directed primarily to the environment of vehicular mobile land-transportation, the general results and approaches used are available for other classes of noise mechanisms, both civilian and military. In so doing, we have also raised various questions that can only be resolved by experiment and/or simulation. Our analytical model includes the physics of propagation, coupling to the medium by means of the source and receiving apertures (beam patterns), source and platform motion (doppler), the general geometry of sources and receiver, and general waveforms for the interference, both broad- and narrow-band. The basic statistical model (BSM) is Poisson in the location in space of possible sources, leading to a Poisson process for the received waveforms [which is shown to be essentially stationary (macrostationary) for the type of emissions

considered here]. The fundamental assumption of independent, transient sources appears entirely reasonable. By suitable modification of Hall's atmospheric model,<sup>5</sup> we have constructed an equivalent statistical model (ESM) that has the great advantage of analytic tractability in its probability distributions, unlike the BSM, for which generally no closed-form, or even simple series developments seem possible. (This, of course, does not preclude simulation of the BSM and its distributions, if need be.) On the other hand, our BSM provides us with the explicit, detailed forms of the various moments of the received process, e.g., the mean (usually zero), the average intensity,  $\langle X^2 \rangle$ , the covariance function,  $K_X$   $\left[ = \left\langle X(t_1) X(t_2) \right\rangle \right]$ , and whatever higher-order and higher degree moments may be desired. By means of these moments we related the non-empirical portion of the equivalent model (ESM) to the detailed physics and geometry of the underlying interfering sources and their radiation. The "equivalent" model requires empirical calibration [for example, two parameters  $(\gamma, \sigma_0)$ , cf. (4.48) are being measured at TSC]. Other measurements [such as testing the invariance of the scale process,  $a(t)$ ] and analytical extensions [higher-order p.d.'s] also mentioned in preceding Secs. 2 - 4, are currently under investigation.

REFERENCES and FOOTNOTES:

1. See, for example, F.L.H.M. Stumpers, "Progress in the Work of CISPR (International Special Committee on Radio Interference)," IEEE Transactions on Electromagnetic Compatibility, Vol. EMC-12, No. 2, May 1970.
2. F.D. Lewis and R.A. Soderman, "Radio-frequency Standardization Activities," Proc. IEEE, Vol. 55, pp. 759-773, June 1967.
3. For example,  $\langle X^k \rangle$ ,  $k > 5$ , is a moment of  $X$  of degree higher than  $\langle X^k \rangle$ ,  $5 > k \geq 0$ , whereas  $\langle X(t_1)X(t_2) \rangle [\equiv M(t_1, t_2)]$  is a moment of higher-order than  $\langle X^k \rangle$  all  $k$ .
4. R. Esposito, "Research in Characterization and Measurement of Man-Made Electromagnetic Noise," 1st Monthly Technical Report, 18 Nov. - 17 Dec., 1970 (Raytheon Research Div., Waltham, Mass. 02154; Contract DOT-TSC-73 [Nov. 1970- ]; see references therein.
5. H.M. Hall, "A New Model for 'Impulsive' Phenomena: Application to Atmospheric-Noise Communication Channels," combined Technical Reports Nos. 3412-8, 7050-7, as SEL Report 66-052, August 1966, under Contract AF(638)1517, U.S. Air Force Office of Scientific Research Grants AFOSR-783-65, 783-66, U.S. Air Force Office of Scientific Research; and Tri-Service Contract Nonr-225(83). Radio-science Laboratory, Systems Theory Laboratory, Stanford Electronics Laboratories (SEL), Stanford Univ., Stanford, California.
6. And probably in the higher-order ones as well, with proper modelling and empirical calibration. See pp. 75-77 of Ref. 5.
7. D. Middleton, "Multidimensional Detection and Extraction of Signals in Random Media," Invited paper, Proc. IEEE, Vol. 58, No. 5, May 1970; pp. 696-796. See Sections IIA, IIIA, B, D in particular.
8. \_\_\_\_\_, "A Statistical Theory of Reverberation and Similar First-Order Scattered Fields, I, II," IEEE Trans. Info. Theory, Vol. IT-13, No. 7, July, 1967, pp. 372-392. See Sections 1, 2, 3, 4, 8.1, 9.2, 10.

9. The superscripts (N) on the operators  $\underline{T}$  indicate that noise (i.e., undesired signals) may be injected into the system at this particular stage. We follow here the formalism and conventions developed by the author in previous applications of Statistical Communication Theory.<sup>7, 10, 11</sup>
10. D. Middleton, "An Introduction to Statistical Communication Theory," McGraw-Hill Book Co., New York, 1960; cf. Chapter 2 and Chapter 18, for example.
11. \_\_\_\_\_, "Topics in Communication Theory," McGraw-Hill Book Co., New York, 1965; Chapters 1 and 5 in particular.
12. This is not too critical an assumption at this stage of the analysis. Later, we shall need to extend the analysis, along the lines developed in Ref. 7, to a full vector treatment, particularly when polarization and diversity effects are to be considered.
13. We can readily include interference of a steady-state nature.
14. See Ref. 10, Sections 11.2, 11.3, and Sec. 10, Ref. 8.
15. Ref. 5, pp. 6-8.
16. Similar remarks apply in principle to the corresponding equivalent model for the noise field:  $N_I(t, \underline{R}) = A(t, \underline{R}) Z(t, \underline{R})$ .
17. Ref. 8, Sec. 2.1; Ref. 7, Sec. III D.
18. In general, for these non-stationary processes, this means that the co-intensity spectra,  $\mathcal{N}_{a, Z}(f_1, f_2) \equiv 2 \int_{-\infty}^{\infty} \int_{-\infty}^{\infty} \mathcal{F} \left\{ K_{a, Z}(t_1, t_2) \right\} [cf. Sec. 8.5, Ref. 8]$ , where  $\mathcal{F}$  denotes the Fourier transform and the star (\*) indicates the complex conjugate, do not overlap. If  $a(t)$ ,  $Z(t)$  are stationary, the condition is on the (auto-) intensity spectrum  $\mathcal{N}_{a, Z}(f) = 2 \int_{-\infty}^{\infty} \mathcal{F} \left\{ K_{a, Z}(\tau) \right\}$
19. We may regard any heterodyning operation, i.e., RF to IF, as essentially linear here. Thus,  $h_{ARI} = h_{IF} * h_{RF}$  is the convolution of the responses in question, and we formally place the source of system noise at the input to  $h_{ARI}$ , of the receiving aperture, i.e., into the RF and IF stages.
20. Section 3 may be bypassed for the time-being by those interested primarily in the statistical portions of the urban radio-noise model sketched in Sec. 2.
21. We confine ourselves to a scalar model here in Part I [cf. Ref. 12].
22. See Secs. 4.1, 4.2, Ref. 8, and Sec. IIIA, Ref. 7.

23. In other words, different beam patterns are produced for different wavelengths of the exciting signal (or field, in the case of reception).
24. Ref. 8, Sec. 4.5; Ref. 7, Sec. IIC.
25. Whether the spreading factor  $(4\pi R_j)^{-1}$  is applied to  $\underline{T}_{AR}$ , or to  $\underline{T}_M^{(N)}$ , is mathematically a matter of convenience, but physically we associate it with the field operator,  $\underline{T}_M^{(N)}$ , as it is sensible to associate the delay  $R_j/c$ , also
26. The wave equation (3.1) becomes  $\nabla^2 \mathcal{L} - 1/e^2 \left[ (\partial/\partial t) + \underline{v}_S \cdot \underline{\nabla} \right]^2 \mathcal{L} = -G_I$ , or 0, where the source is moving, but as long as  $\beta_{SR}, \beta_{RS} \ll 1$  we can ignore terms like  $\underline{v}_S \cdot \underline{\nabla}$ , etc., and the usual wave-equations (3.1) apply.
27. See Ref. 8, Sec. (4.3), Eqs. (4.18) - (4.20), for a discussion of the responses of a (linear) time-variable system.
28. N.W. MacLachlan, "Complex Variables and Operational Calculus," Cambridge Univ. Press, 1939, Chapter IV.
29. Note the Poisson character of the process; the sources are independently, randomly distributed initially in space. This point is discussed more fully in Sec. 4 following.
30. If the receiver has a steerable beam, we replace  $\mathcal{Q}_R$  in (3.43) [as well as in (3.39), (3.39a) - (3.41), (3.42)] by  $\mathcal{Q}_R(\underline{v}_{Rj} - \underline{v}_{0Rj}, f_0)$ , where  $\underline{v}_{0R}$  = a steering spatial frequency  $\equiv \hat{i}_0 f_0/c$ , cf. (3.5), (3.6), and  $\underline{v}_{Rj} = -\hat{i}_{Rj} f_0/c$ . By changing  $\underline{v}_{0R}$ , one can "point" the beam in the direction  $P(\underline{R}_0)$ , where  $\hat{i}_0 \equiv \underline{R}_0/|\underline{R}_0|$ . See the discussion in Sec. 4.1, Ref. 8.
31. Ref. 10, Sec. 7.7, also Secs. 11.2, 11.3.
32. Ref. 7, Sec. IID; Ref. 8, Sec. 9.2.
33. Ref. 10, Sec. 1.3.
34. D. Middleton, "Acoustic Modelling, Simulation, and Analysis of Complex Underwater Targets. II. Statistical Evaluation of Experimental Data," Applied Research Laboratories Report ARL-TR-69-22, 26 June, 1969 (Naval Ships Systems Command, Contract N00024-69-C-1129).
35. T.D. Plemmons, "Spectra, Covariance Functions, and Associated Statistics of Underwater Acoustic Scattering From Lake Surfaces," Doctoral Dissertation, Phys. Dept., Univ. of Texas at Austin, May, 1971.

36. G.N. Watson, "Theory of Bessel Functions," 2nd Edition, MacMillan, New York, 1944.
37. Note, as expected, that all odd-order moments vanish.
38. See the discussion in Ref. 5, pp. 16, 17; 50 - 52.

GLOSSARY OF PRINCIPAL SYMBOLS:

A.	$A_0$	: signal amplitude
	$a(t)$	: scaling process
	$A_I(\underline{\xi}, f)$	: aperture weighting (source)
	$\alpha_I$	: timeform of aperture weighting
	$A_R(\underline{\eta}, f)$	: aperture weighting (receiver)
	$a_I, a_R, a'_I$	: beam patterns
B.	BSM	: Basic Statistical Model
	$\beta_{RS}, \beta_{SR}$	: normalized doppler speeds
	$\beta$	: a combination of doppler speeds
C.	$c$	: velocity of propagation
D.	$\delta( )$	: a delta function
E.	ESM	: Equivalent Statistical Model
	$e(t)$	: envelope of $Z(t)$
	$\underline{\eta}$	: a receiver coordinate
	$\epsilon$	: sum of dopplers
	$\hat{\epsilon}$	: epoch: observer vs. initial source emission
F.	$f, f_0$	: frequencies
	$F_1, F_n$	: characteristic functions
G.	$G(t, \underline{R})$	: gauss noise field
	$G(t)$	: a gauss process
	$G_I$	: source function
	$\gamma$	: parameter of a p.d.

- H.  $h_{RI}$  : weighting function of RF-IF receiver response  
(including receiving aperture)  
 $h_R$  : height of receiver above source plane
- I.  $\hat{i}_R; \hat{i}_x, \hat{i}'_x, \hat{i}_y, \hat{i}'_y, \hat{i}_z, \hat{i}'_z$  : unit vectors
- J.
- K.  $B_X, K_X, K_{N_I}, K_a, K_Z$  : covariance functions  
 $\xi$  : a source coordinate
- L.  $\Lambda_X$  : "sine" component of  $K_X$   
 $\mathcal{L}$  : field of a noise source  
 $\Lambda$  : domain of interfering sources  
 $\lambda$  : a (time) variable  
 $\underline{\lambda}$  : a set of coordinates  
 $L_{\max}$  : max. dimension of source aperture
- M.  $\mu$  :  $1 + a$  doppler speed
- N.  $N_I(t, \underline{R})$  : interference field  
 $\underline{v}$  : vector wave number  
 $v$  : a statistical parameter
- O.  $\omega, \omega_0$  : angular frequencies
- P.  $P(t, \underline{R})$  : Poisson noise field  
 $P(t)$  : a Poisson process  
 $\varphi_0, \varphi$  : phases  
 $\varphi_R$  : azimuthal angle
- Q.

R.	$R_X$	: "cosine" component of $K_X$
	$\rho(\lambda)$	: Poisson source density
	$\underline{r}, \underline{r}', \underline{R}, \underline{R}', R$	: distance (and vectors)
S.	$\sigma_B, \sigma_D, \sigma_S$	: physical densities of sources
	$\sigma_0$	: parameter of a p.d.
	$\hat{S}_0$	: complex signal envelope
	$S_I(t, \underline{R})$	: interfering noise source
	$S_I(f, \underline{\xi})$	: amplitude spectrum of source
T.	$T_S$	: signal duration
	$T_0$	: time delay on path of propagation
	$\underline{T}_{AR}, \underline{T}_M, \underline{T}_{R_0}$	: transformations
	$\underline{\theta}$	: set of parameters of interfering signal
	$\tau$	: correlation time, $t_2 - t_1$
	$t, t_1, t_2, t_S, t_R$	: times
U.	$U_j$	: typical received waveform from $j^{\text{th}}$ source
V.	$V_I, V_R$	: volume of source and receiver aperture
	$\underline{v}_R, \underline{v}_S$	: velocities
W.	$\mathcal{W}_X$	: auto- or cointensity spectrum
	$w_1, W_1$	: p.d.'s
X.	$X(t)$	: the interference process in the receiver
Y.	$Y_I$	: (time-varying) system function of source
	$\mathcal{Y}_I$	: bi-frequency function of source
Z.	$Z(t)$	: a gaussian random process

LIST OF FIGURE CAPTIONS: (DOT: DM, Paper #1)

- Fig. 3.1    Geometry of interfering source and the receiver
- Fig. 3.2    Schema of a typical distribution of urban noise sources and a receiver (R)
- Fig. 4.1    Geometry of an interfering source (at  $P_j$ ) and a receiver at height ( $h_R \geq 0$ ), for an urban region  $\Lambda$  containing independent radio noise sources. (Exaggerated in the vertical direction.)



Transportation Systems Center.  
SC-UMTA-71-6. Ground  
stations & control.

DL	TELEPHONE	DATE
1	461100	3/22/73
2	762-7010	4/30/74

OK CARD

GPO 896-099



00349668